NATIONAL INSTITUTE OF PUBLIC HEALTH AND THE ENVIRONMENT
BILTHOVEN, THE NETHERLANDS

Report no. 722108015

Towards development of a deposition monitoring network for air pollution of Europe

J. W. Erisman[1], M.G. Mennen[1], D. Fowler[2],
C.R. Flechard[2], G. Spindler[3], A. Grüner[3],
J.H. Duyzer[4], W. Ruigrok[5], G.P. Wyers[6]

April 1996

[1] *RIVM, P.O.Box 1, 3720 BA Bilthoven, the Netherlands*
[2] *ITE, Bush Estate, Penicuik, Midlothian, EH26 0QB, U.K.*
[3] *IFT, Permoserstr. 15, 04303 Leipzig, Germany*
[4] *TNO, P.O.Box 6011, 2600 JA Delft, the Netherlands*
[5] *KEMA, P.O.Box 9035, 6800 ET Arnhem, the Netherlands*
[5] *ECN, P.O.Box 1, 1755 ZG Petten, the Netherlands*

This investigation was carried out on behalf and for the account of the LIFE project of the European Commission DG XI, within the framework of project no. 7221010: "LIFE", and on behalf of and for the account of the Directorate-General for Environmental Protection (DGM/LE) within the framework of project no. 722108: "Deposition Research".

RIVM, Antonie van Leeuwenhoeklaan 9, P.O. Box 1, 3720 BA BILTHOVEN, The Netherlands Tel: +31 30 2749111; Fax: +31 30 2742971

Mailing list

1. Directeur Lucht en Energie, ir. G.M. van der Slikke
2. Plv.Directeur-Generaal Milieubeheer, dr.ir. B.C.J. Zoeteman
3. Plv.Directeur-Generaal Milieubeheer, mr. G. Wolters
4. Drs. R.J.T. van Lint, DGM, hoofd afd. Luchtkwaliteit en Verzuring
5. Dr. W.A.H. Asman, NERI, Denmark
6. Dr. D.D. Baldocchi, NOAA, USA
7. Dr. C. Baquero, CIEMAT, Spain
8. Dr. E. Berge, EMEP
9. Dr. R. Bobbink, KUN
10. Dr. P. Borrell, IFU, Germany
11. Dr. F. Bosveld, KNMI
12. Dr. J. Brook, Canada
13. Dr. G.P.J. Draaijers, TNO
14. Dr. L.J. van der Eerden, Ab_DLO
15. Prof. dr. A. Eliassen, EMEP
16. Dr. J. Garland, UK
17. Dr. P. Grennfelt, IVL, Sweden
18. van Heekeren, VROM
19. Dr. B.B. Hicks, NOAA, USA
20. Ir. P. Hofschreuder, LUW
21. Dr. B. van der Hove, LUW
22. Mr. V. Keizer, VROM
23. Dr. J. Kesselmeier, Max Planck Institute, Germany
24. Dr. W. Klaassen, RUG
25. Dr. G. Lövblad, IVL, Sweden
26. Dr. F. Meixner, Max Planck Institute, Germany
27. Dr. J. Padro, Canada
28. Dr. K. Pilegaard, RISØ, Denmark
29. Dr. C. Pio, University of Aveiro, Portugal
30. Dr. R. San Jose, University of Valadolid, Spain
31. Dr. J. Schaug, EMEP
32. Dr. K. Sjöberg, IVL, Sweden
33. Dr. J. Slanina, ECN
34. Drs. J. Sliggers, VROM
35. Ir. S. Smeulders, VROM
36. Dr. T. Spranger, UBA, Germany
37. Dr. M. Sutton, ITE, UK
38. Dr. A. Vermeulen, ECN
39. Dr. W. de Vries, SC-DLO
40. Depot Nederlandse Publicaties en Nederlandse Bibliografie
41. Directie Rijksinstituut voor Volksgezondheid en Milieu
42. Dr. R.M. van Aalst
43. Drs. J.M.M. Aben
44. Dr. ir. R. van de Berg
45. Ing. A. Bleeker
46. Ir. T. Bresser

47. Drs. E. Buijsman
48. Ir. H.S.M.A. Diederen
49. Ing. B.G. van Elzakker
50. Ir. G.J. Heij
51. Dr. J.P. Hettelingh
52. Dr. ing. J.A. van Jaarsveld
53. Ir. F. Langeweg
54. Drs. E. van Leeuwen
55. Dr. ir. D. van Lith
56. Dr. R. Maas
57. Dr. A. van der Meulen
58. Dr. D. Onderdelinden
59. Dr. M. Posch
60. Dr. A. van Pul
61. Ing. E. van Putten
62. Ing. W. Uiterwijk
63. Dr. J. Wiertz
64. Hoofd Bureau Voorlichting en Public Relations
65. Bureau Projekten- en Rapportenregistratie
66.-74. Auteurs
75. Bibliotheek LLO
76-77. Bibliotheek RIVM
78-125. Bureau Rapportenbeheer
125-150. Reserve exemplaren LLO

CONTENTS

List of Figures

List of Tables

Samenvatting

In 1993 werd vanuit het LIFE projekt van de Europese Commissie DG XI voor 50% het projekt 'Towards the development of a deposition monitoring network for air pollution of Europe' (93/NL/A32/NL3547) gefinancierd. Het projekt werd mede gefinancierd door het Ministerie VROM, door de Engelse en Duitse overheid, en door de deelnemende instituten zelf. Het projekt werd uitgevoerd door ITE (UK), IFT (Duitsland), TNO, ECN, KEMA en RIVM (Nederland). Het doel van dit projekt was het ontwikkelen en implementeren van een depositiemonitoring-methode voor luchtverontreiniging in Europa. Een dergelijke methode zou gebruikt moeten worden als uitbreiding van bestaande Europese monitoring netwerken voor het meten van luchtconcentraties, om depositieschattingen op ecosysteemschaal te kunnen maken. In dit projekt werd een monitoringstation ontworpen en op drie plaatsen in Europa gedurende een jaar ingezet: Auchencorth, een semi-natuurlijke lage vegetatie in Schotland; Melpitz, een grasland in Duitsland en Speulder bos, een Douglas sparren bos in Nederland. Dit rapport beschrijft de eindresultaten van het zogenaamde LIFE projekt.

De resultaten van het projekt laten zien dat de ontwikkeling van depositiemonitoring-methoden succesvol was en dat routinematige metingen voor de bepaling van de depositie van luchtverontreiniging uitgevoerd kunnen worden. De inzet van de apparatuur op drie lokaties in Europa, representatief voor verschillende condities en ecosystemen, leverde continu hoge kwaliteit gegevens voor de bepaling van de jaargemiddelde deposities. De droge depositie van SO_2, NH_3 en NO_x werd continu gemeten met behulp van de gradiëntmethode. De evaluaties van parametrisaties voor de uitwisseling van deze komponenten met het oppervlak vormden een belangrijk onderdeel van het projekt, daar deze parametrisaties gebruikt worden voor de bepaling van de depositie van de andere komponenten in de zogenaamde inference methode. Er werden systematische afwijkingen gevonden tussen gemodelleerde en gemeten fluxen. Het was echter niet het doel van dit projekt de modellen te verbeteren. De metingen vormen een goede basis voor modelverbeteringen en zullen in de toekomst daartoe worden geanalyseerd.

Depositiefluxen
De jaargemiddelde droge depositie van geoxideerd zwavel (SO_2, SO_4), geoxideerd en gereduceerd stikstof (NO_x, HNO_3, HNO_2, NH_3, NO_3, NH_4), basische kationen (Na, Ca, Mg) en zware metalen (Pb, Cr, Cd, Zn, Cu, Ni) werd uit metingen in 1995 vastgesteld op de drie lokaties. Natte depositie werd gemeten met wet-only vangers, terwijl de droge depositie werd bepaald met concentratiemetingen en meteorologische metingen. De totale depositie voor deze komponenten is de som van de natte en droge depositie, deze zijn voor de drie lokaties gegeven in onderstaande tabel. De lokaties werden geselekteerd voor het verschil in landgebruik, oppervlakte karakteristieken en klimaten. De noord-Schotse lokatie Auchencorth Moss kan geklassificeerd worden als een semi-natuurlijke lage vegetatie in een vochtig, relatief schoon klimaat, het Speulder bos in het midden van Nederland is een Douglas bos met een hoge ruwheid in een middelmatig belast gebied met hoge ammoniak belasting, Melpitz tenslotte is een grasland in een hoog belast gebied nabij Leipzig in Duitsland onder invloed van een land- klimaat.

Het verschil in omstandigheden en condities is terug te vinden in de droge depositiesnelheden en oppervlakte weerstanden die afgeleid zijn uit de gradientmetingen op de drie lokaties. De

invloed van vocht op het oppervlakte, de stomataire opname en de koppeling tussen verschillende komponenten aan het oppervlakte is in de meetresultaten terug te vinden. Het is duidelijk dat de grote variaties in depositiesnelheden die hiervan het gevolg zijn, nog niet voldoende gemodelleerd kunnen worden. Dit onderschrijft de behoefte aan dergelijke langdurige metingen.

Het verschil in klimaat en milieubelasing volgt direkt uit een vergelijking tussen de verschillende fluxen in onderstaande tabel. De fluxen op Auchencorth Moss zijn over het algemeen het laagste, behalve die van de zeezout komponenten, welke op Melpitz het laagst waren als gevolg van de grote afstand tot de zee. De hoogste droge depositie voor alle komponenten werden gemeten op het Speulder bos, voornamelijk als gevolg van de hoge ruwheid van het bos wat hoge droge depositiesnelheden tot gevolg heeft. De depositie van zware metalen is veel lager dan die van gassen en basische kationen. Zware metalen worden voornamelijk gedeponeerd via de natte depositie. Voor zeezout komponenten is de natte depositie belangrijker dan de droge depositie. De bijdrage van de natte depositie aan de totale depositie verschilt sterk per komponent en per lokatie. Op Auchencorth Moss is de natte depositie verreweg het belangrijkste. Op de andere, meer belaste lokaties, is de droge depositie meer van belang, en op Speuld zelfs dominant. The relatieve bijdrage van HNO_2 en HNO_3 aan de totale geoxydeerde stikstofdepositie blijkt niet te verwaarlozen in centraal Europa, in het noorden, waar de natte depositie domineert, is de bijdrage echter zeer klein.

De totaal potentieel zuur depositie bedroeg in 1995 op Auchencorth, Speuld en Melpitz, respectievelijk 1006, 4914 and 3230 mol H^+ ha^{-1} a^{-1}. De totale basische kation depositie bedroeg respektievelijk 217, 456 en 225 eq ha^{-1} a^{-1}, 20%, 9% en 7% van de totaal potentieel zuur depositie. De totale stikstof depositie bedroeg respectievelijk 586, 3430 en 1240 mol ha^{-1} a^{-1} (8, 48 en 17 kg N ha^{-1}). Het grootste aandeel aan de potentieel zuur en stikstofdepositie werd gevormd door NH_x, behalve voor de bijdrage aan potentieel zuur te Melpitz, waar SO_x het belangrijkste was.

Wolken- en mistwater samplers werden op de drie lokaties geplaatst, maar op geen van de drie is de depositie ten gevolge van mist bepaald. Dit is deels het gevolg van technische problemen, maar ook van de lage frequentie van voorkomen van mist in 1995. Het is raadzaam om deze methode alleen toe te passen in gebieden waar veel mist voorkomt (kust, bergen).

Onzekerheden
Op alle drie de lokaties is een schatting van de onzekerheid gemaakt door de gemeten en gemodelleerde depositieparameters te vergelijken, de belangrijkste onzekerheidsbronnen te kwantificeren en door expert judgements. Het blijkt dat de onzekerheid in de droge depositie van deeltjes het grootst is, vooral voor de zware metalen. Depositiesnelheden voor deeltjes zijn onzeker, maar ook de concentratiebepaling voor zware metalen is, bij de lage koncentraties, onnauwkeurig. Voor het Speulder bos is de bepaling van de deeltjes depositie nauwkeuriger dan voor de andere lokaties, omdat hier recentelijk een groot onderzoek is uitgevoerd naar de depositie van deeltjes. Depositie van gassen is minder onzeker boven lage vegetatie dan boven bos, omdat de concentratieverschillen boven bos, door de goede menging veel kleiner zijn dan boven lage vegetatie. De grootste onzekerheid geldt voor NO_x.

Natte, droge en totale depositie afgeleid uit metingen boven het Speulder bos, Auchencorth Moss en Melpitz (mol ha^{-1} a^{-1}).

	Speulder forest			Auchencorth Moss			Melpitz		
Komponent	Droge depositie	Natte depositie	Totale depositie	Droge depositie	Natte depositie	Totale depositie	Droge depositie	Natte depositie	Totale depositie
SO_4	106	291		11	128		35	209	
SO_2	345			71			751		
SO_x	*452*		*742*	*82*		*210*	*786*		*995*
NH_4	337	806		24	173		47	336	
NH_3	1277			177			518		
NH_x	*1615*		*2420*	*201*		*374*	*565*		*901*
NO_x	203			41			12		
NO_3	267	374		14	133		20	233	
HNO_3	97			18			55		
HNO_2	69			6			20		
NO_y	*636*		*1010*	*79*		*212*	*95*		*340*
Cl	214	855		48	395		12	75	
HCl	69			17			31		
Cl_x	*284*		*1139*	*65*		*460*	*43*		*118*
Na	317	646	963	53	378	431	21	70	91
Ca	37	46	83	3	36	39	32	49	81
K	25	29	54	2	25	27	5	24	29
Mg	40	78	118	6	50	56	3	14	17
Zn	5	4	9	0.13	0.907	1.037	0.35	4	4.35
Pb	0.88	0.11	0.99	0.03	0.065	0.095	0.03	0.08	0.11
Cd	0.03	0.04	0.07	0	0.003	0.003	0.001	0.004	0.005
Cu	0.66	0.19	0.85	0.02	0.144	0.164	0.047	0.05	0.097
Ni	0.25	0.06	0.31	0.01	0.006	0.016	0.005	0.03	0.035
Cr	0.11	0.07	0.18	0	0.016	0.016	0.006	0.01	0.016

Generalisatie

Voor de generalisatie van depositie en de ontwikkeling van reduktiemaatregelen in Europa worden depositiemodellen gebruikt. De depositie in dergelijke modellen wordt geschat door gebruikmaking van parametrisaties van de oppervlakte-uitwisseling, welke zijn afgeleid uit metingen. Tot nu toe zijn deze modellen nog niet gevalideerd met droge depositiemetingen. De resultaten van het LIFE projekt leveren daarom voor het eerst de mogelijkheid een onafhankelijke evaluatie uit te voeren. De resultaten van het EDACS model, dat het enige model is dat depositiefluxen op kleine schaal kan bepalen in Europa, werden vergeleken met de metingen. De modelresultaten waren alleen voor 1993 beschikbaar omdat de emissies voor latere jaren niet beschikbaar waren, terwijl de metingen uitgevoerd zijn in 1995. Ondanks dat, kan gekonkludeerd worden dat EDACS de zwaveldepositie overschat. Dit is voornamelijk te wijten aan het verwaarlozen van horizontale concentratiegradienten op kleine schaal en aan de parametrisaties van de oppervlakte- uitwisseling. Ammoniakdepositie werd onderschat met EDACS, door het verwaarlozen van de grote ruimtelijke variaties in koncentraties. De gemodelleerde NO_y waarden kwamen redelijk overeen met de metingen. Het is duidelijk dat het model verder ontwikkeld moet worden voor een meer accurate bepaling van ecosysteem-speciefieke fluxen. Vooral de modellering van concentratiegradienten en de oppervlakte-uitwisseling verdient hierbij de nodige aandacht. Verder is gebleken dat de resultaten van de metingen op de LIFE lokaties van groot belang zijn voor de ontwikkeling en evaluatie van depositiemodellen.

Monitoring strategie

Het is onmogelijk om Europa-dekkend de depositie met metingen in kaart te brengen. De droge- en mistdepositie laten zeer grote ruimtelijke gradienten zien als gevolg van gradienten in concentraties, verschil in landgebruik en oppervlakte condities. Metingen zullen daarom complementair moeten zijn aan modellen. Daarnaast zijn metingen nodig voor de ontwikkeling van modellen die de processen beschrijven, en om trends te detekteren voor onafhankelijke beleidsevaluatie. Deze punten vergen elk een eigen meet/monitoring inspanning. Voor een goede evaluatie van modellen en voor beleidsontwikkeling in Europa, is een uitbreiding van het aantal depositiemeetpunten noodzakelijk. Voor ontwikkeling en testen van modellen is een uitbreiding van 'intensieve' meetlokaties, zoals in dit projekt opgezet, naar meer ecosystemen onder verschillende omstandigheden noodzakelijk. Ongeveer 5 à 10 van dergelijke lokaties in Europa zijn voldoende. Twee à drie zijn nodig in Zuid-Europa, drie à vier in centraal en oost- Europa en drie in achtergrond gebieden (noord- en West-Europa). Voor modelevaluatie alleen zouden de huidige koncentratie monitoring netwerken (o.a. EMEP en nationaal) uitgebreid moeten worden met ongeveer 100 lokaties waar met goedkope methoden de depositie gemonitoord wordt. Kandidaten voor een dergelijke methode zijn langdurig gemiddelde gradienten en de Relaxed Eddy Accumulation (REA) methode Deze methoden moeten echter nog verder worden ontwikkeld en getest, voor routinematige metingen kunnen worden uitgevoerd.

Summary

In January 1993 within the framework of the LIFE programme a project was financed (50%) which aim was to develop a deposition monitoring method for air pollution of Europe (93/NL/A32/NL/3547). The project was co-financed by the Dutch, German and Brittish governments and by the participating institutes. The project was executed by ITE (UK), IFT (Germany), TNO, ECN, KEMA and RIVM (The Netherlands). The monitoring method should be used to extend existing European monitoring networks of air concentrations to provide deposition inputs on an ecosystem scale. A monitoring station for atmospheric deposition was designed and constructed using existing methods. Three such stations were applied in a pilot project for a year on three sites in different regions in Europe to estimate local inputs and to validate deposition models which are currently developed for estimation of ecosystem-specific deposition in Europe.

The results of this project show that the developed deposition monitoring method is successful in determining the deposition of pollutants and can be applied on a routine basis. The equipment for flux measurements provided continuous high quality data for SO_2, NH_3 and NO_x, and concentration data for all major gaseous and particulate pollutants throughout the range of pollution climates present in Central and Northern Europe. The monitoring facility was therefore highly successful. The sites selected were representative of the major ecosystems of Europe and the range of air pollution climates (excepting urban areas and Mediterranean regions).

Deposition budgets
Detailed annual deposition budgets for all components, i.e. oxidised sulphur (SO_2, SO_4) oxidised and reduced nitrogen (NO, NO_2, HNO_3, HNO_2, NH_3, NO_3, NH_4) for base cations (Na, Ca, Mg) and heavy metals (Pb, Cr, Cd, Zn, Cu, Ni) were obtained from measurements throughout the year (1995) at 3 contrasting sites; Melpitz (SE Germany), Speulder forest (Central Netherlands) and Auchencorth Moss (Southern Scotland). The sites were selected for their difference in land use type, surface characteristics and environmental climates. The northern Scottish site can be classified as humid background site. Speulder forest is characterised as a rough surface in a humid, sea climate with moderate pollution levels, except for NH_3. Melpitz can be considered as a site with a land climate, with relatively high sulphur loads. The difference in surface characteristics is reflected in the dry deposition velocities and surface resistances determined from the gradients measured at the different sites.

The influence of surface wetness, stomatal uptake, but also coupling of uptake at the external leaf surface between different components is clearly shown. One important result of this project is that it is shown that the variations in processes affecting surface uptake is not yet quantified by current surface resistance parametrisations, although the SO_2 parametrisations compared quite good with measurements at the three sites. The discrepancies between modelled and measured surface uptake reflects the need for these long-term measurements, as the large variability has up till now not yet been identified by campaign type of measurements. Surface resistance parametrisations were tested using the continuous gradient measurements and applied here to estimate annual average dry deposition. No improvements were made yet, as this was not within the aims of this project.

The annual fluxes obtained at the three sites are listed in the table in this summary. The differences in pollution level is clearly identified in the different fluxes measured at the sites. The fluxes at Auchencorth Moss are generally lowest, except for components of sea salt origin (Na^+, Mg^{2+}, Cl^-). For these components, Melpitz has lower fluxes than Auchencorth Moss, as the result of the difference in distance to the sea. Speulder forests yields highest input for all components, mainly as the result of the roughness of the forest and the resulting high dry deposition velocities. Heavy metal inputs are much lower than gases and base cations. It is remarkable that heavy metal fluxes are much higher in Auchencorth than in Melpitz. Heavy metal inputs are mainly resulting from wet deposition. It must be emphasised here that uncertainties associated with heavy metal inputs are highest of all. The percentage wet deposition of the total deposition varies very much per component and per site. At Auchencorth Moss, the background site, wet deposition is clearly the dominant input. At the higher pollution sites, dry deposition becomes more important, and is generally dominating total deposition at the forest site (high roughness). For sea salt components, wet deposition is higher than dry deposition.

The relative contribution of the minor nitrogen species (HNO_2, HNO_3) to input budgets has been quantified at 3 locations and demonstrates that HNO_3 (and to a lesser extent HNO_2) are important components of the input throughout continental Europe but is a minor component in NW Europe where wet deposition dominates the input.

Wet, dry and total deposition derived from measurements above the Speulder forest, Auchencorth Moss and Melpitz (mol ha^{-1} a^{-1}).

	Speulder forest			Auchencorth Moss			Melpitz		
Component	Dry deposition	Wet deposition	Total deposition	Dry deposition	Wet deposition	Total deposition	Dry deposition	Wet deposition	Total deposition
SO_4	106	291		11	128		35	209	
SO_2	345			71			751		
SO_x	*452*		*742*	*82*		*210*	*786*		*995*
NH_4	337	806		24	173		47	336	
NH_3	1277			177			518		
NH_x	*1615*		*2420*	*201*		*374*	*565*		*901*
NO_x	203			41			12		
NO_3	267	374		14	133		20	233	
HNO_3	97			18			55		
HNO_2	69			6			20		
NO_y	*636*		*1010*	*79*		*212*	*95*		*340*
Cl	214	855		48	395		12	75	
HCl	69			17			31		
Cl_x	*284*		*1139*	*65*		*460*	*43*		*118*
Na	317	646	963	53	378	431	21	70	91
Ca	37	46	83	3	36	39	32	49	81
K	25	29	54	2	25	27	5	24	29
Mg	40	78	118	6	50	56	3	14	17
Zn	5	4	9	0.13	0.907	1.037	0.35	4	4.35
Pb	0.88	0.11	0.99	0.03	0.065	0.095	0.03	0.08	0.11
Cd	0.03	0.04	0.07	0	0.003	0.003	0.001	0.004	0.005
Cu	0.66	0.19	0.85	0.02	0.144	0.164	0.047	0.05	0.097
Ni	0.25	0.06	0.31	0.01	0.006	0.016	0.005	0.03	0.035
Cr	0.11	0.07	0.18	0	0.016	0.016	0.006	0.01	0.016

The total potential acid input in 1995 at Auchencorth Moss, Speulder forest and Melpitz amounted 1006, 4914 and 3230 mol H^+ ha^{-1} a^{-1}, respectively. Total base cation input amounted respectively 217, 456 en 225 eq ha^{-1} a^{-1}, 20%, 9% and 7% of the total potential acid deposition. The total nitrogen input was 586, 3430 and 1240 mol ha^{-1} a^{-1} (8, 48 and 17 kg N ha^{-1}). The main contribution to the total potential acid and nitrogen deposition was from NH_x at the three sites, except for Melpitz where the main contribution to the total potential acid input was formed by SO_x.

Cloud/fog-water collectors were deployed at each site but any of the cloud/fog frequency was too small to characterise the chemistry or deposition at any of the sites, a high altitude site would be necessary to achieve this.

Uncertainty
For each site, the uncertainty has been estimated based on the comparison of modelled and measured dry deposition velocities, quantification of major uncertainty sources and expert judgement. It shows that the uncertainty in particle input is highest, especially for heavy metals. Particle deposition velocities are uncertain, and for heavy metals, the detection of concentration is uncertain as the result of the very low concentrations. For forests, especially for Speulder forest, there is more information on particle deposition than for low vegetation. In a recent study, many methods to determine particle deposition were used, in order to evaluate particle deposition models for rough surfaces. Therefore, uncertainty in particle fluxes to the forest is lower than for other sites. Gas deposition yields lower uncertainties for low vegetation than for rough surfaces, because the vertical concentration differences are higher and because much more measurements are available over low vegetation. The highest uncertainty for gaseous input is found for NO_x.

Generalisation
For generalisation of deposition and for development of abatement strategies of Europe deposition models are used. In these models, deposition is estimated using surface exchange parametrisations derived from deposition measurements. Untill now, it has not been possible to test these models with dry deposition measurements. The results from the LIFE project provides the first independent check of model results. Results of the EDACS model, which is currently the only model capable of estimating deposition on a small sclae in Europe, were compared to the measurements made at the three sites. Model results were only available for 1993, whereas measurements were made during 1995. Despite this, it is concluded that EDACS overestimates sulphur deposition. This is mainly the result of the neglecting of horizontal concentration gradients and of the deposition velocity parametrisation. For ammonia, EDACS underestimates the deposition. This is due to the neglecting of horizontal concentration gradients in the model. NO_y deposition from the two methods compares reasonably well. It is concluded from the comparison that the model needs further development to estimate local (ecosystem specific) inputs. Main emphasis must be on development of surface resistance parametrisations and concentration resolution. Furthermore, the current demands for high spatial resolution deposition data for the application of critical load assessment to determine the scale of emission reduction necessary for Europe make the use of flux monitoring stations such as the three LIFE sites invaluable to underpin the models used.

Monitoring strategy

It is impossible to obtain an accurate annual average deposition map of Europe based on actual deposition measurements. Dry, cloud and fog deposition show very strong horizontal gradients due to variations in ambient concentrations in land use, in surface conditions and in meteorology. Measurements should therefore be supplementary to models. Furthermore, measurements are used for developing process descriptions and for evaluation of model results. Finally, measurements can act as an independent tool for assessing policy targets (trend detection). These issues require different measuring/monitoring strategies. For a thorough evaluation of models and of policy development, more measuring sites of deposition are needed in Europe. For development and testing of deposition models, more 'intensive' sites, as developed within the project reported here, placed at different ecosystems in different conditions are needed. It is estimated that about 5 to 10 of such monitoring stations will be sufficient. Two or three of such stations are needed in southern Europe, three or four in central Europe and three in background areas. For validation of model results several (about 100) sites in Europe are needed, in addition to current concentration monitoring networks. The intensive monitoring sites are, however, much too expensive for large scale application. Therefore, the development of low cost deposition monitoring methods is needed. For this, the long-term average gradients or the Relaxed Eddy Accumulation (REA) method seems appropriate. Such methods need testing and further development.

1. Introduction

Effects of air pollution exposure and deposition to European ecosystems have been widely recognised and have resulted in legislation to limit gaseous emissions. Ecosystem vitality is influenced by interactions with acidifying compounds, euthrophying compounds, heavy metals and persistent organic compounds of atmospheric origin (Grennfelt and Thörnelöf, 1992). Air pollutants are deposited to the surface in dry and in wet form. Deposition by cloud or fog is also important at some sites. The biosphere - atmosphere exchange of air pollutants has been studied in campaign measurements and has been extended using measurements and models.

Several national networks and a few European monitoring network (OSPAR, HELCOM, EMEP, Schaug *et al.*, 1991) exist, where routinely ambient concentrations and wet deposition measurements are made of a range of components. Dry deposition is more difficult to measure. To date, measurements of dry deposition have been made in intensive field campaigns. Monitoring of dry deposition for some gases has only recently been reported (Erisman *et al.*, 1993a, Erisman *et al.*, 1993b, Erisman and Wyers, 1993; Erisman and Draaijers, 1995).

Area average deposition can not be measured directly. Therefore, long-range transport models are used to describe the concentration and deposition variations on a national or European scale. The long-range transport EMEP model (Iversen *et al.*, 1991) is used for deriving blame matrices and as a basis for the first SO_x and NO_x protocols for emission reduction agreements in Europe. These protocols are aimed at deposition targets. In the future, these deposition targets will probably be based on the critical load concept, as has been done for the second SO_2 protocol. Emission reductions are derived from estimated exceedances of these critical loads. Long-range transport models estimate deposition based on emission estimates and transport modules on a large spatial scale (50x50 to 150x150 km). Specific ecosystem interactions such as surface characteristics and terrain roughness are not taken into account. At this moment, models are under development which can deal with these small scale processes (see Lövblad *et al.*, 1993). These models will be more suitable for estimating the actual ecosystem exposures and loads and thus for estimating critical load exceedances.

At the workshop on deposition (3-6 November 1992 Göteborg, Sweden) organised by the Nordic Council of Ministers in co-operation with EMEP (European Monitoring and Evaluation Programme) and BIATEX (Biosphere Atmosphere Exchange of pollutants), the need for routine measurements of dry and wet deposition at several locations in Europe was stressed (Lövblad *et al.*, 1993). The purposes of such a deposition monitoring network should be:

- long-term measurements of dry and wet deposition of air pollution over several types of receptors under different pollution climates;
- identification of sites and ecosystems at risk;
- testing of existing long-range transport models;
- support of European policy on pollution control.
- trend analysis and monitoring of effectiveness of emission reduction plans, i.e. evaluation of critical load exceedances.
- improvements of parametrisations currently used in long range transport models.

It was recommended during the workshop to equip several locations in Europe with intensive deposition monitoring methods. Such a network will be an extension of existing monitoring programmes such as that run by EMEP. The intensive monitoring locations should be selected based on pollution climates and type of vegetation, common in Europe.

The *objective* of the project reported here was to develop a deposition monitoring method for air pollution of Europe. This method will be used to extend existing European monitoring networks of air concentrations to provide deposition inputs on an ecosystem scale.

A monitoring station for atmospheric deposition was designed and constructed using existing methods. Three such stations were applied in a pilot project for a year on three sites (Speulder forest in The Netherlands, Auchencorth in Scotland and Melpitz in Germany) in different regions in Europe to estimate local inputs and to validate deposition models which are currently used or developed to estimate ecosystem specific deposition in Europe.

The components considered in this project are the acidifying components: sulphur dioxide (SO_2), particulate sulphate (SO_4), nitrogen oxides (NO and NO_2), nitrous acid (HNO_2), nitric acid (HNO_3), particulate nitrate (NO_3), ammonia (NH_3), particulate ammonium (NH_4), and the heavy metals: lead (Pb), cadmium (Cd), arsenic (As), mercury (Hg), chrome (Cr), zinc (Zn), copper (Cu) and nickel (Ni). The methods developed in this pilot project to estimate total deposition will be suitable also for other components, such as persistent organic compounds.

In this report the main results of the project are presented. The theoretical aspects and experimental set-up for the deposition monitoring methods are described in chapter 2. In chapter 3, the results of the measurements are described for the three sites. For each site, a description of the site, an overview of the successful measurements and the deposition parameters will be described. In chapter 4, a description of the deposition model will be given and deposition maps for the areas surrounding the three sites will be described. In chapter 5, a proposal for a European deposition monitoring strategy will be described.

2. Theoretical background

After transport and possible transformations, pollutants eventually deposit on a surface by wet, dry, or cloud/fog water deposition. Wet deposition is the process by which atmospheric pollutants are delivered to the earth's surface by rain, hail or snow. Dry deposition is the process where gases and particles are deposited directly from the atmosphere onto vegetation, soil or other surfaces without the hydrometer as medium. Cloud and fog water deposition is the process where cloud and fog water droplets are directly intercepted by the earth's surface. This deposition process is often referred to as 'occult' deposition. In this chapter, deposition processes will be explained and different measurement techniques used for deposition monitoring will be described.

2.1 Deposition processes

2.1.1 Wet deposition

Wet scavenging is defined as the natural process by which atmospheric pollutants are attached to and dissolved in cloud and precipitation droplets (or particles), and as a result of this are transported to the earth's surface. The amount of compounds thus received per unit of surface area and per unit of time is defined as wet deposition flux. The amount of pollutant wet deposition is strongly dependent on the amount of rain and the location of the receptor with respect to sources. Wet deposition patterns depend on the topography (Fowler *et al.* 1991). At high altitudes an enhancement of wet deposition may occur because of increased aerosol scavenging due to so-called seeder-feeder effects (Fowler *et al.*, 1988). Seeder-feeder scavenging results from the incorporation of particles into orographic clouds above hills and the scavenging of the hill cloud droplets by rain droplets falling from a higher level cloud. Such effects are found to be pronounced in north-west Europe and western Scandinavia. Over the central and southern European uplands, where convective processes dominate, the above effect is less important (Fowler *et al.*, 1992; Lövblad and Erisman, 1992). The characteristics of the receptor area do not have much influence on the wet deposition. However, in areas with large roughness elements (like forests or urban areas), the catchment of small droplets could be expected to be possibly more efficient than it would over smooth homogeneous surfaces. This might be due either to increased turbulence or the kinds of scavenging effects associated with forest edges, for example.

2.1.2 Dry deposition

The dry deposition of gases and particles from the atmosphere to a receptor surface is governed by the concentration in air and by turbulent transport processes in the boundary layer, as well as by the chemical and physical nature of the depositing species and the capability of the surface to capture or absorb gases and particles. The transport of gases and particles from the atmosphere to close to the receptor surface is governed by the level of atmospheric turbulence, generated by both wind shear and buoyancy. The higher the level of atmospheric turbulence, the more efficiently gases and particles are transported to a given

receptor surface. Given a constant sink strength for a particular pollutant of interest, the concentration gradients above the receptor will vary according to the intensity of atmospheric turbulence. A well-mixed unstable boundary layer leads to relatively small concentration gradients and to low resistance to vertical transport. For a boundary layer with near neutral stability, buoyancy has essentially no influence on the level of turbulence. Stable stratified boundary layers are associated with much larger gradients, because vertical motions are suppressed.

Generally, two layers can be distinguished in the boundary layer for transport of pollutants to the receptor: the fully turbulent layer and the quasi-laminar layer. The quasi-laminar layer is introduced to quantify the way in which pollutant transfer differs from momentum transfer in the immediate vicinity of the surface (Hicks *et al.*, 1987). In this layer, the transport to the receptor surface is dominated by molecular diffusion. Once at the surface, the chemical, biological and physical nature of the surface determines the capture or absorbency of the gases and particles. For gases, surface uptake is controlled by the ability of the surface to absorb the specific chemical species. For reactive trace gases, such as HNO_3, molecules are collected immediately upon contact with all surfaces (Huebert and Robert, 1985; Dollard *et al.*, 1986). Less reactive, but soluble, gases, such as SO_2 and NH_3, tend to be taken up through stomata or through the leaf cuticle (Garland, 1977; Schwela, 1977; Fowler, 1984; Duyzer *et al.*, 1987; Grennfelt, 1987). These gases can also be absorbed in water layers at the leaf surface, or at the soil (Fowler *et al.*, 1991; Hicks *et al.*, 1989). The chemical composition of the surface is important for snow, ice and water (Hicks *et al.*, 1989; Erisman *et al.*, 1994).

2.1.3 Cloud and fog deposition and dew

Vegetation may intercept cloud and fog droplets or directly collect water vapour that forms dew. Hill cloud and lowland fog droplets generally have diameters between 3 and 50 μm, and can be efficiently captured by vegetation (Fowler, 1984; Fowler *et al.*, 1989; Hicks *et al.*, 1989; Fowler *et al.*, 1992). Deposition of such droplets occurs similar to that of coarse particles and thus is only limited by the resistance to aerodynamic transfer (Dollard *et al.*, 1983; Gallagher *et al.*, 1988). As the droplets are rather small, their sedimentation rate is slow, but impaction and interception by foliage, and other obstacles in their path can be effective. Cloud droplets usually contain higher concentrations of pollutants than are found in rain, and cloud water deposition may exceed annual precipitation, especially at high elevation sites (Lovett, 1988). In Europe, at altitudes higher than 400 m above sea level, low clouds are present between 500 and 2000 h per year (Fowler *et al.*, 1991). Cloud water deposition might be a significant input mechanism for such regions in Europe. The major limitation for estimating inputs by cloud and fog droplet deposition is the lack of information on cloud and fog water composition, and on liquid water content. In general, concentrations of SO_4^{2-}, NO_3^- and NH_4^+ in cloud and fog droplets are found to be 10-50 times those in precipitation.

2.2 Measuring methods and flux estimation

2.2.1 Wet deposition

Wet deposition is measured by placing samplers in the open field to collect precipitation. Precipitation is collected in bottles for two weeks or a month; after this the sample is analysed for its chemical composition. Wet deposition is the amount of precipitation multiplied by the concentration of the pollutant. In former days, the most commonly used sampler was the bulk or open sampler, which has no provision to exclude dry deposition during dry periods. Dry deposition of gases and particulate matter may therefore influence the chemical composition of precipitation passing the contaminated funnel at the entrance of the sampler (Slanina *et al.*, 1982; Ridder *et al.*, 1984). The use of wet-only samplers, in which the funnel is open to the atmosphere only during precipitation events, is widely recommended. Short exposure periods are also recommended when sample deterioration due to bacterial or chemical action is expected.

Aspects which might influence the composition of the precipitation sample (Buijsman and Erisman, 1988) include:
- transformation of components under the influence of light or enhanced temperature,
- storage conditions or time elapsed before analysis of the samples,
- bird droppings, insects, etc.

Other errors may be introduced by analytical methods and handling of the samples. Usually, these error sources were minimised by using light protected bottles, by minimising the sampling (bi-weekly) and storage periods, and by quality assurance through standardisation in sampling handling and analysis (Schaug *et al.*, 1989; Buijsman, 1989).

2.2.2 Dry deposition

Several methods exist with which dry deposition is estimated, see Fowler and Duyzer (1989) or Erisman and Draaijers (1995) for an overview. Among these methods are surface wash techniques (throughfall measurements, artificial or natural surface accumulation measurements), chamber methods, watershed mass balance methods and micrometeorological methods. Among the methods for measuring dry deposition, micrometeorological methods are the most suitable for determining the dry deposition of many gases (Fowler and Duyzer, 1989), and they are therefore used in this project. The flux to the total system may be determined with these methods, and the relationship between air concentrations, meteorology and the flux is directly established. In a flat homogeneous terrain, the flux measured at a sampling point above the surface within the constant flux layer represents the average vertical flux over the upwind fetch. A constant flux layer is required to make sure that the flux measured above the surface is that at the surface. Several micro-meteorological measuring methods exist for measuring dry deposition. The flux can be derived from measurements of the vertical component of the wind velocity and the gas concentration. The most direct of these methods is the eddy correlation method. With another method, the gradient technique, the flux is derived from measurements of air concentrations at several heights above the receptor surface and from meteorological variables. The principles of the eddy correlation method and gradient technique will be described in this section. Other techniques consist of

Bowen ratio approaches, variance and a variety of so-called conditional sampling methods. The latter are not described in this book; information on these techniques can be found in such references as Businger (1986), Hicks *et al.* (1989), Baldocchi *et al.* (1988) or Fowler and Duyzer (1989)

Eddy correlation method
The vertical flux density F of an entity is given as

$$F = \overline{\omega\rho} \qquad [2.1]$$

where ω is the vertical wind velocity and ρ the density of the entity. This may be considered as the sum of two components, the product of mean vertical wind speed ω and density ρ, and fluctuations about the means of the same quantities ω' and ρ':

$$F = \overline{\omega}\,\overline{\rho} + \overline{\omega'\rho'} \qquad [2.2]$$

where ω' and ρ' are the instantaneous vertical wind velocity and the departure from the mean concentration, respectively (Baldocchi *et al.*, 1988). When ρ represents a pollutant concentration, F is simply the pollutant flux. When ρ is the momentum, F represents the momentum flux, more commonly denoted as the stress τ. The sensible heat flux H is represented as

$$H = \rho_a c_p \overline{\omega\,\theta} \qquad [2.3]$$

where ρ_a is the air density, c_p the specific heat of air and θ the potential air temperature. In the constant flux layer, the eddy correlation method provides direct fluxes from measurements of the co-variance of ω and ρ. In order to measure the contribution of all eddies to the flux, fast sensors are necessary. For meteorological quantities such as momentum or sensible heat fluxes this method has proven to give reliable results (Montheith, 1975; Businger, 1986; Baldocchi *et al.*, 1988; Duyzer and Bosveld, 1988; Fowler and Duyzer, 1989).

When conducting an experiment with the eddy correlation technique, the sampling frequency and the length of the sampling period must be carefully chosen to ensure that the whole spectrum of eddies that contribute to the transfer processes is accounted for. Sampling rates in the order of 5 - 10 Hz are normally required for this method over most surfaces when measurements are made from tower-based systems.

Although the eddy correlation technique provides a direct measurement of the vertical flux for gases and small particles. The requirement for fast responding chemical instruments limits the application of this technique to just a few chemical species. Relatively fast response analysers are available for O_3 and NO_2.

Aerodynamic gradient method
Before the measurements required for the aerodynamic gradient method are described, the basic theory will be summarised. In the turbulent layer, transport of heat, momentum and mass are similar (Thom, 1975). The diffusivity K of a property at any point in a particular fluid medium can be defined as the ratio of the property flux through the medium to its

concentration gradient (in the same direction) at that point. The flux towards or away from the surface is found as the product of this gradient and the diffusivity.
For the momentum flux (τ):

$$\tau = K_m(z)\frac{\partial(\rho u)}{\partial z} \qquad [2.4]$$

For sensible heat flux (H):

$$H = K_h(z)\frac{\partial(\rho_a c_p \theta)}{\partial z} \qquad [2.5]$$

For pollutant mass flux (F):

$$F = K_c(z)\frac{\partial c}{\partial z} \qquad [2.6]$$

where u is the wind speed, z the vertical distance and c the pollutant concentration. Fluxes directed towards the earth are defined positive throughout this report.
The approximate similarity of:

$$K_m \approx K_h \approx K_c \qquad [2.7]$$

appears to be valid in neutral and stable conditions (Thom, 1975; Droppo, 1985; Zeller, 1990). In unstable conditions, experiments showed that the equality of K_h and K_c with K_m does not hold (Droppo, 1985), although K_h and K_c were similar in these conditions too (Hicks *et al.* 1989; Droppo, 1985; Zeller *et al.*, 1989).

The shearing stress, or momentum flux τ, is defined as the drag force per unit area of a horizontal plane caused by horizontal air motion (Thom, 1975). τ is related to the air density and the effectiveness of vertical turbulent exchange in the air flow over the surface:

$$\tau = \rho_a u_*^2 \qquad [2.8]$$

where u_* is the 'eddy velocity' or friction velocity associated with the momentum flux is. The term u_* may be defined in terms of gradient theory, such that:

$$u_* = l\frac{\partial u}{\partial z} \qquad [2.9]$$

where l is the mixing length for momentum, or rather the effective eddy size, at level z. The value for l may be given by:

$$l = \frac{\kappa(z-d)}{\phi_m} \qquad [2.10]$$

where κ is the Von Karman constant, established experimentally to be about 0.41 (see discussion in Pasquill and Smith, 1983); ϕ_m is the empirically estimated dimensionless correction for stability effects upon this ratio, while d is the zero displacement height.

The eddy diffusivity K_m may be found from Eqns. 2.4, 2.8, 2.9 and 2.10:

$$K_m = \frac{\kappa(z-d)u_*}{\phi_m} \qquad [2.11]$$

This equation may be used to estimate K_c, given the similarity between K_m, K_h and K_c. For K_c, ϕ_h is used rather than ϕ_m. Thus, given the equality of ϕ_h and ϕ_c:

$$K_c = \frac{\kappa(z-d)u_*}{\phi_h} \qquad [2.12]$$

which may be substituted into the mass flux (Eqn. 2.6), yielding:

$$F = \frac{\kappa(z-d)u_*}{\phi_m}\frac{\partial c}{\partial z} \qquad [2.13]$$

u_* is derived from 2.9 and 2.10:

$$u_* = \frac{\kappa(z-d)}{\phi_m}\frac{\partial u}{\partial z} \qquad [2.14]$$

Similarly, the eddy concentration can be defined as:

$$c_* = \frac{\kappa(z-d)}{\phi_h}\frac{\partial c}{\partial z} \qquad [2.15]$$

and thus the mass flux becomes:

$$F = u_* c_* \qquad [2.16]$$

As a result, the flux of a pollutant may be derived from information on the wind profile, the concentration gradient and the effect of stability. The empirical estimation of ϕ_h for different conditions has been the subject of much investigation (Dyer and Hicks, 1970; Pasquill and Smith, 1983). The stability function is a correction for the departure of the neutral profile. Therefore under neutral conditions $\phi_m=\phi_h=\phi_c=1$. The stability correction is a function of height. Therefore ϕ should be included in the integration of Eqns. (2.14) and (2.15). In the literature, results obtained by Dyer and Hicks (1970) are widely used (e.g. Thom, 1975; Denmead, 1983). Under stable conditions these results are:

$$\phi_m = \phi_h = \phi_c = 1 + 5.2\frac{(z-d)}{L} \qquad [2.17]$$

and under unstable conditions, ϕ_h and ϕ_c are represented by the square of ϕ_m:

$$\phi_m^2 = \phi_h = \phi_c = [1-16\frac{(z-d)}{L}]^{-0.5} \quad [2.18]$$

where L is the Monin Obukhov length used as stability parameter (L>0: stable; L<0: unstable; $|L| \rightarrow \infty$: neutral), given as:

$$L = \frac{-T\rho_a c_p u_*^3}{\kappa g H} \quad [2.19]$$

where T is the absolute temperature and g, the acceleration of gravity. The sensible heat flux H and u_* can be derived from sonic anemometer measurements or calculated from the net radiation using the Priestly-Taylor model parameterised (modified by Holtslag and De Bruin, 1988). This modified model was tested using experiments at a meteorological mast at Cabauw in the centre of the Netherlands. The model was used in subroutines for the calculation of H, L and u_* by Beljaars *et al.* (1987).

Integration of (2.14) and (2.15) between the roughness length z_0 and z, yields:

$$u_* = \frac{\kappa u(z)}{\ln(\frac{z-d}{z_0}) - \psi_m(\frac{z-d}{L}) + \psi_m(\frac{z_0}{L})} \quad [2.20]$$

and:

$$c_* = \frac{\kappa c(z)}{\ln(\frac{z-d}{z_0}) - \psi_h(\frac{z-d}{L}) + \psi_h(\frac{z_0}{L})} \quad [2.21]$$

where

$$\psi_m(\frac{z-d}{L}) = \psi_h(\frac{z-d}{L}) = -5.2\frac{(z-d)}{L} \quad [2.22]$$

for stable conditions and,

$$\psi_m(\frac{z-d}{L}) = 2\ln(\frac{1+x}{2}) + \ln(\frac{1+x^2}{2}) - 2\arctan(x) + \frac{\pi}{2}$$

$$\psi_h(\frac{z-d}{L}) = 2\ln(\frac{1+x^2}{2}) \quad [2.23]$$

$$x = [1-16\frac{(z-d)}{L}]^{0.25}$$

for unstable conditions. $\psi_m((z-d)/L)$ and $\psi_h((z-d)/L)$ are the integrated stability corrections for momentum and heat.

The application of the aerodynamic gradient method is limited by the accuracy and other characteristics, such as the interference of chemical instruments. Concentration differences between two levels in the order of 1 - 5% have to be detected accurately. The noise level of the instrument should therefore be very small (Mennen *et al.*, 1995). To avoid systematic differences, gradients are often determined with the same sensor.

Concentrations at two or more heights within about 10 m above a horizontally homogeneous surface (low vegetation) are used to evaluate a local gradient that is assumed to be representative of the area of interest. Next to the concentration gradient, measurements are made to estimate K_c (Eqn. 2.13) and the stability corrections to estimate the pollutant flux. These measurements usually comprise wind profile measurements, sonic anemometer measurements, or measurements on wind speed, temperature, global radiation and standard deviation of wind direction at one level.

Limitations to the micrometeorological methods
Time-average measurements at a point provide an area-integrated average of the exchange rates between the surface and the atmosphere. The measuring height must be well within the constant flux layer and near to the earth's surface (5 - 10 m). This means that usually only local fluxes can be measured (low measuring heights to meet these demands). Extrapolating these fluxes or derived deposition parameters to larger areas is still a great problem because of varying surface properties and roughness characteristics, and accordingly non-homogeneous turbulent behaviour. Fluxes cannot be derived from measurements with these methods in a complex terrain or near to sources where there is no constant flux layer. Measurements must be made over a terrain with an upwind fetch over a homogeneous surface large enough to establish a fully developed constant flux layer. In addition to fetch requirements, the development of the constant flux layer requires that no sources or sinks exist in the atmosphere above the surface, and that the concentration of the constituent does not vary significantly with time (Baldocchi *et al.*, 1988; Hicks *et al.*, 1987; Businger, 1986; Erisman *et al.*, 1989). Sources or sinks might also be the result of rapid reactions among reactive species between the point of flux measurement and the surface. Such an influence of reactions has been suggested for NH_3 and acidic gases, such as HNO_3 and HCl (Huebert and Robert, 1985; Erisman *et al.*, 1988; Brost *et al.*, 1988; Allen *et al.*, 1989), and has been demonstrated for the photostationary equilibrium between NO, NO_2 and O_3 (Lenschow, 1982; Duyzer, 1991; Wesely *et al.*, 1989; Kramm, 1989).

2.2.3 Cloud and fog water deposition

Several techniques have been applied by which droplet deposition can be separated from wet and dry deposition. Cloud water can be collected by impaction of the droplets on a collection surface (Weathers *et al.*, 1986; Waldman *et al.*, 1982; Mallant and Kos, 1990). Furthermore, estimates of cloud water deposition have been made using throughfall measurements, together with sensors for cloud occurrence and measurements of cloud water amount (Joslin and Wolfe, 1992). Dollard *et al.* (1983) and Gallagher *et al.* (1988) report micrometeorological measurements of cloud water deposition to short vegetation, while Wyers *et al.* (1995) and Vermeulen *et al.* (1994) report similar measurements over the Speulder forest. From these studies, it was found that cloud water deposition rates averaged over the droplet size spectrum

in these measurements are close to the reciprocal of the aerodynamic resistance for momentum.

2.3 *Frameworks for the description of atmosphere - surface exchange*

The dry deposition flux of gases and particles from the atmosphere to a receptor surface is governed by: 1) the concentration in air and turbulent transport processes in the boundary layer; 2) the chemical and physical nature of the depositing species and 3) by the efficiency of the surface to capture or absorb gases and particles.

Resistance analogy for trace gases
A common framework is provided to describe the exchange of a range of gases with very different chemical and physical properties. In this framework, three stages in dry deposition to the surface are distinguished. The most widely used is that of the resistance analogy (Thom, 1975, Chamberlain, 1966; Garland, 1977; Fowler, 1978). The analogy of trace gas fluxes to a current in an electrical circuit is described by Ohm's law (resistance = potential difference/current). Assuming one-dimensional transfer over a homogeneous surface, the total resistance R_t is defined by:

$$R_t(z) = \frac{c(z_1) - c(z_2)}{F} \qquad [2.24]$$

where z_1 and z_2 are two heights above the surface. The flux F is taken as negative when directed towards the surface. The absorbing surface is often assumed to have zero surface concentration; the flux is therefore viewed as being linearly dependent on atmospheric concentration. In this case, if z_2 is considered to be the notional height of the absorbing surface (z_0+d), the total resistance from a height z to the surface becomes:

$$R_t(z) = -\frac{c(z)}{F} = \frac{1}{V_d} \qquad [2.25]$$

In effect, (z-d) is the height above the aerodynamic ground level. The turbulent boundary layer flow over a receptor surface of uniform height h behaves as if the vertically distributed elements of the receptor were located at a certain distance d from the ground. The bulk effectiveness as a momentum absorber is specified by z_0, while the parameter d can be considered to indicate the mean level at which momentum is absorbed by the individual elements of the receptor surface. This concept is valid for the momentum flux, as the wind speed decreases to zero at the receptor surface. For mass transport, however, this does not hold, as surface concentrations might not be zero for gases (or particles). However, the concept of z_0 is used for mass transport as well (Thom, 1975). Values for roughness length, z_0, and displacement height, d, can be obtained from tables with landscape classifications, e.g. those proposed by Davenport (1960), revised by Wieringa (1992) or Voldner *et al.* (1986).

The inverse of the total resistance is the deposition velocity (V_d). The latter, providing a measure of conductivity of the atmosphere - surface combination for the gas, is widely used to

parametrise gas uptake at the ground surface (Wesely and Hicks, 1977; Hicks *et al.*, 1989; Fowler, 1984; Fowler *et al.*, 1989; Wesely, 1989). V_d is the inverse of three resistances:

$$V_d(z) = \frac{1}{R_a(z) + R_b + R_c} \qquad [2.26]$$

The three resistances represent the three stages of transport: the aerodynamic resistance R_a for the turbulent layer, the laminar layer resistance R_b for the quasi-laminar layer, and the surface or canopy resistance R_c for the receptor itself. The atmospheric resistance to transport of gases across the constant flux layer is assumed to be similar to that of heat (see e.g. Hicks *et al.*, 1989 for an overview). R_a depends mainly on the local atmospheric turbulence intensities. Turbulence may be generated through mechanical forces of friction with the underlying surface (forced convection) or through surface heating (buoyancy or free convection). Unless wind speeds are very low, free convection is small compared to mechanical turbulence. In the case of rough (uneven) surfaces like forest canopies, the aerodynamic characteristics of the canopy and the wind speed control the generation of turbulence to a large extent and regulate vertical mixing of pollutant-laden air layers in the vicinity of the canopy. In this study R_a is approximated following the procedures used by Garland (1978):

$$R_a(z) = \frac{1}{\kappa u_*}\left[\ln\left(\frac{z-d}{z_0}\right) - \psi_h\left(\frac{z-d}{L}\right) + \psi_h\left(\frac{z_0}{L}\right)\right] \qquad [2.27]$$

The second atmospheric resistance component R_b is associated with transfer through the quasi-laminar layer in contact with the surface. R_b quantifies the way in which pollutant or heat transfer differs from momentum transfer in the immediate vicinity of the surface. R_b depends on both turbulence characteristics and the molecular diffusion of the gas considered (Thom, 1975; Garrat and Hicks, 1973; Erisman, 1992). Transport of a pollutant gas through the quasi-laminar layer by molecular diffusion depends on the thickness of the layer, the concentration gradient over the layer, and on a diffusion constant which, in turn, depends on the radius of the gas molecule considered and on temperature. Although a great deal is known about quasi-laminar layer transport to artificial surfaces, the complexity of vegetation limits the accuracy with which the magnitude of this transport mechanism can be estimated in the field. The thickness of the quasi-laminar boundary layer, for example, is found to depend on size, shape and orientation of the receptor surface, and on wind speed. Real-life events like 'fluttering' of leaves make it extremely difficult to model quasi-laminar boundary layer transport accurately (Chamberlain, 1975). The quasi-laminar layer resistance R_b can be approximated by the formulation presented by Hicks *et al.* (1987):

$$R_b = \frac{2}{\kappa u_*}\left(\frac{Sc}{\mathrm{Pr}}\right)^{\frac{2}{3}} \qquad [2.28]$$

where Sc and Pr are the Schmidt and Prandtl numbers, respectively. Pr is 0.72 and Sc is defined as: $Sc = \upsilon/D_i$, with υ the kinematic viscosity of air (0.15 $cm^2\ s^{-1}$) and D_i the molecular diffusivity of pollutant i, and thus component specific. The Schmidt and Prandtl number correction in Eqn. 2.28 is listed in Table 1 for different gases. Usually R_b values are of less importance than values of R_a and R_c, so Eqn. 2.28 can be considered as appropriate. Over very rough surfaces such as forest canopies, however, R_a may be small and the reliability of the R_b

estimate becomes important. This is especially the case for trace gases with a small or zero surface resistance.

The surface or canopy resistance, R_c, is the most difficult of the three resistances to describe. R_c values can in principle be obtained from theoretical considerations based, for instance, on solubility and equilibrium calculations in combination with simulations of vegetation specific processes, such as accumulation, transfer processes through stomata, mesophyll and cuticles, absorption, etc. (Baldocchi *et al.*, 1987; Wesely, 1989). Many theoretical approaches are, however, hard to validate by measurements because of the complexity of the processes involved. R_c values presented in the literature are primarily based on measurements of V_d. By determining R_a and R_b from the meteorological measurements, R_c can be calculated as the residual resistance using Eqn 2.27. Values of R_c can then be related to surface conditions, time of day, etc., yielding parametrisations. Unfortunately, measurements by existing techniques are still neither accurate nor complete enough to obtain accurate R_c values under most conditions. Furthermore, R_c is usually specific for a given combination of component, type of vegetation and surface conditions; measurements are available for only a limited number of combinations. Bache (1986) demonstrated that in cases of low surface resistances, the R_c values obtained using the resistance analogy are likely to contain aerodynamic factors. In such conditions, the surface and aerodynamic components cannot be fully separated.

Parametrisations of surface resistances derived from measurements and literature are described in Erisman *et al.* (1994). These have been used here and are summarised in Appendix A.

Table 1. Schmidt and Prandtl number correction for several gases (Hicks et al., 1987).

Component	$(Sc/Pr)^{2/3}$
SO_2	1.34
NO	1.14
NO_2	1.19
HNO_3	1.34
NH_3	0.87
HNO_2	1.24
HCl	1.14
H_2O	0.87
O_3	1.14

Particles

The resistance analogy is not used for particles. Transport from the free atmosphere to the receptor surface is more-or-less similar to gas transport. However, transport processes through the quasi-laminar layer differ considerably between gases and particles. Whereas gases are transported primarily through molecular diffusion, particle transport and deposition basically take place through sedimentation, interception, impaction and/or Brownian diffusion. *Sedimentation* under the influence of gravity is especially significant for receptor surfaces with horizontally oriented parts. *Interception* occurs if particles moving in the mean air motion pass sufficiently close to an obstacle to collide with it. Like interception, *impaction* occurs when there are changes in the direction of airflow, but unlike interception a particle subject to impaction leaves the air streamline and crosses the laminar boundary layer with inertial energy imparted from the mean airflow. The driving force for *Brownian diffusion*

transport is the random thermal energy of molecules. Transport is a function of atmospheric conditions, characteristics of the depositing contaminant and the magnitude of the concentration gradient over the quasi-laminar layer (Davidson and Wu, 1990).

Which type of transport process dominates is largely controlled by the size distribution of the particles (Chamberlain, 1966; Sehmel, 1980; Slinn, 1982). The deposition of particles with mass median diameter (*MMD*) near 0.1-1.0 μm is the least efficient. Deposition of particles falling in this *MMD* range is very much affected by turbulent transfer from the free atmosphere to the receptor surface and, therefore, depends heavily on wind speed and the aerodynamic roughness of the receptor surface (Slinn, 1982). Deposition velocity for particles to low vegetation with a diameter in this range can be obtained from parametrisations on u_* (Wesely *et al.*, 1989; Erisman *et al.*, 1994). Particles with *MMD*s smaller than 0.1 μm deposit through Brownian diffusion, which efficiency is inversely related to particle size (Fowler, 1980). For particles with *MMD*s between 1 and 10 μm, the deposition velocity increases sharply with the *MMD*. These particles deposit mainly through impaction and/or interception. Here we see relatively efficient removal processes, which depend to a large extent on wind speed and aerodynamic characteristics of the receptor surface. This determines transport from the free atmosphere to the receptor surface. The processes also depend on in-canopy wind speeds controlling inertial impaction through quasi-laminar boundary layers (Thorne *et al.*, 1982). For particles with *MMD*s larger than 10 μm, turbulent transfer is less important and sedimentation is the main deposition process. Bounce-off or blow-off effects may be important for such large particles (Slinn, 1982; Wu *et al.*, 1992). Sticky or hairy surfaces limit these effects considerably. Parametrisations of the particle V_d used in this project are summarised in Appendix A.

2.4 Dry deposition monitoring methods used in this project

The selected monitoring methods and concentration measuring equipment, and developed software has been extensively tested in the field. During this test, performance and quality of measurements were evaluated. Furthermore, individual operational methods have been implemented in one deposition monitoring station. After the field test, three monitoring stations were produced, tested and stationed at three different locations in Europe (the Netherlands, UK and former East-Germany). During 1995 continuous measurements have been made. The monitoring equipment, the operational procedures and measuring and calibration protocols are described extensively in the attached report (Duyzer *et al.*, 1996). The three sites, data collection and measurements are extensively described in the attached reports for the individual sites (Fowler *et al.*, 1996; Erisman *et al.*, 1996 and Spindler and Grüner, 1996). Here only an overview of the methods is presented.

2.4.1 Wet deposition and Cloud/fog deposition

In this project, total deposition of acidifying components and heavy metals has been estimated at each site from wet and dry deposition measurements. Wet deposition has been measured fortnightly using a wet-only sampler. The precipitation collector for wet-only measurements was provided by van Essen Instruments of The Netherlands. The collection interval was one week. The samples are split in the lab; one sample is used for measuring acidifying

components, while the other is used for measuring heavy metals. All major anions and cations were analysed by ion chromatography. Heavy metals were send to ECN and analysed.

The fog sampler system from KEMA in The Netherlands was used to measure both the frequency and the chemical composition of fog at the site. Sequential fog samples were analysed in the lab with the same methods for the precipitation samples.

2.4.2 Dry deposition

Dry deposition of three gases (SO_2, NO_x and NH_3) has been measured semi-continuously using the aerodynamic gradient technique. SO_2 concentration gradients have been measured at 4 heights above the surface (three at Auchencorth Moss) using an UV pulsed-fluorescence monitor, a second monitor is used to measure continuously the concentration at the highest level; a change in SO_2 concentration during a measuring cycle can thus be detected and corrected for (Erisman *et al.*, 1993; Mennen *et al.*, 1993). The same measuring method is used for NO_x, concentrations have been measured with a chemiluminescent monitor (Duyzer *et al.*, 1991). For NH_3, gradients have been measured using three continuous-flow denuders (Wyers *et al.*, 1993). Meteorological measurements were made with a sonic anemometer and the Bowen ratio method, as described in Duyzer *et al.*, (1996). A method to estimate annual average dry deposition fluxes was developed by Erisman *et al.* (1993a). Although the aim of the project is to monitor annual average dry deposition fluxes, we do not monitor fluxes, but we rather derive them from monitored data. Continuous measurement of the fluxes using the gradient method is not possible because several theoretical demands have to be fulfilled before application of the theory, such as: ideal fetch, wind speeds above 1 m/s, stationarity, concentration measurements well above the detection limit of monitors, etc. (see previous sections). Only gradients, which fulfil theoretical demands are therefore selected from the total dataset. Normally, no more than 40 to 60% of the data is left after selection. To obtain annual averages from these data, there are two possibilities: *i)* take the 40-60% of selected data and assume that they are representative for a whole year, i.e. no systematic bias is introduced by the selection procedure; *ii)* take the selected data and test or derive parametrisations of the surface resistance with these data, apply the parametrisations to the rejected data using the inferential technique (Hicks *et al.*, 1987; Erisman *et al.*, 1994a) and extend the selected dataset with fluxes obtained with this technique. With the second method, it is assumed that the tested parametrisations are also valid for the circumstances found during the rejected hours. In fact, method *i)* assumes that the frequency distribution of all parameters (c, c_*, u, etc.) for the selected periods are equal to those during the year, while in method *ii)* this assumption only regards the parameters relevant for the parametrisation (rh, T, Q, etc.). The latter is in general more valid than the first. For instance, the assumption cannot be valid for c, since periods with low concentrations are rejected. The second method has been applied for several datasets in the Netherlands (Erisman and Draaijers, 1995) and has proved to be reliable. This method is therefore applied here.

The quality of the annual deposition estimate depends on the site characteristics and the quality of the measurements (selection) and of the surface resistance parametrisation. The surface resistance parametrisation is based on literature values and experimental data obtained at several experiments in Europe (Erisman *et al.*, 1994, see Appendix A) and was tested using the current (selected) data. Through this project, improvements to the existing

parametrisations have been made. The surface resistance parametrisation was available to all LIFE project participants as a FORTRAN subroutine which uses general meteorological data derived from measurements as (selected) input values. In this way areas were identified where development is needed. The resistance analogy and surface resistance parametrisation are summarised in Appendix A. These parametrisations are used together with concentration and meteorological measurements to infer dry deposition of other gases (Hicks *et al.*, 1987).

The concentration measurements of these gases and aerosol components have been made using existing methods. Aerosols were measured using a Partisol 2000 provided by Ruppert and Patashnick Company Incorporated, USA. The instrument provided measurements of the PM 2.5 particles and the PM 10 particles, and was operated on a weekly basis to provide a daytime value and a night-time value for each of the two size fractions. The filters including blanks were pre-weighted and were then divided into sections and analysed by ion chromatography for anions and cations and for heavy metals by ECN in The Netherlands. The batch denuder of the annular type provided hourly averaged concentration measurements of HNO_2, HNO_3 and HCl. The denuder was operated one day per week to provide both diurnal and seasonal concentration patterns for these gases. These measurements were obtained at a single height.

3. Overview of the results for the three monitoring sites

In this chapter the results of the one year of monitoring are summarised. Because of technical problems and/or late implementation of (parts) of the equipment, the common monitoring period for all three sites range from 1-2-1995 to 1-12-1995. Averages were extrapolated to annual averages. It is expected that the annual deposition is not influenced to a large extend by not taking the winter month into account. The activities and monitoring results are extensively described in Fowler *et al.* (1996) for Auchencorth, Scotland; in Spindler and Grüner (1996) for Melpitz, Germany, and in Erisman *et al.* (1996) for Speulder forest, The Netherlands. For each site, a site description will be given followed by the result description for the concentration measurements, dry deposition fluxes, wet deposition, cloud/fog deposition and total deposition. In a separate section of this chapter, the results for the three sites will be compared in a synthesis.

3.1 Auchencorth Moss

3.1.1 Site description

The site selected for a moderately high rainfall, low temperature regime in north western Europe was an open moorland some 10 km south east of Edinburgh, called Auchencorth Moss (see Figure 1Figure 1). This site was selected because of its very good fetch, needed for obtaining good flux measurements under remote conditions. The site was provided with calibration facilities, mains electrical power and was reasonably accessible even though it was a moorland station. The instrumentation was set up in a way that provided unattended operation for several days. The placement of instrumentation is shown in Figure 2.

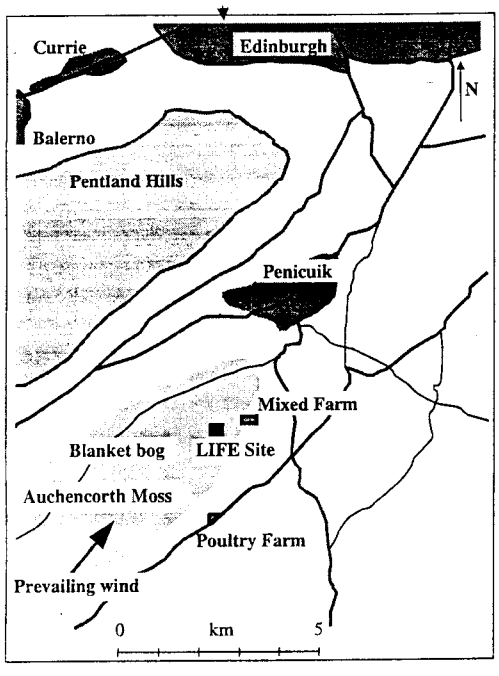

Figure 1. Location of the measurement site, Auchencorth Moss (Southern Scotland).

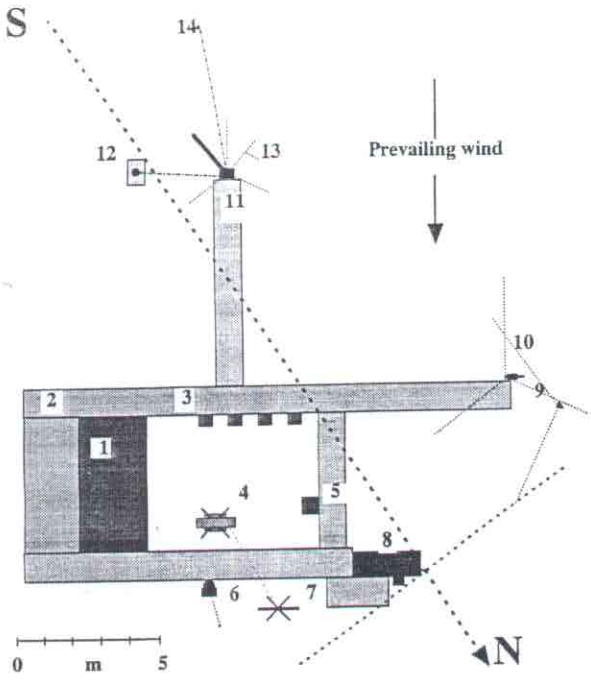

Key:

1	Cabin; $SO_2/NO_x/O_3$ analysers and data acquisition system
2	Board walk
3	Aerosol sampler (Partisol 2000, Ruppert & Pataschnick Co)
4	Fog & cloudwater collector (KEMA)
5	HCl, HNO3 & HNO2 Batch Denuder (ECN)
6	Wet-only precipitation collector (Van Essen Instruments bv)
7	Fog detector (KEMA)
8	Ammonia wet annular denuder gradient system (ECN)
9	Sonic (Solent)
10	SO_2, NO_x & O_3 gradient air intakes
11	Bowen ratio system and global radiometer (Campbell Sc.)
12	Tipping bucket precipitation collector (Campbell Sc.)
13	Soil heat flux plates (Campbell Sc.)
14	Net radiometer (Campbell Sc.)

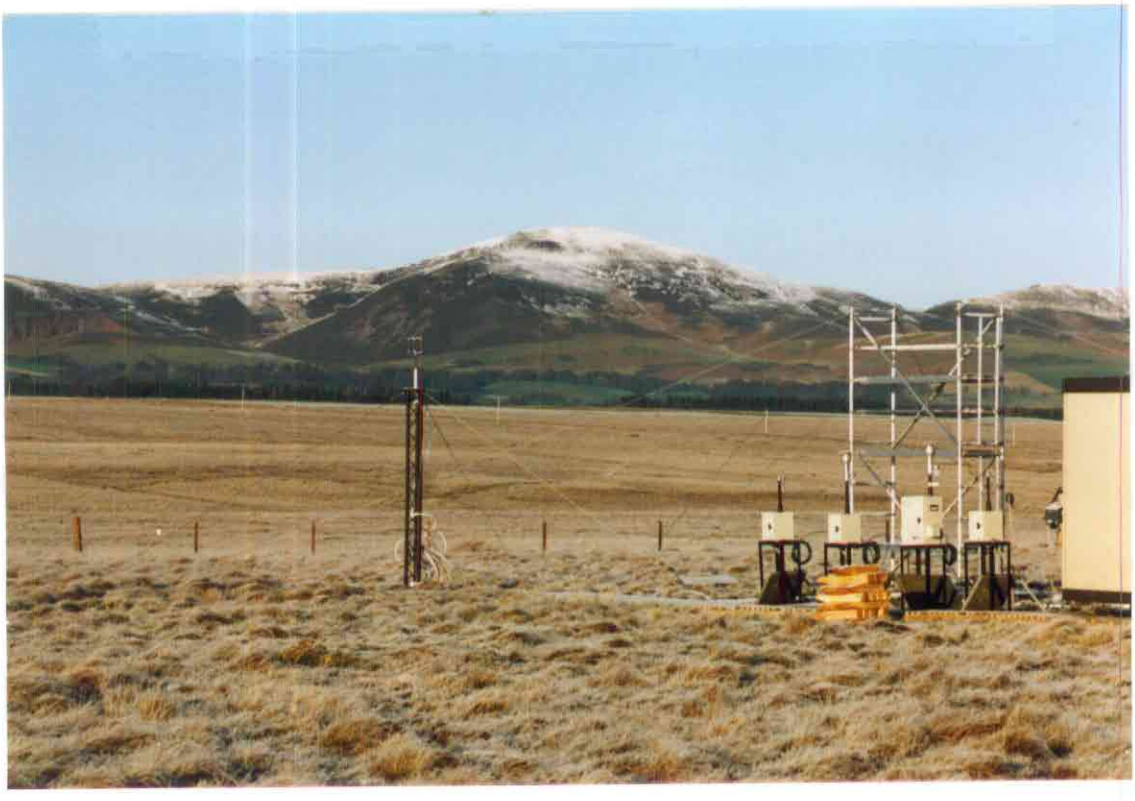

Figure 2. Site diagram of Auchencorth Moss and instrumentation.

3.1.2 Concentrations and meteorological parameters

The concentrations conceal considerable variability in the directional dependence of the concentrations. Figure 3 shows the wind sector dependence of SO2 concentrations. One major source can be identified on a bearing of 310° from the measurement site. This source is a major refinery some 50 km distant. Three other significant sources lie on bearings of 20, 100 and 130°. Concentrations are very small in the south west sector. This is the sector from which winds are blowing most of the time (Figure 5). In the case of NH_3 there are two major sources that contribute to the concentrations measured at this site (Figure 3) The first one is situated south from the site and is a large poultry farm about 3.5 km distant. The other, a much smaller farm is situated closer to the site in south easterly direction. For all other sectors the average concentration is below 1 μg m^{-3}. The sector dependence of NO concentrations identifies three major sources (Figure 4). Those to the north east on a bearing of approximately 30° and those to the west on a bearing of about 250° and again as a source at about 310° which is almost certainly the same as the large SO_2 source. Considering ozone, the wind sector dependence shows almost constant concentrations, with a significant depletion at 10 and 120°, associated with local sources of nitrogen oxide. The winds are almost always blowing from south west to north east, or the other way around, because of the valley and surrounding hills. The south west direction is more frequent than the north east (Figure 5). Wind speeds are highest during south westerly winds (Figure 5).

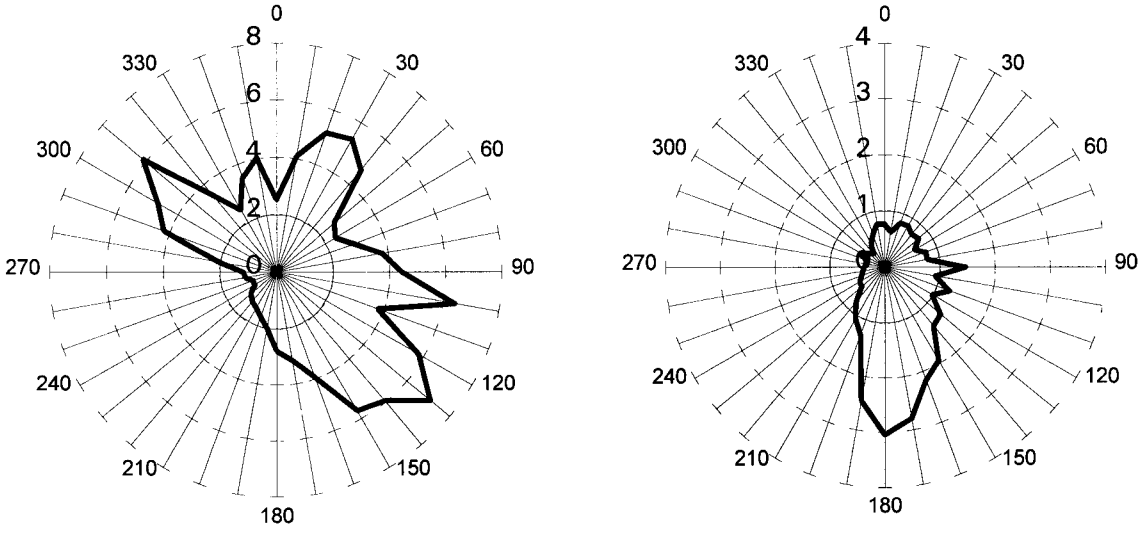

Figure 3. Average SO_2 and NH_3 concentration (μg m^{-3}) at 36 m per wind direction sector of 10°.

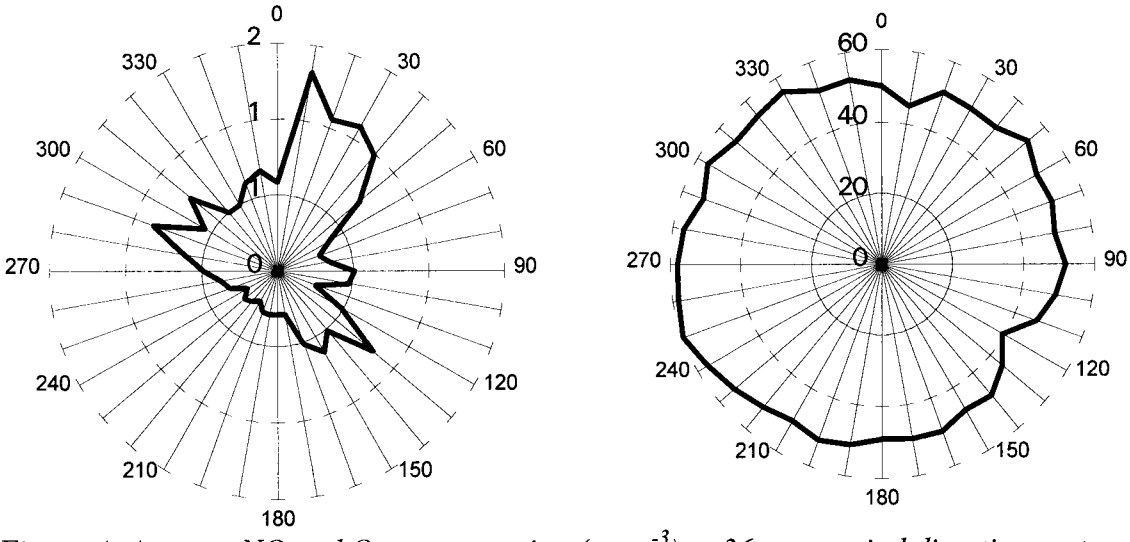

Figure 4. Average NO and O_3 concentration ($\mu g\ m^{-3}$) at 36 m per wind direction sector of 10^o.

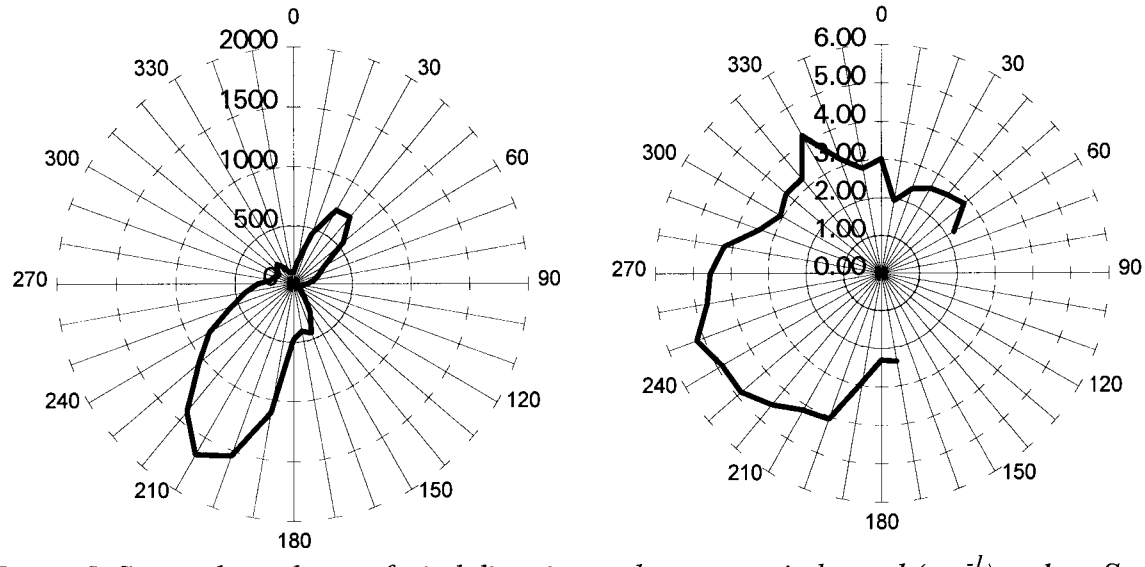

Figure 5. Sector dependence of wind direction and average wind speed ($m\ s^{-1}$) at 1 m. Sectors without wind speed values represent wind directions with poor fetch.

Diurnal variations

Diurnal variations are available for SO_2, NH_3, NO_x, O_3, HNO_2, HNO_3 and HCl, these are shown in Figure 6. The aerosol concentrations were measured as daytime and night-time averages. There is a distinct difference between the different gases. HNO_2 shows a minimum in the afternoon, while the other gases show minimum values at night, except for NO_2 showing an early morning minimum. For HNO_2 the diurnal cycle is governed by photochemical destruction during daytime, and for NO_2 photochemical formation during the afternoon. For NH_3 there is no distinct diurnal variations, the early morning peaks are probably the result of a build-up of concentration during stable conditions. SO_2 and O_3 show diurnal variations with highest concentrations during the afternoon.

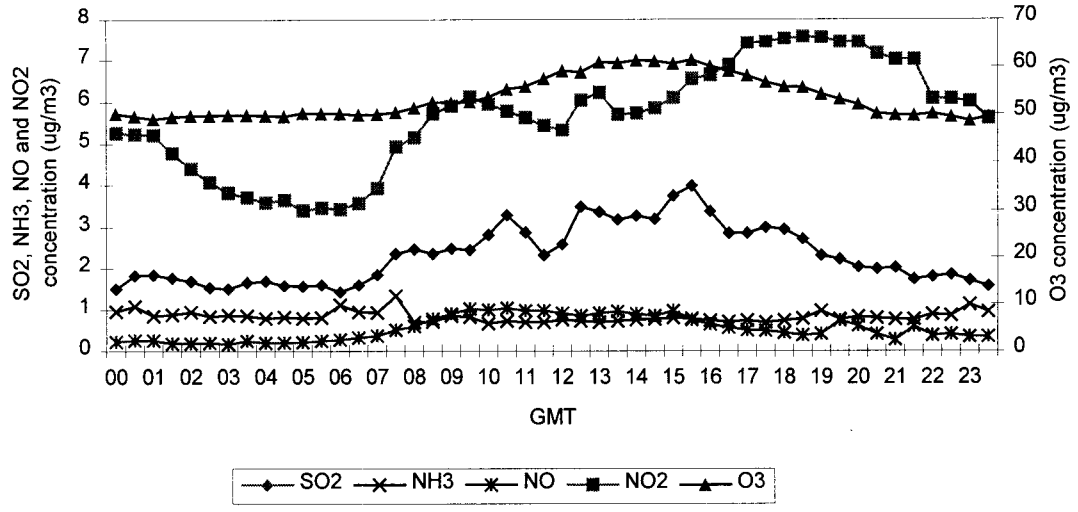

Figure 6. Diurnal variation of gases measured over Auchencorth Moss at 1 m (μg m^{-3}).

Annual average concentrations

Annual average concentrations and their standard deviation are listed in Table 2. Concentrations show a log-normal distribution, median values are lower than averages. Concentrations in aerosol are dominated by NH_4^+, NO_3^- and SO_4^{2-}. Aerosol SO_4^{2-} and NO_3 are almost completely bound to NH_4. Concentrations of Na^+ , Ca^{2+} and Mg^{2+} are higher in the larger particles, as can be expected from the sources such as sea salt and wind blown dust (e.g. Milford and Davidson, 1985; Draaijers *et al.*, 1996). All other aerosols are mostly found in the smaller fractions. Heavy metal concentrations are generally small compared to the other particle concentrations, and also to the detection limits.

Table 2. Annual concentrations measured at Auchencorth Moss (1 m) in 1995 (μg m^{-3}).

Component	MMD (μm)	Average	Standard deviation	No. half hours	Min	Max	Median
SO_4-S	2.5	0.550	0.415	52	0.122	2.379	0.420
	10.0	0.097	0.087	38	0.006	0.386	0.070
SO_2		2.530	5.720	17382	0.001	122.434	0.880
NH_4-N	2.5	0.633	0.498	52	0.020	2.768	0.526
	10.0	0.075	0.048	34	0.002	0.196	0.068
NH_3		1.020	1.850	10462	0.002	27.778	0.500
NO		0.440	1.910	17300	0.004	60.792	0.120
NO_2		6.010	7.040	17069	0.001	143.579	3.590
O_3		52.460	18.560	15789	1.002	359.369	53.380
NO_3-N	2.5	0.197	0.150	52	0.037	0.627	0.149
	10.0	0.087	0.077	45	0.001	0.381	0.065
HNO_3-N		0.077	0.118	855	0.047	0.055	0.042
HNO_2-N		0.022	0.027	856	0.032	0.050	0.015
Cl	2.5	0.338	0.259	51	0.011	1.416	0.306
	10.0	0.567	0.390	47	0.037	1.790	0.548
HCl-Cl		0.171	0.294	855	0.134	0.270	0.111
Na	2.5	0.188	0.100	51	0.012	0.407	0.158
	10.0	0.394	0.209	50	0.087	0.957	0.336
Ca	2.5	0.046	0.081	50	0.007	0.553	0.026
	10.0	0.051	0.059	45	0.002	0.383	0.035
K	2.5	0.043	0.018	44	0.018	0.103	0.040
	10.0	0.023	0.013	40	0.002	0.046	0.020
Mg	2.5	0.031	0.017	51	0.002	0.061	0.028
	10.0	0.044	0.023	50	0.008	0.114	0.040
Zn *	2.5	5.976	3.042	52	0.450	10.817	5.618
	10.0	4.554	5.019	38	0.192	16.476	2.771
Pb *	2.5	8.419	4.894	47	3.164	20.250	6.523
	10.0	3.798	5.003	32	0.267	14.111	1.150
Cd *	2.5	0.060	0.007	42	0.043	0.071	0.060
	10.0	0.068	0.054	14	0.001	0.126	0.090
Cu *	2.5	0.230	0.202	47	0.055	0.706	0.144
	10.0	0.478	0.356	50	0.000	1.291	0.321
Ni *	2.5	0.222	0.101	47	0.115	0.416	0.183
	10.0	0.888	1.866	30	0.000	5.554	0.170
Cr *	2.5	0.157	0.109	47	0.050	0.345	0.093
	10.0	0.197	0.144	26	0.000	0.433	0.232

* in ng m^{-3}

3.1.3 Dry deposition

Annual average dry deposition fluxes for the different compounds were derived by the inferential method or by a combination of fluxes derived from gradients and by inference. For each hour, dry deposition velocities were calculated using the dry deposition parametrisation described in Erisman *et al.* (1994) (chapter 2). This was done for hours where all the necessary meteorological information was available. For SO_2, NH_3 and NOx, these hourly values for the rejected periods were multiplied with the concentrations at the reference height, 1 m, to obtain hourly fluxes. Annual average fluxes and V_d's were calculated using all hours from the rejected and selected datasets. For all other components, modelled dry deposition velocities were combined with measured concentrations to obtain hourly average, and eventually annual average fluxes. Before the dry deposition fluxes are described, first the results for the measured gradients and resulting deposition parameters for SO_2, NH_3, O_3 and NO_x are described.

Gradient measurements
For each half hour the gradients were averaged and c^*, F, V_d, R_a, R_b and R_c were calculated. The dataset thus obtained has to be 'cleaned' by selection of hours during which the theoretical demands for the gradient technique were fulfilled, during which the concentrations were well above the detection limit, and during which there was no loss of necessary measurements due to technical problems. The criteria which were applied are listed in Table 3. In this table the percent of the total number of half hourly averaged measurements which remained after applying the selection criteria is also given. For SO_2 42% survived the selection criteria. Most of the data were rejected as a result of the random error in individually measured concentrations. At concentrations below 0.5 μg m^{-3} the random error was found to be the dominating error in deposition parameters. For NH_3, O_3 and NO_2 more than 50% remained after selection. This can be regarded as very high, especially in view of the very low concentrations at this site.

Table 3. Selection criteria for gradients measured over the Auchencorth Moss and the percentage of measurements left after selection in 1995 (remaining total: 3153 half hours of continuous SO_2 measurements 3479 half hours of NO_x measurements, 3691 half hours of O_3 measurements and; 3577 half hours of continuous NH_3).

Criteria	Percentage of remaining data				
	SO_2	NO	NO_2	O_3	NH_3
Fetch requirements: θ < 60 and θ > 170°	89	89	89	89	88
Extreme stability |L| > 5 m, u > 0.8 m s^{-1} (1 m)	82	82	82	82	80
Detection limits (SO_2 > 0.5 μg m^{-3}, NH_3 > 0.05 μg m^{-3}, NO, NO_2 > 0.1 ppb	60	51	81	82	79
Instrumentation installation, failure, maintenance and calibration	42	31	61	61	57

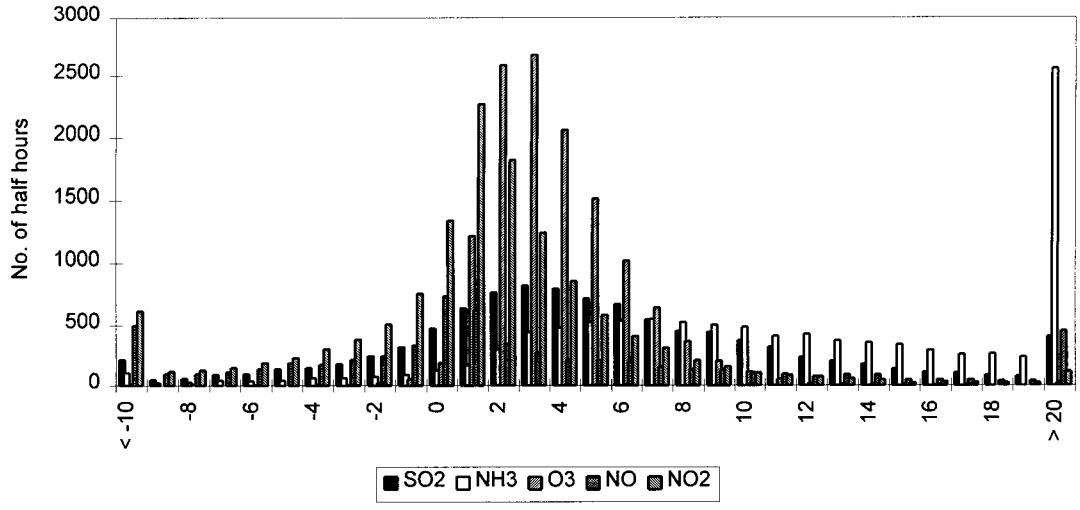

Figure 7. Frequency distribution of Vd values for selected hours (cm s^{-1}).

The frequency distribution of dry deposition velocities for SO_2, NH_3, O_3 and NO_x for the remaining (selected) hours are given in Figure 7. The distributions show log-normal curves, with a normal distribution of random errors. Most negative values for SO_2 are the result of the random error in vertical concentration gradient measurements, although 'real' emission fluxes have been observed after periods with high sulphur loads due to high concentrations, followed by some hours with very low ambient concentrations. The accumulated sulphite concentrations not yet fixed as SO_4^{2-} can be evaporated during these conditions. The same effect, although less strong, is observed for NH_3 in addition to stomatal emissions. If ambient concentrations fall below the compensation points for NH_4^+ concentrations in stomatal apoplast, and/or at the outer leaf surface, emission of NH_3 is expected.

Some statistical parameters for dry deposition velocities in selected periods are given in Table 4. The median values are lower than the averages, as the result of the log-normal distributions. For those components where the median value is about the same as the average, the Vd values are influenced by the random error in the concentration gradients. NH_3 deposition velocities are highest, SO_2 show a surface resistance to uptake at the surface. NO_x show small V_d's, the net-exchange being towards the surface. Microbial emissions from the surface and photo-chemical conversions might have influenced the results. Errors listed in the table are estimated by the methods described in Duyzer *et al.*, 1996). In the table median error values are given, because the distribution of hourly values is log-normal and averages are therefore influenced by a few very high values. The error for selected V_d values is 10% for SO_2, 3% for O_3, 21% for NO, 10% for NO_2 and 14% for NH_3, these values are relatively small, reflecting the high quality of the measurements. The error is largest for NO_x, due to the small gradients (low V_d).

Table 4. Statistical parameters for Vd (m s^{-1}) derived from measurements of selected hours.

Statistic	SO_2	NH_3	O_3	NO	NO_2
Average	0.0045	0.0133	0.0033	0.0012	-0.0002
Standard deviation	0.0088	0.0132	0.0031	0.0155	0.0105
Median	0.0040	0.0105	0.0029	0.0002	0.0009
Min	-0.1495	-0.0525	-0.2183	-0.1990	-0.3990
Max	0.1101	0.1630	0.0349	0.2212	0.1932
Error (median value, %)	10	14	3	21	10

Frequency distributions of R_c for SO_2, NH_3 and NO_x are shown in Figure 8. The median R_c value for SO_2 is 170 s m^{-1}, whereas that for NH_3 is much lower: 30 s m^{-1}. Median values for R_c NO, NO_2 and O_3 are >1000, 1000 and 275 s m^{-1}, respectively. NH_3 is most effectively taken up at the surface, O_3 is taken up with rates higher than the stomatal limited uptake. Even during winter time with a snow covered surface uptake of O_3 was observed. SO_2 is not taken up as effectively as suggested in literature, despite the frequent occurrence of surface wetness. R_c values are, however, smaller than stomatal resistances stressing the importance of external leaf uptake.

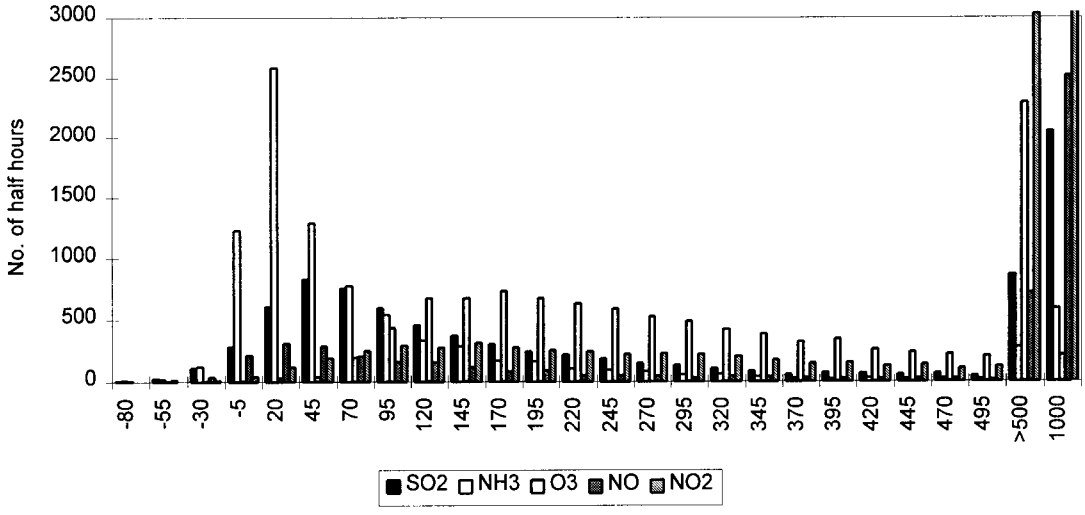

Figure 8. Frequency distribution of Rc values for selected half hours (s m^{-1}). Please note that figures in the 1000 s m-1 class denote emission fluxes and therefore no real canopy resistances

Testing of dry deposition parametrisations

The parametrisations listed in the Appendix were only tested at Auchencorth Moss for SO_2. Figure 9 shows the results of the comparison between modelled and measured values, both averaged per concentration class. Error bars, reflecting the standard deviation per class have not been shown, because these are very large, 300% for measured values and 60% for modelled values, and would therefore disturb the picture. The results show high correlation between the modelled and measured values, with modelled values being systematically higher than measured values.

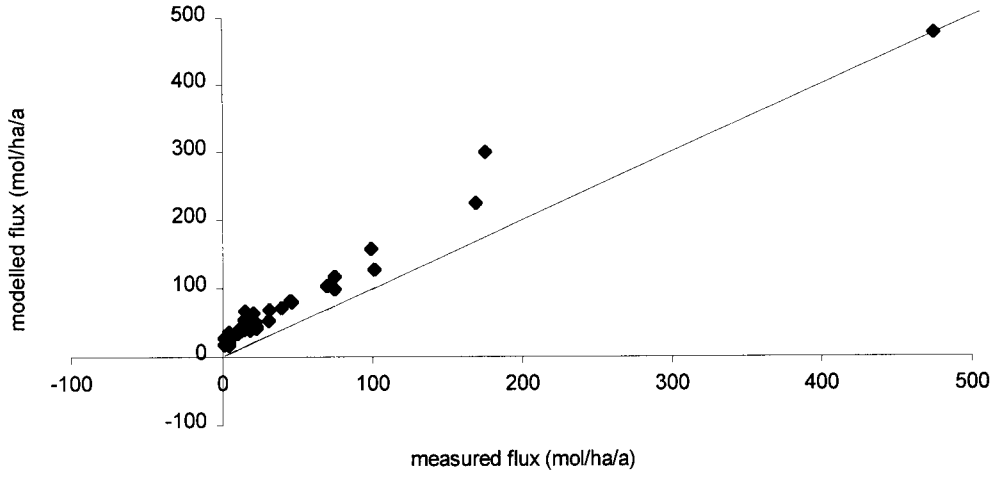

Figure 9. Comparison of modelled SO_2 fluxes and measurements.

Dry deposition velocities
Dry deposition velocities were estimated every half hour using measured quantities and the dry deposition parametrisations outlined in chapter 2. For SO_2, NH_3, O_3 and NO_x only the V_d's for hours which are rejected after selection are calculated using the parametrisation, the other V_d values are from measured concentration gradients.

Diurnal variations
Diurnal variations of V_d for gases and aerosols are displayed in Figure 10 and 11, respectively. As turbulence intensities are higher during daytime than at night, V_d values are higher during daytime. V_d values for HNO_3 are highest (not shown), because it is assumed that uptake rates are entirely governed by turbulent transport, without any surface resistance. O_3 show diurnal variations determined by turbulence and stomatal uptake, although the influence of the surface cannot be neglected. SO_2 uptake is both determined by stomata and external leaf water layers. SO_2 V_d does not show a diurnal variation, probably because of saturation of the external surface with SO_4^{2-}. NO_2 shows lowest values during the afternoon, which is unexpected. This is not the result of atmospheric chemistry, rather than frequent NO_2 production at the surface during daytime. The diurnal variation in NH_3 deposition velocities shows lowest values during daytime as the result of net upward fluxes. These occur when the ambient concentrations fall below stomatal or external leaf surface compensation points.

Model results for aerosols show the same diurnal variations, there is only a difference in magnitude: base cation V_d being highest, followed by NO_3^-, SO_4^{2-} and NH_4^+. This reflects the size distributions of these particles. Indications of the distribution of particle concentration with size can be obtained from the concentration differences for PM 2.5 and 10 as shown in Table 3. Base cation concentrations are higher in the PM 10 classes, whereas e.g. for NH_4^+ concentrations is nearly only found in the PM 2.5 class.

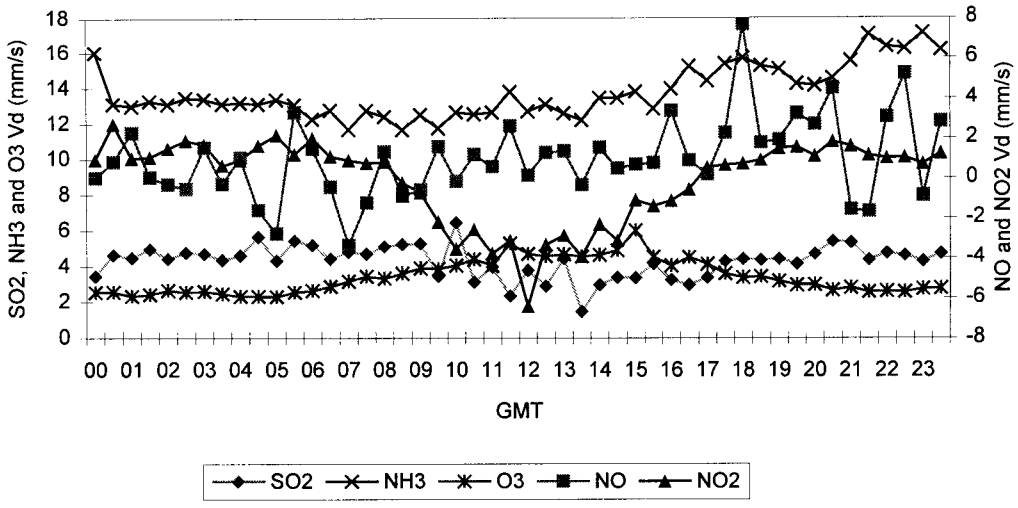

Figure 10. Diurnal variations of gas Vd (mm s^{-1}) at 1 m height.

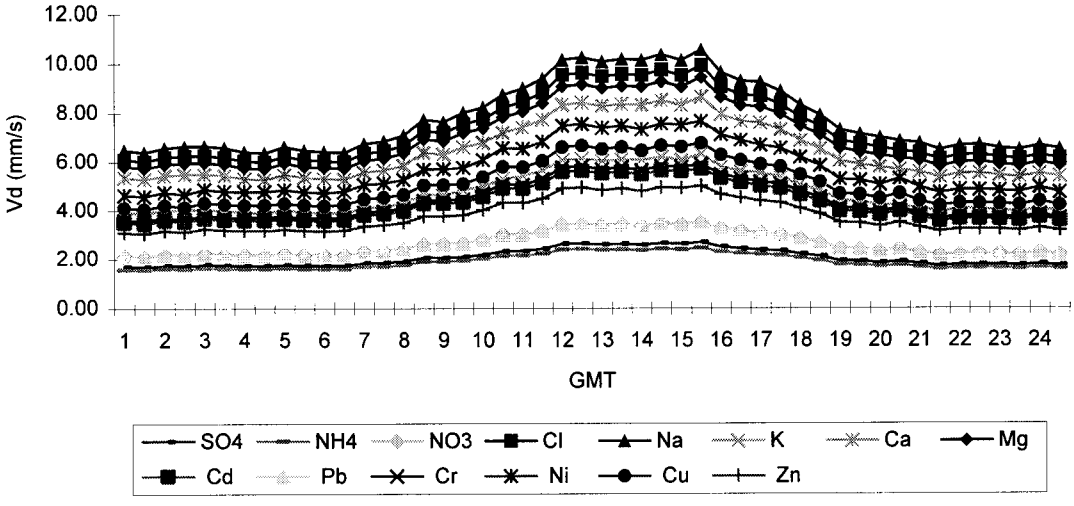

Figure 11. Diurnal variations of aerosol Vd (mm s^{-1}) at 1 m height.

Annual averages

Annual averages, standard deviation and median values of V_d are listed in Table 5. The maximum V_d is about 1.8 m s^{-1}, estimated for HNO_3 and HCl with a negligible surface resistance. NH_3 deposition velocities are quite high, showing only small resistances to uptake. This is mainly the result of the occurrence of surface wetness, which is about 50% of the time.

Table 5. Annual dry deposition velocities estimated from measurements over Auchencorth Moss in 1995 (cm s^{-1}).

Component	MMD	Average	Standard deviation	No. of half hours	Min	Max	Median
SO_4	2.5	0.148	0.049	53	0.032	0.276	0.147
	10.0	0.527	0.248	53	0.123	1.305	0.496
SO_2		0.454	0.884	7409	-14.949	11.011	0.404
NH_4	2.5	0.148	0.049	53	0.032	0.276	0.147
	10.0	0.527	0.248	53	0.123	1.305	0.496
NH_3		1.329	1.316	9081	-5.249	16.300	1.050
NO		0.121	1.546	5383	-19.901	22.124	0.023
NO_2		-0.025	1.047	10735	-39.899	19.324	0.087
O_3		0.330	0.313	10680	-21.832	3.494	0.293
NO_3	2.5	0.148	0.049	53	0.032	0.276	0.147
	10.0	0.527	0.248	53	0.123	1.305	0.496
HNO_3		1.816	0.553	855	0.595	3.241	1.833
HNO_2		1.015	0.240	856	0.473	1.702	1.014
Cl	2.5	0.148	0.049	53	0.032	0.276	0.147
	10.0	0.843	0.307	53	0.331	1.796	0.808
HCl		2.020	0.628	855	0.634	3.731	2.034
Na	2.5	0.148	0.049	53	0.032	0.276	0.147
	10.0	0.843	0.307	53	0.331	1.796	0.808
Ca	2.5	0.148	0.049	53	0.032	0.276	0.147
	10.0	0.843	0.307	53	0.331	1.796	0.808
K	2.5	0.148	0.049	53	0.032	0.276	0.147
	10.0	0.843	0.307	53	0.331	1.796	0.808
Mg	2.5	0.148	0.049	53	0.032	0.276	0.147
	10.0	0.843	0.307	53	0.331	1.796	0.808
Zn	2.5	0.148	0.049	53	0.032	0.276	0.147
	10.0	0.688	0.279	53	0.227	1.559	0.654
Pb	2.5	0.148	0.049	53	0.032	0.276	0.147
	10.0	0.527	0.248	53	0.123	1.305	0.496
Cd	2.5	0.148	0.049	53	0.032	0.276	0.147
	10.0	0.688	0.279	53	0.227	1.559	0.654
Cu	2.5	0.148	0.049	53	0.032	0.276	0.147
	10.0	0.688	0.279	53	0.227	1.559	0.654
Ni	2.5	0.148	0.049	53	0.032	0.276	0.147
	10.0	0.688	0.279	53	0.227	1.559	0.654
Cr	2.5	0.148	0.049	53	0.032	0.276	0.147
	10.0	0.688	0.279	53	0.227	1.559	0.654

Dry deposition fluxes

Diurnal variations

The annual average diurnal variation in dry deposition fluxes is given in Figure 12 and 13. Diurnal variation for SO_2 show highest fluxes in the afternoon, due to the maximum concentrations in the afternoon. HNO_3, HCl and particles also show highest dry deposition fluxes in the afternoon, but as the result of highest turbulence. NH_3 does not show a distinct minimum or maximum. This is because there is a anti-correlation between concentrations and dry deposition velocities. HNO_2 show maximum values in early morning, when turbulence intensities increase and concentrations are highest.

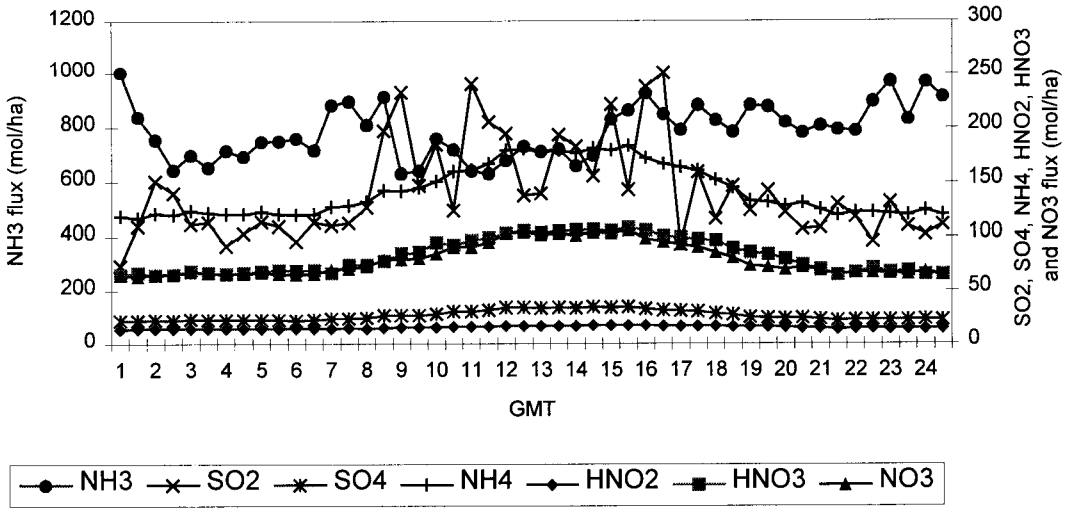

Figure 12. Annual diurnal variation in dry deposition fluxes of SO_2, SO_4^{2-}, NH_3, NH_4^+, HNO_2, HNO_3 and NO_3^- (mol ha^{-1} a^{-1}).

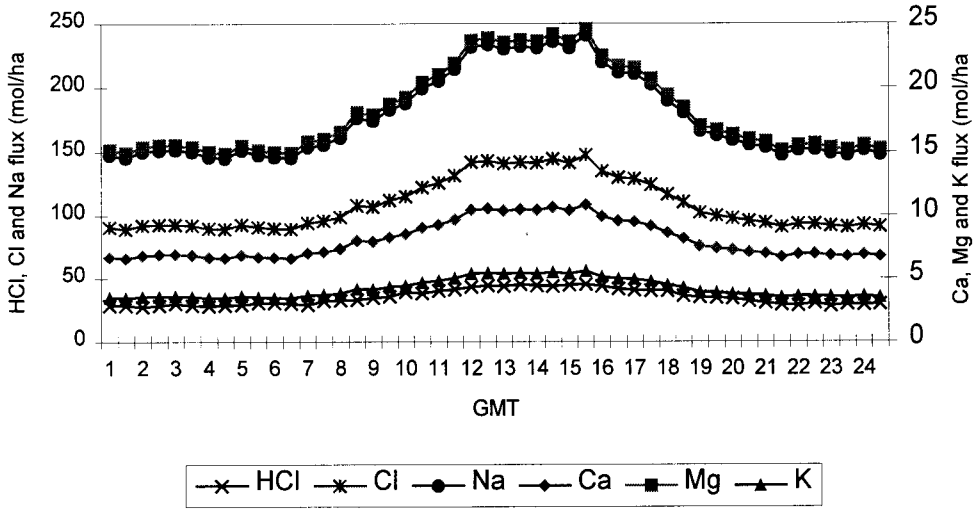

Figure 13. Annual diurnal variation in dry deposition fluxes of HCl, Cl, Na^+, Ca^{2+}, Mg^{2+}, and K^+ (mol ha^{-1} a^{-1}).

Annual average fluxes

Annual average dry deposition fluxes, standard deviations, minimum, maximum and median values are listed in Table 6. Highest input is from NH_3, about 180 mol ha^{-1} a^{-1}. NH_4^+ aerosol deposition contributes about 12% to total NH_x dry deposition. The contribution of SO_4^{2-} aerosol to total SO_x deposition is about 13% and of NO_3^- to NO_y 18%. Chloride input is dominated by aerosol input, mainly as the result of sea salt particles. Auchencorth Moss is relatively near to the coast (about 40 km?). Median fluxes are generally lower than averages as the result of the log-normal distribution of the fluxes. SO_2, NH_3 and NO_x show a large negative minimum and a positive maximum. For these gases, partly, the Vd values derived from the gradient measurements are used, and these extreme values are the result of the normal distribution around the mean values. Maximum values occur at high concentrations combined with appreciable wind speeds.

Base cation input is relative large, mainly as the result of the relatively small distance to the North sea (Na^+, Mg^{2+}) and as the result of nearby emissions from unpaved roads and agricultural practice. Dry deposition of heavy metals is generally small. Highest input is from zinc (0.13 mol ha^{-1} a^{-1}). Lowest input is from Cadmium, concentrations of this metal were usually near to the detection limit. The uncertainty in this value is therefore very high.

Table 6. Annual statistics of dry deposition fluxes inferred at Auchencorth Moss .

Component	Average	Standard deviation	Count	Min	Max	Median
SO_4	11	9	106	0	44	8
SO_2	71	327	7409	-8729	9061	24
NH_4	24	18	106	0	82	20
NH_3	177	265	9081	-4277	331	93
NO	4	123	5383	-3765	1550	1
NO_2	37	191	10735	-3357	2660	21
NO_3	14	12	106	0	55	10
HNO_3	18	21	855	4	125	19
HNO_2	3	3	856	0	9	6
Cl	48	50	106	0	245	33
HCl	17	12	855	10	70	24
Na	53	46	106	0	196	36
Ca	3	5	106	0	31	3
K	2	2	106	0	6	1
Mg	6	5	106	0	21	4
Zn	0.13	0.15	106	0.00	0.67	0.10
Pb	0.03	0.04	106	0.00	0.17	0.02
Cd	0.00	0.00	106	0.00	0.00	0.00
Cu	0.02	0.01	106	0.00	0.06	0.01
Ni	0.01	0.03	106	0.00	0.15	0.00
Cr	0.01	0.04	106	0.00	0.15	0.00

Total sulphur, nitrogen and base cation inputs are listed in Table 7. The total potential acid dry deposition, calculated as $2SO_x+NO_y+NH_x$ (Heij and Schneider, 1991) is about 450 mol ha^{-1} a^{-1}. Largest contribution to the potential acid deposition is from NH_x, 45%. Base cation deposition, calculated as K+2Ca+2Mg is estimated to be 20 eq ha^{-1} a^{-1}, about 5% of total dry potential acid deposition. Na^+ is assumed not to contribute to the neutralisation of acids as it originates from sea salt.

Table 7. Total sulphur, nitrogen and base cation input by dry deposition (eq. ha^{-1} a^{-1}).

Component	Dry deposition flux (eq. ha^{-1} a^{-1})
SOx	164
NOy	79
NHx	201
potential acid	444
BC	20

3.1.4 Wet deposition and cloud/fog deposition

Wet deposition

Wet deposition was measured using wet-only samplers. Weekly samples were collected and transported to the lab to be analysed for anions and cations. Table 8 shows the annual average fluxes and standard deviations of the wet deposition measurements for all components considered in this project. Potential acid wet deposition fluxes amount about 990 eq ha^{-1} a^{-1}, the main contribution is formed by SO_4^{2-} (42%). Base cation deposition ($Ca^{2+}+K^{+}+Mg^{2+}$) contributes about 150 eq ha^{-1} a^{-1}, 15% of the potential acid deposition.

Table 8. Annual average wet deposition fluxes and standard deviations measured at Auchencorth Moss (mol ha^{-1} a^{-1}).Rainfall amounted 895 mm.

Component	Average	Standard deviation
SO_4^{2-}	128	2.5
NO_3^{-}	133	2.7
NH_4^{+}	173	3.1
Cl^{-}	395	9.3
Na^{+}	378	8.1
Ca^{2+}	36	0.6
K^{+}	25	0.5
Mg^{2+}	50	1.0
Zn^{2+}	0.907	0.048
Pb^{2+}	0.065	0.0026
Cd	0.003	0.0003
Cu^{2+}	0.144	0.0070
Ni^{+}	0.006	0.0007
Cr^{2+}	0.016	0.0024

Cloud/fog deposition

Cloud/fog deposition: no results

3.1.5 Annual average deposition

Table 9 shows the overall average dry, wet and total deposition for the period 1-2-95 to 1-12-95 (extrapolated to annual averages). At this remote site wet deposition is higher than dry deposition for each component except for NH_x. Highest input on equivalent basis is for SO_x and NH_x. The contribution of NH_x to the total nitrogen deposition is 1.5 times that for NO_y. Base cation input is high for components of sea salt origin. Heavy metal input is generally low, ranging from 1 mol ha^{-1} a^{-1} for Zn to 0.003 mol ha^{-1} a^{-1} for Cd. Total sulphur, nitrogen and base cation inputs are listed in Table 10. Total potential acid input is about 1000 eq ha^{-1} a^{-1}, 217 eq ha^{-1} a^{-1} of this is encountered by base cations. The main contribution to the potential acid is formed by sulphur (42%) and reduced nitrogen (37%). Oxidised nitrogen contributes about 21% to the total potential acid deposition.

Table 9. Average dry, wet and total deposition fluxes to Auchencorth Moss for the period 1-2-95 to 1-12-95 (mol ha^{-1} a^{-1}).

Component	Dry deposition	Wet deposition	Total deposition
SO_4	11	128	
SO_2	71		
SO_x	82		210
NH_4	24	173	
NH_3	177		
NH_x	201		374
NO_x	41		
NO_3	14	133	
HNO_3	18		
HNO_2	6		
NO_y	79		212
Cl	48	395	
HCl	17		
Cl_x	65		460
Na	53	378	431
Ca	3	36	39
K	2	25	27
Mg	6	50	56
Zn	0.13	0.907	1.037
Pb	0.03	0.065	0.095
Cd	0	0.003	0.003
Cu	0.02	0.144	0.164
Ni	0.01	0.006	0.016
Cr	0	0.016	0.016

Table 10. Total sulphur, nitrogen and base cation input at Auchencorth Moss (eq. ha^{-1} a^{-1}).

Component	Dry deposition flux (eq. ha^{-1} a^{-1})
SOx	420
NOy	212
NHx	374
potential acid	1006
BC	217

3.2 Melpitz

The monitoring site at Melpitz was installed and run by the Institute of Tropospheric Research (IFT) in Leipzig. The activities and results obtained at Melpitz are extensively described in Spindler and Grüner (1996), the reader is referred to this report for more details. Here only a summary of the results achieved between 1-2-1995 and 1-12-1995 is given.

3.2.1 Site description

The IFT research station is situated near Melpitz Saxony, Germany) in an old meadow at an altitude of 87 m (51° 32' N, 12° 54' E, see Figure 14. This region was one of the most exposed as the result of SO_2 and NO_x emission areas in the former GDR. Permanent meteorological and some chemical measurements started here in May 1992 within the framework of the former national research project SANA (Scientific observations programme for the rehabilitation of the atmosphere above the new countries of Germany). One of the scientific aims of this project was the registration of the change of emission and its effect on the concentration and deposition of pollutants. The very flat and large meadow is very suitable for micrometeorological experiments through its good fetch. The site diagram is shown in Figure 15. The grassland consists mainly of Lolium perenne (Deutsches Weidelgras), Taraxacum officinale (Gemeiner Löwenzahn) and Leontodon autumnales (Herbst-Löwenzahn). The displacement height at this site varies between 0.10 m in winter to 0.25 m in June, just before cutting. The main wind direction (SW) transports air from the conurbation Leipzig to Melpitz (distance 41 km). The second most important wind direction (ENE) transports emissions from the high chimneys of brown coal heated power plants located in the Lusatian area near the border of Poland, about 80 to 150 km away from the site.

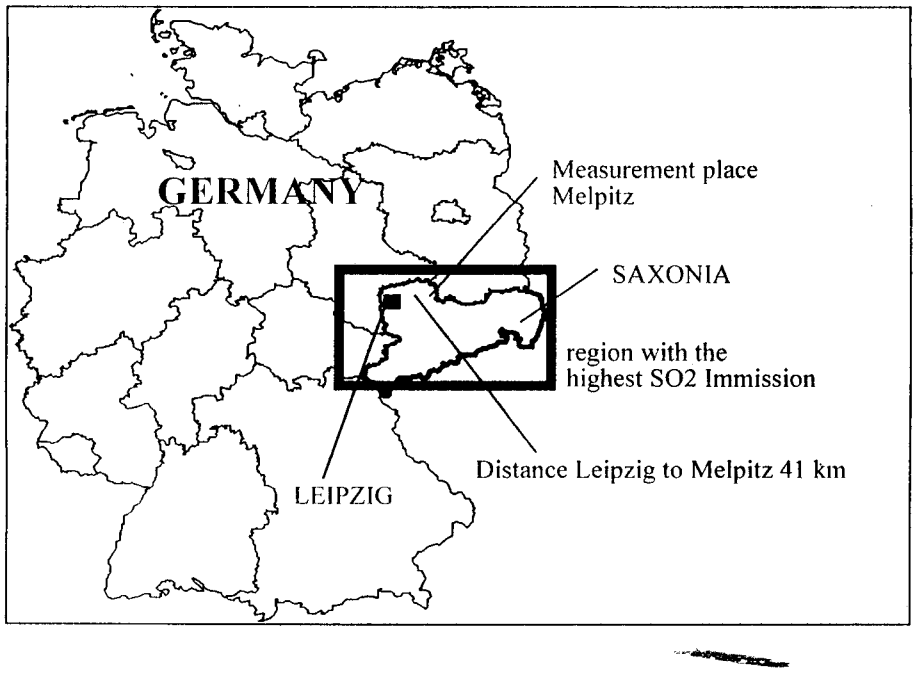

Figure 14. Location of the measurement site, Melpitz (Germany).

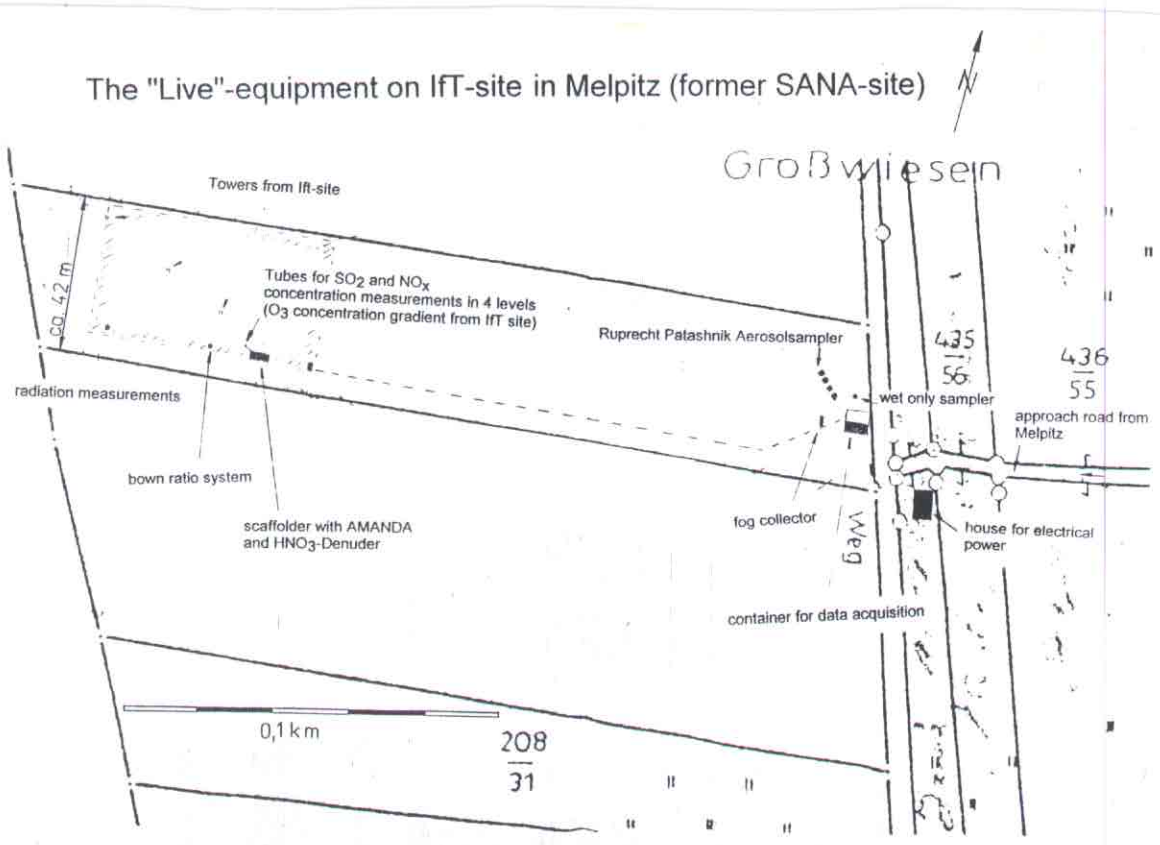

Figure 15. Site diagram Melpitz and a picture showing part of the equipment.

3.2.2 Concentrations and meteorological parameters

The concentrations conceal considerable variability in the directional dependence of the concentrations. Figure 16 shows the wind sector dependence of SO_2 and NH_3 concentrations. Concentrations of SO_2 do not show great variability, only the concentrations in the south west sector being lower than other directions, because in most cases the wind speed is high from these directions (Fig. 18). In the case of NH_3, the north east sector shows highest concentrations, wind speeds are usually low when the wind is from this direction (Fig. 18). The site is surrounded by sources influencing the large scale concentration variations per sector. The sector dependence of NO concentrations (Fig. 17) identifies two major sources: traffic on a road in the north and a single source in the south east. Considering ozone on Figure 17, the wind sector dependence shows almost constant concentrations, with a significant depletion at the south west sector. The winds are almost always blowing from the west, with highest wind speeds from the south to west (Fig. 18).

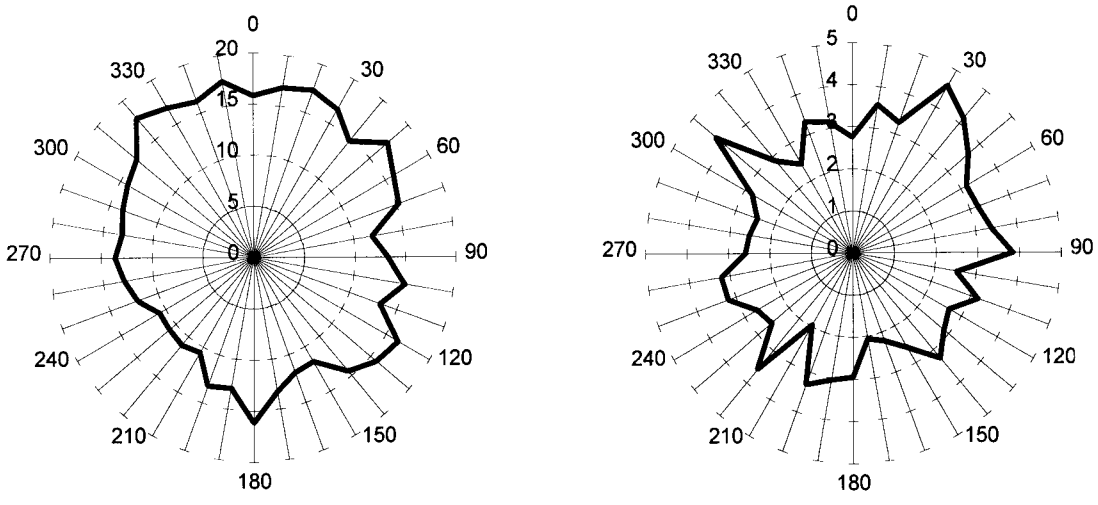

Figure 16. Average SO_2 and NH_3 concentration ($\mu g\ m^{-3}$) at 5 m per wind direction sector.

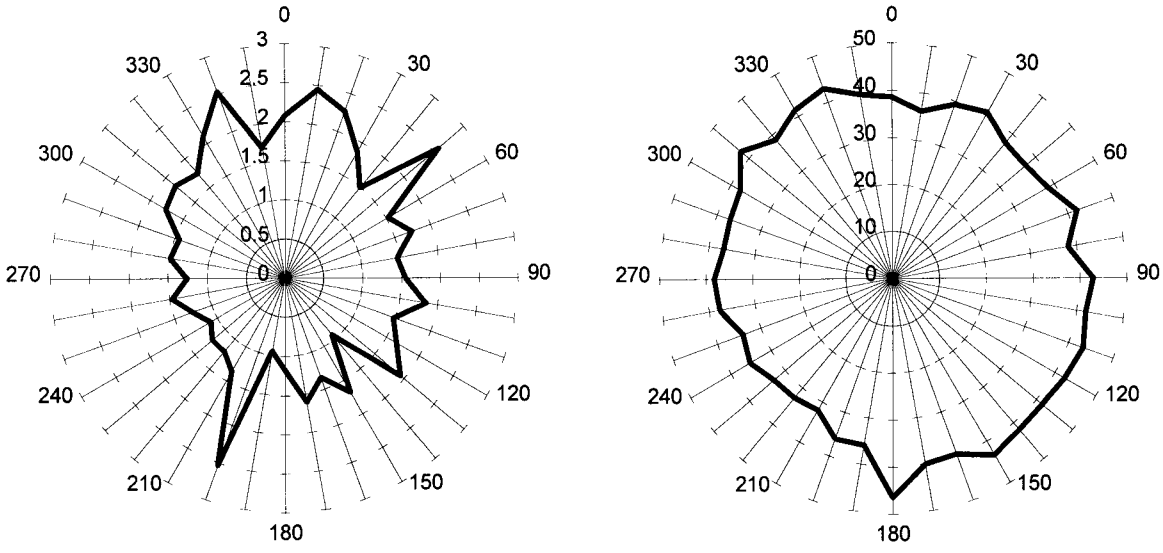

Figure 17. Average NO and O_3 concentration ($\mu g\ m^{-3}$) at 5 m per wind direction sector of 10^o.

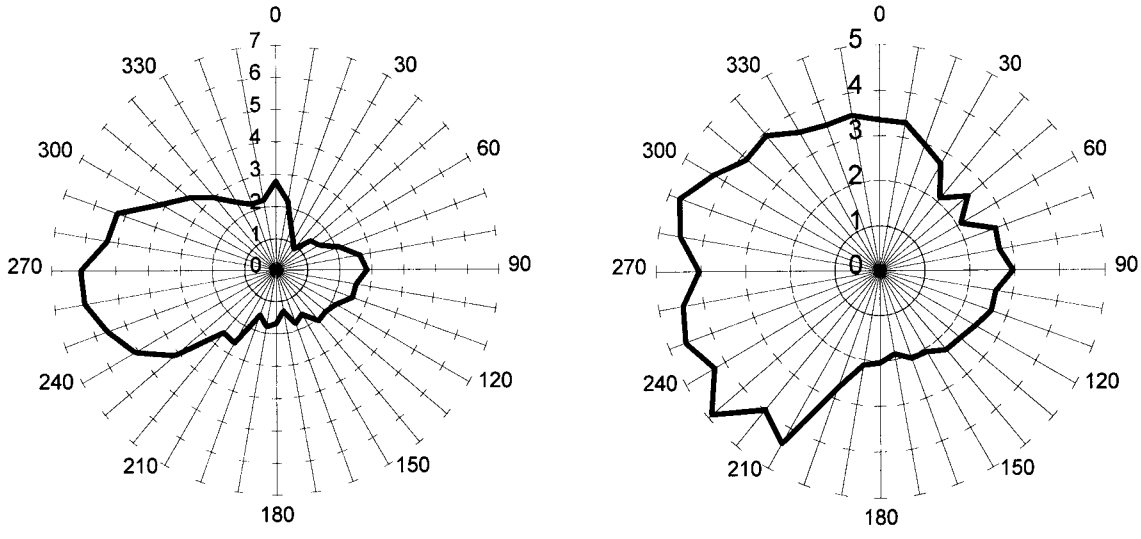

Figure 18. Sector dependence of wind direction and average wind speed ($m\ s^{-1}$) at 1 m.

3.2.3 Dry deposition

Annual average dry deposition fluxes for the different compounds were derived by the inferential method or by a combination of fluxes derived from gradients and by inference. For each half hour, dry deposition velocities were calculated using the dry deposition parametrisation described in Erisman *et al* (1994) (chapter 2). This was done for half hours where all the necessary meteorological information was available. For SO_2, NH_3 and NOx, these half hourly values for the rejected periods were multiplied with the concentrations at the reference height, 1 m, to obtain hourly fluxes. Annual average fluxes and V_d 's were calculated using all half hours from the rejected and selected datasets. or all other components, modelled dry deposition velocities were combined with measured concentrations to obtain half hourly average, and eventually annual average fluxes. Before the dry deposition fluxes are described, first the results for the measured gradients and resulting deposition parameters for SO_2, NH_3, O_3 and NO_x are described.

Gradient measurements

For each half hour the gradients were averaged and c_*, F, V_d, R_a, R_b and R_c were calculated. The dataset thus obtained has to be 'cleaned' by selection of half hours during which the theoretical demands for the gradient technique were fulfilled, during which the concentrations were well above the detection limit, and during which there was no loss of necessary measurements due to technical problems. The criteria which were applied are listed in Table 11. In this table the percent of the total number of half hourly averaged measurements which remained after applying the selection criteria is also given. For SO_2 66.9% survived the selection criteria. Most of the data were rejected as a result of the random error in individually measured concentrations. At concentrations below 5 $\mu g\ m^{-3}$ the random error was found to be the dominating error in deposition parameters. For NH_3, O_3 and NO_2 more than 50% remained after selection. This can be regarded as very high, especially in view of the very low concentrations at this site.

Table 11. Selection criteria for gradients measured over the Melpitz and the percentage of measurements rejected after selection in 1995 (remaining total half hours of continuous measurements: 67% for SO_2, 63% of NO_x, 58% of O_3 and 26% of NH_3.

Criteria	Percentage of remaining data				
	SO_2	NO	NO_2	O_3	NH_3
Fetch requirements: $\theta < 85$ and $\theta > 90^o$	2.9	3.9	3.9	3.4	5.7
Extreme stability $\|L\| > 3$ m, $u > 0.9$ m s^{-1} (7.9 m)	12.5	16.8	16.4	14.6	24.7
Detection limits ($SO_2 > 5\ \mu g\ m^{-3}$, $NH_3 > 0.3\ \mu g\ m^{-3}$, NO, $NO_2 > 0.2\ \mu g\ m^{-3}$, $O_3 > 6\ \mu g\ m^{-3}$	44.4	43.9	0	4.3	6.3
Instrumentation installation, failure, maintenance and calibration	11.6	34.3	32.6	24.3	55.3

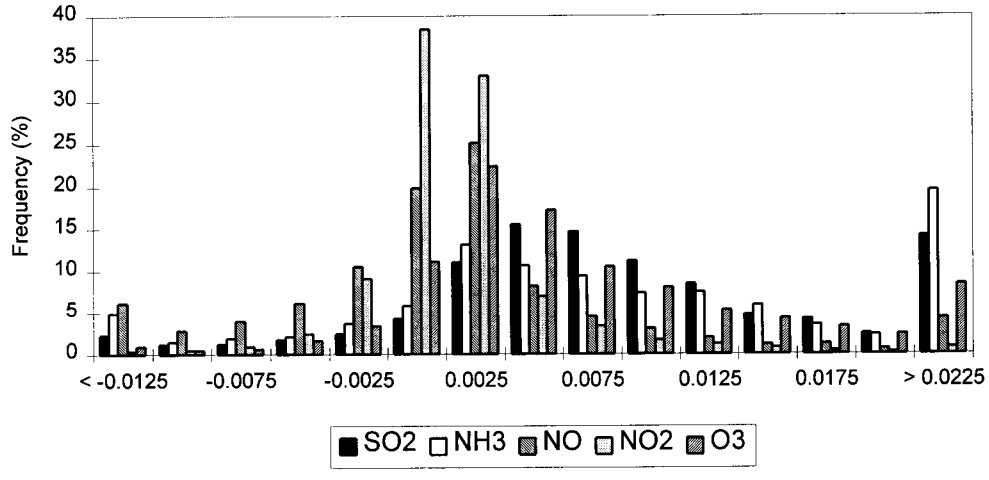

Figure 19. Frequency distribution of Vd values for selected hours ($m\ s^{-1}$).

The frequency distribution of dry deposition velocities for SO_2, NH_3, O_3 and NO_x for the remaining (selected) hours are given in Figure 19. The distributions show log-normal curves, with a normal distribution of random errors. Most negative values for SO_2 and O_3 are the result of the random error in vertical concentration gradient measurements, although 'real' emission fluxes of SO_2 have been observed after periods with high sulphur loads due to high concentrations, followed by some hours with very low ambient concentrations. The accumulated sulphite concentrations not yet fixed as SO_4^{2-} can be evaporated during these conditions. The same effect, even stronger, is observed for NH_3 in addition to stomatal

emissions. If ambient concentrations fall below the compensation points for NH_4^+ concentrations in stomatal apoplast, and/or for NH_4^+ concentrations at the outer leaf surface, emission of NH_3 is expected. The distributions of SO_2 and NH_3 are similar in shape and in classes. NO and NO_2 deposition velocities show distributions around zero, probably due to atmospheric chemistry and random noise.

Some statistical parameters for dry deposition velocities in selected periods are given in Table 12. The median values are lower than the averages, as the result of the log-normal distributions. NH_3 deposition velocities are highest, SO_2 show a surface resistance to uptake at the surface. NO_x show very small deposition velocities. Errors listed in the table are estimated by the methods described in Duyzer *et al.*, 1996). In the table median error values are given, because the distribution of hourly values is log-normal and averages are therefore influenced by a few very high values. The error for selected Vd values is 36% for SO_2, 47% for O_3, 62% for NO, 60% for NO_2 and 49% for NH_3, these values are relatively small, reflecting the high quality of the measurements. The error is largest for oxidised nitrogen, because of the small gradients and the influence of chemical reactions on the gradients.

Table 12. Statistical parameters for Vd (m s^{-1}) derived from measurements of selected hours.

Statistic	SO_2	NH_3	NO	NO_2	O_3
Average	0.0089	0.0098	-0.0001	0.0004	0.0062
Standard deviation	0.016	0.0236	0.0183	0.0077	0.0105
Median	0.014	0.0064	-0.001	-0.001	0.037
Min	-0.1672	-0.2383	-0.4741	-0.1823	-0.1460
Max	0.1531	0.2605	0.2374	0.1852	0.1237
Error (median value, %)	36	49	62	60	47

Frequency distributions of R_c for SO_2, NH_3 and NO_x are shown in Fig. 20. The median R_c value for SO_2 is 75 s m^{-1}, whereas that for NH_3 is lower: 40 s m^{-1}. Median values for NO, NO_2 and O_3 are 350, >500 and 50 s m^{-1}, respectively. R_c values for O_3 are low, probably these are influenced by chemical reactions. NH_3 is most effectively taken up at the surface, O_3 is taken up with rates lower than the stomatal limited uptake. SO_2 is not taken up as effectively as suggested in literature, despite the frequent occurrence of surface wetness. R_c values are, however, smaller than stomatal resistances stressing the importance of external leaf uptake.

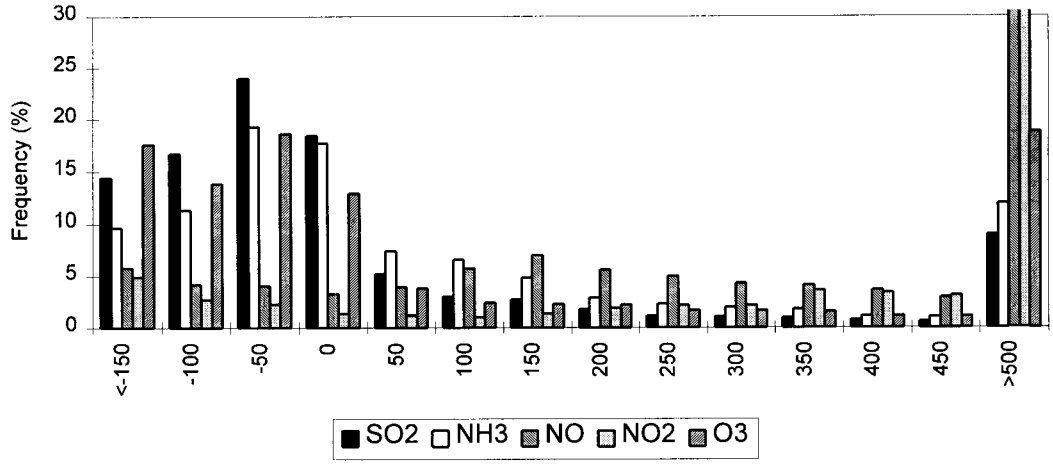

Figure 20. Frequency distribution of Rc values for selected half hours (s m^{-1}).

Testing of dry deposition parametrisations

The surface resistance parametrisations outlined in Appendix A (Erisman *et al.*, 1994) were applied to the half hour data which remained after selection. Figure 21 to 23 show comparisons between modelled and measured V_d values for SO_2, NH_3 and O_3, respectively. The error bars in the plot represent the standard deviation determined for the class average V_d. V_d was averaged per class of modelled values. The comparison shows reasonable agreement between modelled and measured V_d for SO_2 and O_3. On an annual basis, average V_d do not differ significantly from measured values. However, individual modelled V_d for half hours can deviate substantially from measured values. For NH_3 systematic differences can be observed: the modelled values do not represent the strong variations found in the measurements.

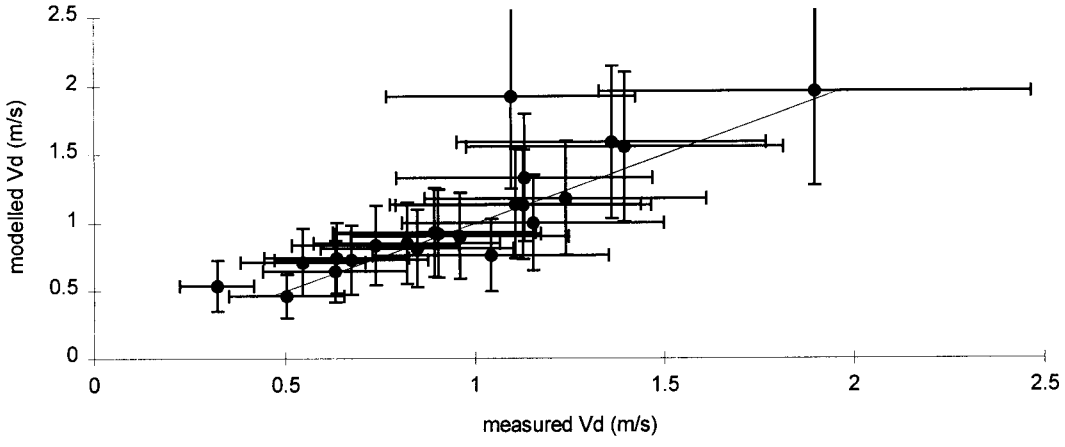

Figure 21. Comparison of modelled and measured V_d *values for* SO_2.

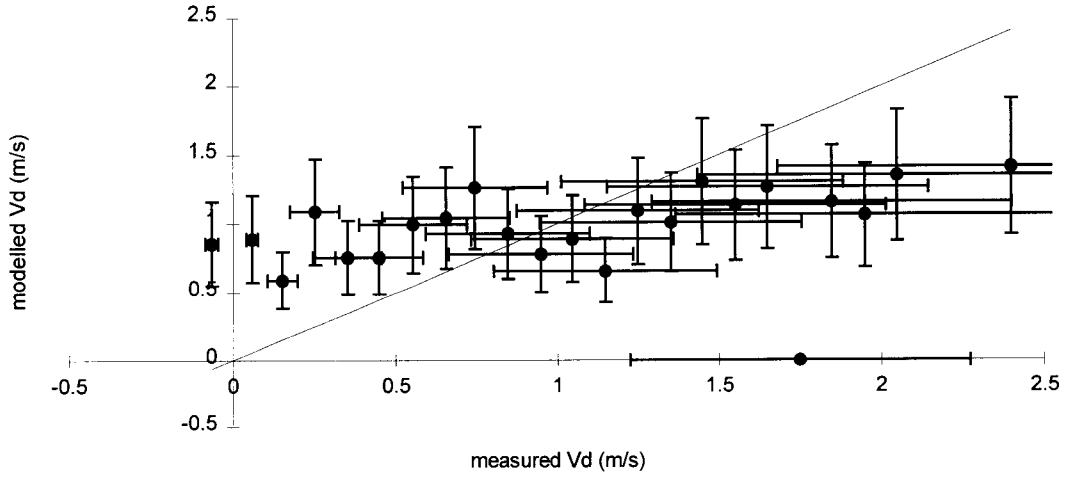

Figure 22. Comparison of modelled and measured V_d *values for* NH_3.

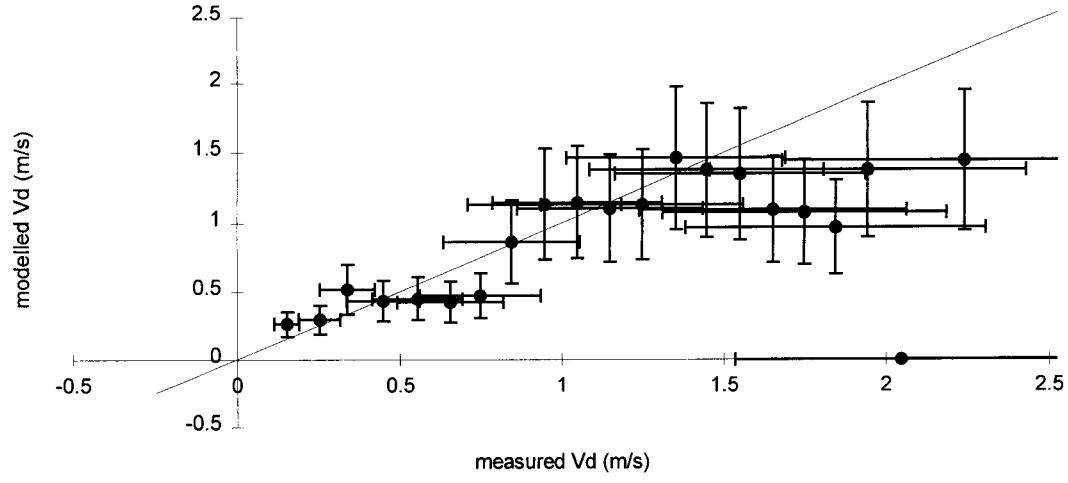

Figure 23. Comparison of modelled and measured V_d *values for* O_3.

Dry deposition velocities

Dry deposition velocities were estimated every half hour using measured quantities and the dry deposition parametrisations outlined in chapter 2. For SO_2, NH_3, O_3 and NO_x only the Vd's for hours which are rejected after selection are calculated using the parametrisation, the other Vd values are from measured concentration gradients.

Diurnal variations

Diurnal variations of V_d for gases and aerosols are displayed in Fig. 24 and 25, respectively. As turbulence intensities are higher during daytime than at night, V_d values for HNO_3 are highest during daytime, because it is assumed that for this gas uptake rates are entirely governed by turbulent transport, without any surface resistance. SO_2 and NH_3 show diurnal variations which are similar, with lowest concentrations during midday. This is unexpected, at least for SO_2. The lower values during daytime than during night-time are probably the result of surface saturation with SO_4^{2-} at the high SO_2 concentrations. The diurnal variation in NH_3 deposition velocities shows lowest values during daytime as the result of net upward fluxes. These occur when the ambient concentrations fall below stomatal or external leaf surface compensation points. O_3 deposition is determined by stomatal uptake, showing a smooth diurnal variation with highest values in the afternoon. NO_2 shows no distinct diurnal variation, whereas NO shows emission during the afternoon. The V_d values for both parameters can be strongly influenced by atmospheric chemistry.

Model results for aerosols show the same diurnal variations, there is only a difference in magnitude: base cation Vd being highest, followed by NO_3^-, SO_4^{2-} and NH_4^+. This reflects the size distributions of these particles. Indications of the distribution of particle concentration with size can be obtained from the concentration differences for PM 2.5 and 10 as shown in Fig. 32 in Spindler and Grüner (1996). Base cation concentrations are higher in the PM 10 classes, whereas e.g. for NH_4^+ concentrations is nearly only found in the PM 2.5 class.

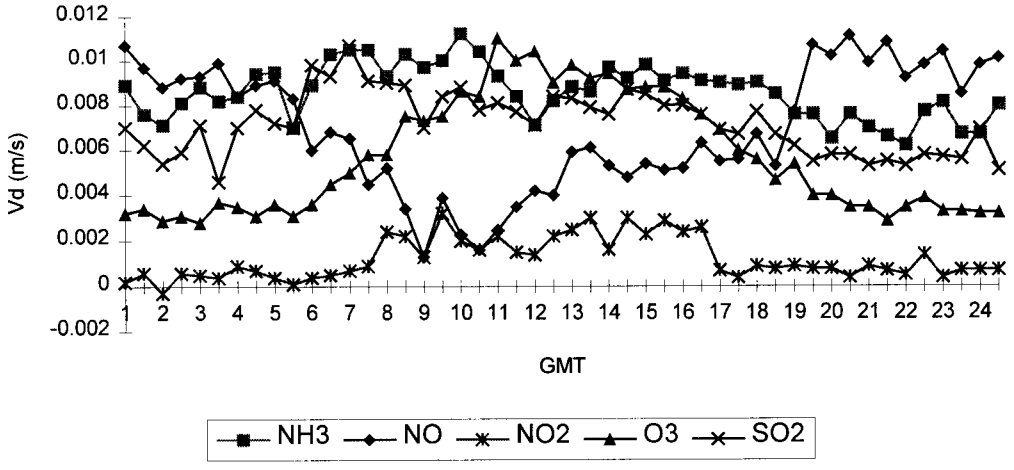

Figure 24. Diurnal variations of gas Vd (m s^{-1}) at 1 m height.

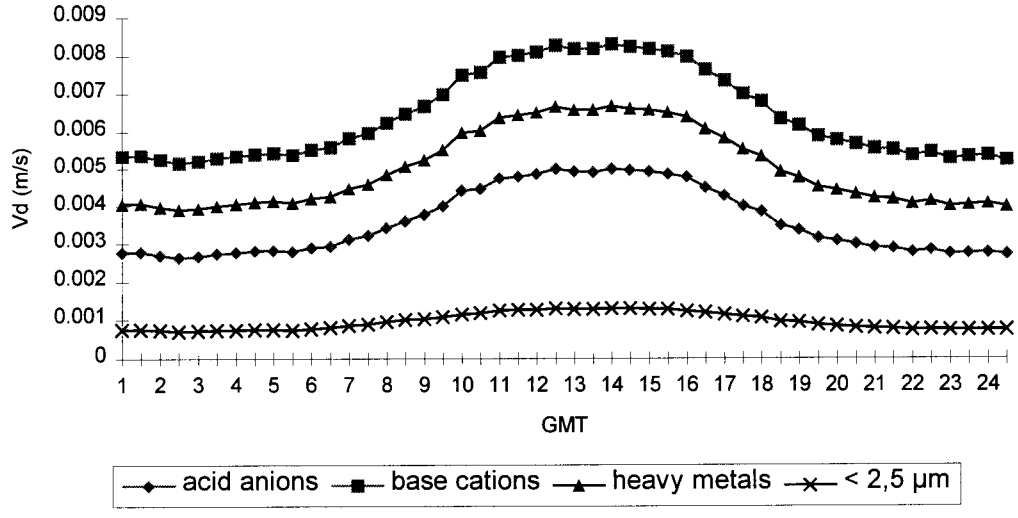

Figure 25. Diurnal variations of aerosol Vd (m s^{-1}) at 1 m height.

Annual averages

Annual averages, standard deviation and median values of V_d are listed in Table 13. V_d is highest for large particles, 2.3 cm s^{-1}. The maximum V_d for gases is about 1.1 cm s^{-1}, estimated for HNO_3 and HCl with a negligible surface resistance. NH_3 deposition velocities are quite high, showing only small resistances to uptake. This is mainly the result of the occurrence of surface wetness, which is about 50% of the time.

Table 13. Annual dry deposition velocities estimated from measurements over Melpitz in 1995 (cm s^{-1}).

Component	Size classes	Average	Standard deviation	No. of half hours	Min	Max	Median
SO_4^{2-}	2.5	0.10	0.07	13198	0.00	0.62	0.09
	10	0.36	0.31		0.00	5.48	0.25
SO_2		0.72	1.09	13165	-16.70	18.30	0.60
NH_4^+	2.5	0.10	0.07		0.00	0.62	0.09
	10	0.36	0.31		0.00	5.48	0.25
NH_3		0.86	1.35	12982	-23.80	26.00	0.70
NO_3^-	2.5	0.10	0.07		0.00	0.62	0.09
	10	0.36	0.31		0.00	5.48	0.25
NO		0.70	1.36	13280	-47.40	23.70	0.50
NO_2		0.12	6.20	13312	-18.20	18.30	0.00
O_3		0.57	0.80	13069	-14.60	12.40	0.40
HNO_3		1.10	2.16		0.00	0.00	0.00
HNO_2[a]		0.72	1.09	13165	-16.70	18.30	0.60
Cl	2.5	0.10	0.07	13198	0.00	0.62	0.09
	10	0.64	0.41	13198	0.00	6.90	0.49
HCl		1.90	2.11		0.00	0.00	0.00
Na^+	2.5	0.10	0.07	13198	0.00	0.62	0.09
	10	0.64	0.41	13198	0.00	6.90	0.49
Ca^{2+}	2.5	0.10	0.07	13198	0.00	0.62	0.09
	10	0.64	0.41	13198	0.00	6.90	0.49
K^+	2.5	0.10	0.07	13198	0.00	0.62	0.09
	10	0.64	0.41	13198	0.00	6.90	0.49
Mg^{2+}	2.5	0.10	0.07	13198	0.00	0.62	0.09
	10	0.64	0.41	13198	0.00	6.90	0.49
Zn	2.5	0.10	0.07	13198	0.00	0.62	0.09
	10	0.50	0.36	13198	0.00	6.20	0.37
Pb	2.5	0.10	0.07	13198	0.00	0.62	0.09
	10	0.50	0.36	13198	0.00	6.20	0.37
Cd	2.5	0.10	0.07	13198	0.00	0.62	0.09
	10	0.50	0.36	13198	0.00	6.20	0.37
Cu	2.5	0.10	0.07	13198	0.00	0.62	0.09
	10	0.50	0.36	13198	0.00	6.20	0.37
Ni	2.5	0.10	0.07	13198	0.00	0.62	0.09
	10	0.50	0.36	13198	0.00	6.20	0.37
Cr	2.5	0.10	0.07	13198	0.00	0.62	0.09
	10	0.50	0.36	13198	0.00	6.20	0.37

Dry deposition fluxes

Diurnal variations

The annual average diurnal variation in dry deposition fluxes is given in Fig. 26 and 27. The diurnal variation in HNO_2, HNO_3 and HCl fluxes as hourly values is given in Spindler and Grüner (1996). O_3, HNO_3, HCl and particles show highest dry deposition fluxes in the afternoon, as the result of highest turbulence. SO_2 does not show a distinct minimum or maximum. This is because there is a anti-correlation between concentrations and dry

deposition velocities. NH_3 fluxes are lowest during the afternoon, where both concentrations and V_d are lowest. NH_3 shows an early morning peak.

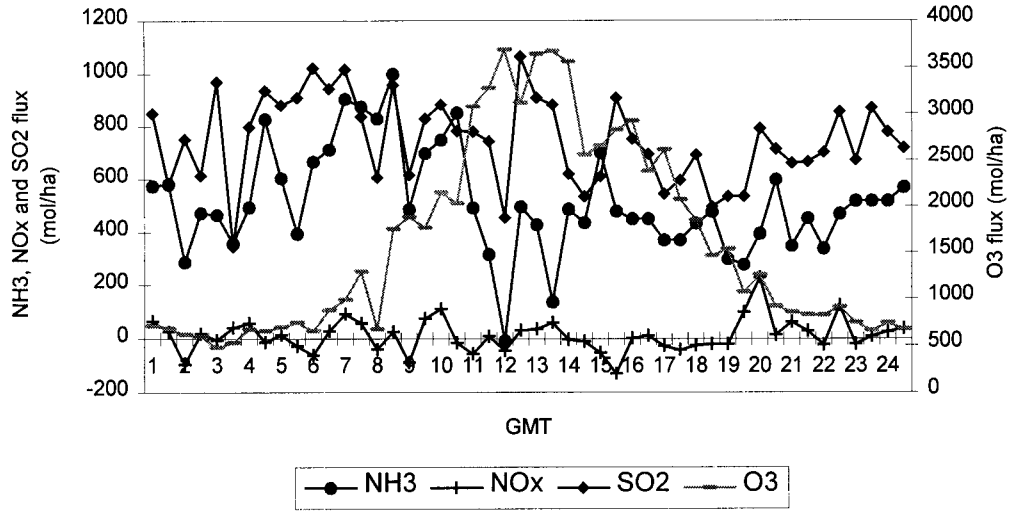

Figure 26. Annual diurnal variation in dry deposition fluxes of SO_2, NH_3, and NO_x (mol ha^{-1} a^{-1}).

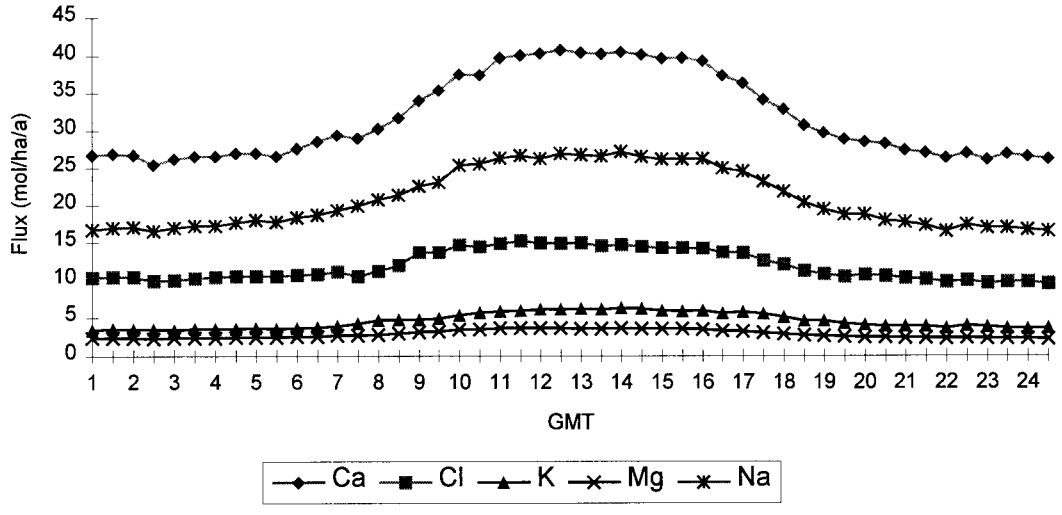

Figure 27. Annual diurnal variation in dry deposition fluxes of Cl, Na^+, Ca^{2+}, Mg^{2+}, and K^+ (mol ha^{-1} a^{-1}).

Annual average fluxes

Annual average dry deposition fluxes, standard deviations, minimum, maximum and median values are listed in Table 14. Highest input is from SO_2 751 (mol ha^{-1} a^{-1}) and NH_3 518 (mol ha^{-1} a^{-1}). NH_4^+ aerosol deposition contributes about 9% to total NH_x dry deposition. The contribution of SO_4^{2-} aerosol to total SO_x deposition is about 5% and of NO_3^- to NO_y 21%. Chloride input is dominated by HCl, contrary to the other sites. Aerosol input is generally low, compared to gaseous deposition. Median fluxes are generally lower than averages as the result of the log-normal distribution of the fluxes SO_2, NH_3 and NO_x show a large negative minimum and a positive maximum. For these gases, partly, the V_d values derived from the gradient measurements are used, and these extreme values are the result of the normal

distribution around the mean values. Maximum values occur at high concentrations combined with appreciable wind speeds.

Table 14. Annual statistics of dry deposition fluxes inferred at Melpitz.

Component	Average	Standard deviation	No. half hours	Min	Max	Median
SO_4	35	30	13198	-5	367	24
SO_2	751	1668	5247	-11083	13667	79
NH_4	47	53	13198	-86	1418	33
NH_3	518	1399	4640	-12454	28470	182
NO	-1	438	3975	-9142	10746	-2
NO_2	13	722	7253	-15586	10167	-6
NO_3	20	29	13198	-260	241	11
HNO_3	55					
HNO_2	20					
Cl	12	22	13198	-16	237	4
HCl	31					
Na	21	27	13198	-19	330	11
Ca	32	35	13198	-2	381	19
K	5	7	13198	-24	95	3
Mg	3	3	13198	-2	95	2
Zn	0.35	0.31	13198	0	4	0.3
Pb	0.03	0.03	13198	0	2.4	0.02
Cd	0.001	0.001	13198	0	0.38	0
Cu	0.047	0.038	13198	0	0.237	0.03
Ni	0.005	0.022	13198	-0.2	0.141	0.005
Cr	0.006	0.008	13198	0	0.237	0.004

Base cation input is relative small, mainly as the result of the low V_d over grassland. Dry deposition of heavy metals is generally small. Highest input is from zinc (0.35 mol ha^{-1} a^{-1}). Lowest input is from Cadmium, concentrations of this metal were usually near to the detection limit. The uncertainty in this value is therefore very high.

Total sulphur, nitrogen and base cation inputs are listed in Table 15. The total potential acid dry deposition, calculated as $2SO_x+NO_y+NH_x$ (Heij and Schneider, 1991) is about 2230 mol ha^{-1} a^{-1}. Largest contribution to the potential acid deposition is from SO_x, 70%. Base cation deposition, calculated as K+2Ca+2Mg is estimated to be 75 eq ha^{-1} a^{-1}, about 3% of total dry potential acid deposition. Na^+ is assumed not to contribute to the neutralisation of acids as it originates from sea salt.

Table 15. Total sulphur, nitrogen and base cation input by dry deposition (eq. ha^{-1} a^{-1}).

Component	Dry deposition flux (eq. ha^{-1} a^{-1})
SOx	786
NOy	95
NHx	565
potential acid	2232
BC	75

3.2.4 Wet deposition and cloud/fog deposition

Wet deposition
Wet deposition was measured using wet-only samplers. Weekly samples were collected and transported to the lab to be analysed for anions and cations. Table 16 shows the annual average fluxes and standard deviations of the wet deposition measurements for all components considered in this project. Potential acid wet deposition fluxes amount about 990 eq ha^{-1} a^{-1}, the main contribution is formed by SO_4^{2-} (42%). Base cation deposition ($Ca^{2+}+K^{+}+Mg^{2+}$) contributes about 150 eq ha^{-1} a^{-1}, 15% of the potential acid deposition.

Table 16. Annual average wet deposition fluxes and standard deviations measured at Melpitz (mol ha^{-1} a^{-1}).

Component	Average	Standard deviation
SO_4^{2-}	209.1	34.5
NO_3^-	233.3	33.7
NH_4^+	335.8	63.1
Cl^-	75.1	6.6
Na^+	61.9	9.3
Ca^{2+}	48.9	9.0
K^+	23.7	4.5
Mg^{2+}	13.5	1.2
Zn^{2+}	0.00346	05.8
Pb^{2+}	0.08	0.02
Cd	0.004	0.00
Cu^{2+}	0.05	0.05
Ni^+	0.03	0.01
Cr^{2+}	0.01	0.01

Cloud/fog deposition
Cloud/fog deposition could be detected only during two periods. Fluxes estimated for these periods were, however, very small (Spindler and Grüner, 1996).

3.2.5 Annual average deposition

Table 17 shows the overall average dry, wet and total deposition for the period 1-2-95 to 1-12-95 (extrapolated to annual averages). Wet deposition is generally lower than dry deposition, except for base cations and heavy metals. For these components the dry deposition is limited by the small V_d. Highest input on equivalent basis is for SO_x and NH_x. Total potential acid input at Melpitz is about 3230 mol H^+ ha^{-1} a^{-1}. Total base cation input is 225 eq mol ha^{-1} a^{-1}, about 7% of the total potential acid deposition. Total nitrogen input is 1240 mol ha^{-1} a^{-1}. The contribution of NH_x to the total nitrogen deposition is 3 times that for NO_y.

Table 17. Average dry, wet and total deposition fluxes to the Melpitz site for the period 1-2-95 to 1-12-95 (mol ha^{-1} a^{-1}).

Component	Dry deposition	Wet deposition	Total deposition
SO_4	35	209	
SO_2	751		
SO_x	786		995
NH_4	47	336	
NH_3	518		
NH_x	565		901
NO_x	12		
NO_3	20	233	
HNO_3	55		
HNO_2	20		
NO_y	95		340
Cl	12	75	
HCl	31		
Cl_x	43		118
Na	21	70	91
Ca	32	49	81
K	5	24	29
Mg	3	14	17
Zn	0.35	4	4.35
Pb	0.03	0.08	0.11
Cd	0.001	0.004	0.005
Cu	0.047	0.05	0.097
Ni	0.005	0.03	0.035
Cr	0.006	0.01	0.016

3.3 Speulder forest

3.3.1 Site description

The Speulder and Sprielder forest (52° 15' N, 5° 41' E) is located in the Veluwe, a large undulating area with forests and heathlands in the central part of the Netherlands (Fig. 28). The measuring site covers an area of 2.5 ha and is planted with Douglas fir of the Arlington provenance. By the end of 1995 the trees were 35 years old. The canopy is well closed with the maximum leaf area density at a height of 10-14 m. The one-sided Leaf Area Index LAI was between 13.9 and 9.7 for the 1987-1993 period of measurement (Steingröver and Jans, 1994). The stem density varies between 765 trees per ha in the east part of the stand and 1216 in the west part of the stand. In 1993 the average Diameter at Breast Height DBH was 25.4 cm and the trees were approximately 22 m in height (Jans *et al.*, 1994). The stand is surrounded by a larger forested area of approximately 50 km^2; the nearest edge is at a distance of 1.5 km from the site. The stand itself is surrounded by Larix, Betula, Quercus, Pinus and Pseudotsuga trees, with mean tree heights varying between 12 and 25 m. A small clearing of 1 ha is situated to the north of the stand. Large source areas of SO_2 and NOx are located about 200 km to the south-east (industrial Ruhr area) and about 100 km to the south-west (Rotterdam port) of the site. The forested area is surrounded by large agricultural areas with intensive livestock farming acting as a source of NH_3 due to ammonia volatilisation from animal manure. A site diagram is displayed in Figure 29.

Figure 28. Location of the measurement site, Speulder forest (The Netherlands).

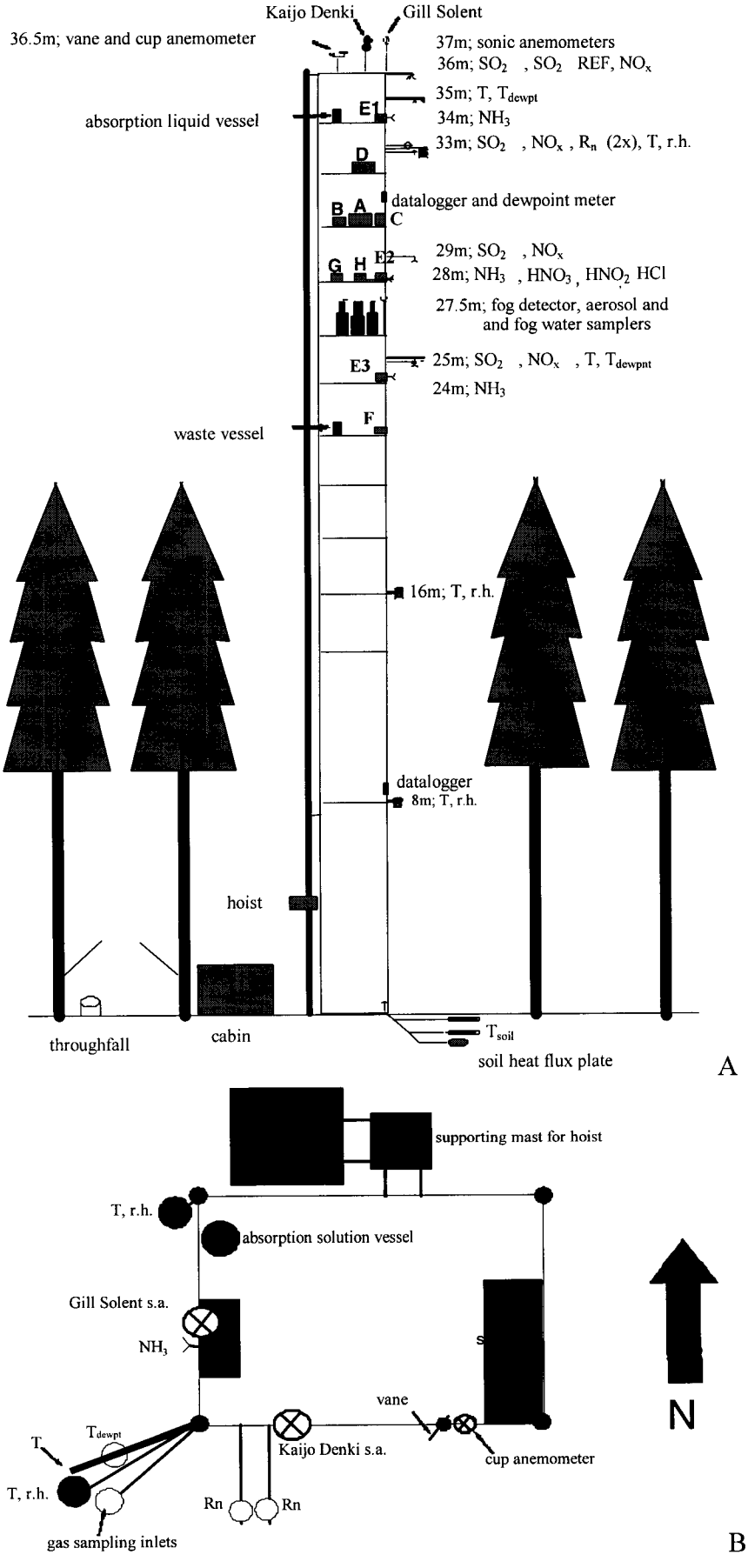

Figure 29. Site diagram and instrumentation.

3.3.2 Concentrations and meteorological parameters

Wind direction dependence

The concentrations measured at Speulder forest depend strongly on wind direction. Figure 30 to 32 show average concentrations of SO_2, NH_3 and NO_x for each wind direction sector. There is a clear wind direction dependence, showing the influence of sources or source areas. For SO_2 concentrations are highest in easterly direction, showing the influence of the Ruhr area in Germany and the 'Amer Centrale'(??) , situated about 30 km to the south-east. Lowest concentrations can be found in air masses coming from northerly direction, i.e. over the North sea. NH_3 concentrations are highest when the wind comes from south-west and from north-east. Major sources areas are the 'Gelderse Vallei' and the 'Achterhoek'. NO_x concentrations are lowest for northerly wind directions. Highest concentrations are measured when the wind is blowing from the south or south-east, because of nearby roads and small towns in these sectors.

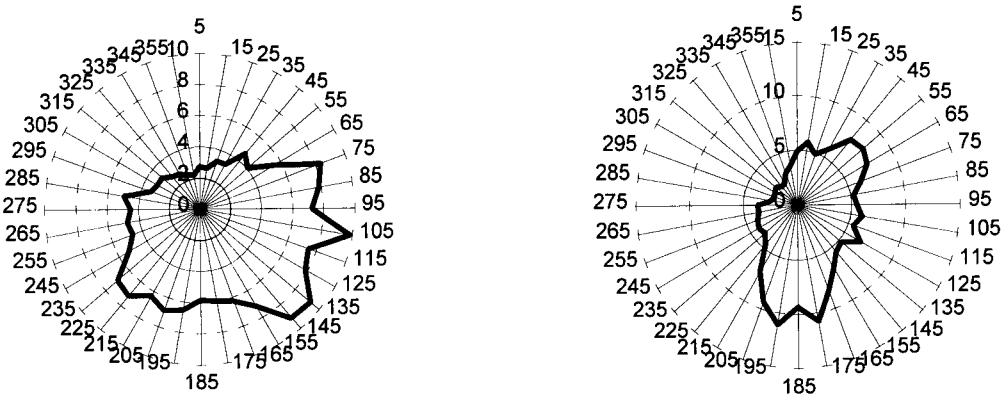

Figure 30. Average SO_2 and NH_3 concentration ($\mu g\ m^{-3}$) at 36 m per wind direction sector of 10^o.

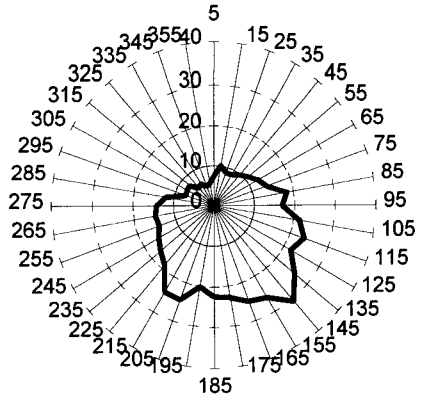

Figure 31. Average NO_x concentration (µg NO m^{-3}) at 36 m per wind direction sector of 10^o.

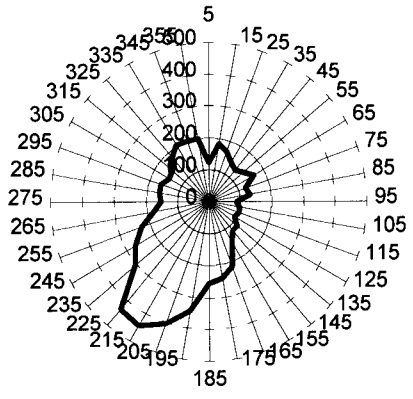

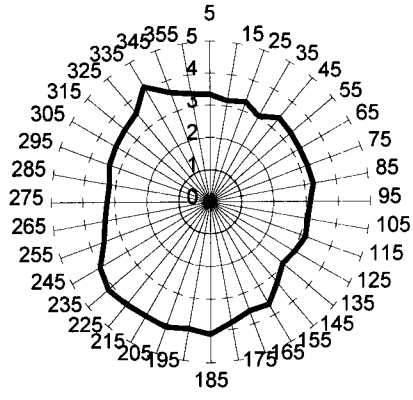

Figure 32. Sector dependence of wind direction and average wind speed (m s^{-1}) at 36.5 m per wind direction sector of 10^o.

Most of the time in 1995 wind blew from south-westerly directions, the prevailing wind direction in The Netherlands (Fig. 32). Wind speeds are more evenly distributed over the wind direction sectors. Somewhat higher wind speeds are experienced when the wind blows from the south-west. For NH_3 conditions for high dry deposition fluxes are optimal, i.e. the concentration is highest in the sector where wind speeds are highest on the average, and where the wind is blowing from most of the time. For SO_2 conditions are less optimal for high dry deposition fluxes.

Diurnal variations

Diurnal variations are available for SO_2, NH_3, NO_x, HNO_2, HNO_3 and HCl. The aerosol concentrations were measured as daytime and night-time averages. There is a distinct difference between the different gases. NH_3 and HNO_2 show a minimum in the afternoon, while the other gases show minimum values at night. For HNO_2 the diurnal cycle is governed by photochemical destruction during daytime. NO_x concentrations show an early morning peak, probably due to the traffic intensities. For NH_3 the daily minimum is the result of the increased dispersion during the day, whereas at night there is a build-up of concentration during stable conditions. Chemical conversion is also higher during the day (Erisman *et al.*, 1988).

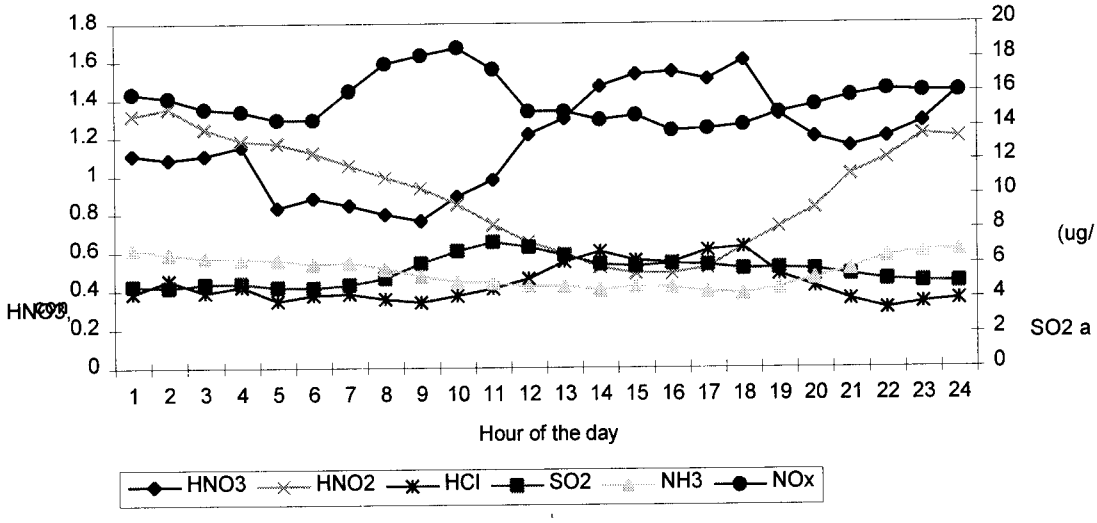

Figure 33. Diurnal variation of gases measured over Speulder forest ($\mu g\ m^{-3}$).

Annual average concentrations

Annual average concentrations and their standard deviation are listed in Table 19. The concentrations of the gases are about equal to country average values derived from measurements made in the National Air Quality Monitoring Network for the Netherlands (RIVM, 1995). Concentrations show a log-normal distribution, median values are lower than averages. Maximum SO_2 concentrations reached to about 50 $\mu g\ m^{-3}$, whereas maximum NH_3 concentrations reach 90 $\mu g\ m^{-3}$. Acid gas concentrations are around 1 $\mu g\ m^{-3}$ for HNO_2 and HNO_3 and below 0.5 $\mu g\ m^{-3}$ for HCl. During episodes, values up to 10 $\mu g\ m^{-3}$ are reached.

Concentrations in aerosol are dominated by NH_4^+, NO_3^- and SO_4^{2-}. Aerosol SO_4^{2-} and NO_3 are almost completely bound to NH_4. Concentrations of Na^+, Ca^{2+} and Mg^{2+} are higher in the larger particles, as can be expected from the sources such as sea salt and wind blown dust (e.g. Milford and Davidson, 1985; Draaijers *et al.*, 1996). All other aerosols are mostly found in the smaller fractions. Heavy metal concentrations are generally small.

Table 18. Annual concentrations measured at Speulder forest in 1995 (μg m^{-3}).

Component	MMD (μm)	Average	Standard deviation	Count	Min	Max	Median
SO_4	2.5	4.7	2.7	7632	0	13	3.4
	10	0.5	0.7	7632	0	5.6	0.3
SO_2		5.5	5.9	6474	0.01	46.8	3.5
NH_4	2.5	3.1	1.9	7632	0.6	9.1	2.4
	10	0.2	0.3	7632	0	1.6	0.1
NH_3		5.5	6.1	4085	0.01	90.4	3.5
NO_x[a]		15.5	12.8	2418	0.64	69.8	11.4
NO_3	2.5	4.8	3.4	7632	0.3	15.8	3.3
	10	1.1	0.6	7632	0	3.3	1.0
HNO_3		1.2	1.3	970	0	9.1	
HNO_2		0.9	0.8	983	0	9.0	
Cl	2.5	0.4	0.4	7632	0	1.5	0.2
	10	0.7	0.6	7632	0	2.7	0.3
HCl		0.4	0.4	966	0	5.9	
Na	2.5	0.264	0.246	7632	0.069	2.170	0.174
	10	0.527	0.337	7548	0.033	1.750	0.403
Ca	2.5	0.040	0.027	7296	0.004	0.160	0.030
	10	0.162	0.102	7212	0.019	0.584	0.118
K	2.5	0.087	0.044	7632	0.001	0.234	0.068
	10	0.045	0.022	7548	0.000	0.120	0.041
Mg	2.5	0.033	0.031	7632	0.006	0.265	0.022
	10	0.078	0.043	7548	0.013	0.234	0.061
Zn	2.5	0.028	0.017	7632	0.004	0.089	0.020
	10	0.008	0.008	7548	0.000	0.059	0.005
Pb	2.5	0.018	0.011	7632	0.003	0.057	0.015
	10	0.003	0.004	7632	0.000	0.026	0.002
Cd	2.5	0.0003	0.0002	7632	0.0000	0.0014	0.000
	10	0.0001	0.0001	7632	0.0000	0.0005	0.000
Cu	2.5	0.003	0.003	7632	0.000	0.023	0.002
	10	0.002	0.002	7632	0.000	0.014	0.002
Ni	2.5	0.001	0.001	7632	0.000	0.004	0.001
	10	0.0004	0.0004	7632	0.0000	0.0029	0.000
Cr	2.5	0.0004	0.0003	7632	0.0000	0.0013	0.000
	10	0.0003	0.0010	7632	0.0000	0.0108	0.000

[a] expressed as μg NO m^{-3}.

3.3.3 Dry deposition

Annual average dry deposition fluxes for the different compounds were derived by the inferential method or by a combination of fluxes derived from gradients and by inference. For each hour, dry deposition velocities were calculated using the dry deposition parametrisation described in Erisman *et al* (1994) (chapter 2). This was done for hours where all the necessary meteorological information was available. For SO_2, NH_3 and NOx, these hourly values for the rejected periods were multiplied with the concentrations at the reference height, 36 m, to obtain hourly fluxes. Annual average fluxes and V_d's were calculated using all hours from the rejected and selected datasets. or all other components, modelled dry deposition velocities were combined with measured concentrations to obtain hourly average, and eventually annual

average fluxes. Before the dry deposition fluxes are described, first the results for the measured gradients and resulting deposition parameters for SO_2, NH_3 and NO_x are described.

Gradient measurements
For each hour the four vertical SO_2, eight NO_2 and ten NH_3 gradients were averaged and c*, F, V_d, R_a, R_b and R_c were calculated. The dataset thus obtained has to be 'cleaned' by selection of hours during which the theoretical demands for the gradient technique were fulfilled, during which the concentrations were well above the detection limit, and during which there was no loss of necessary measurements due to technical problems. Selection criteria for SO_2 derived from measurements over a heathland (Erisman *et al.*, 1993a,b) were adjusted and applied here. These criteria are listed in Table 19. In this table the percent of the total number of hourly averaged measurements which remained after applying the selection criteria is also given. For SO_2 about 30% survived the selection criteria. Most of the data were rejected as a result of the random error in individually measured concentrations. At concentrations below 3 $\mu g\ m^{-3}$ the random error is the dominating error in deposition parameters. The largest errors in the deposition parameters are caused by the vertical concentration gradient measurements. Even small errors in concentration measurements can lead to very large errors in the concentration gradient c_* because c_* is small as a result of the large turbulence induced by the forest. The influence of random noise of the SO_2 (and NO_2) monitors on the error in c_* was estimated by Zwart *et al.* (1994). They estimated that by using an averaging time of 1 min for the concentration detection, the error in an individually measured gradient, at concentration levels of 7 μg m-3, is 100% for unstable, 70% for neutral and 40% for stable conditions (one σ level). At higher concentrations this error reduces, but at lower concentrations it will be larger. In the field larger random errors are expected as a result of the valve system, the tubes and filters. The influence of random errors in the field was investigated by placing all tubes at one height (36 m) and sampling SO_2 concentrations for one week according to the normal measuring scheme. In this way random errors in concentration measurements due to the complete system (monitors, valves, heated tubes and filters) were estimated. It was shown that by measuring the gradient in time using one monitor, a random error is introduced due to concentration changes within one measuring cycle. The correction with measurements from the reference monitor are therefore inevitable (see Equation 5). Furthermore, it was found that by applying Equation [5] the changes in concentration were accounted for and no extra random errors were introduced (Erisman *et al.*, 1993b). The random error in c_* becomes larger at smaller concentrations. For hourly average concentrations of 5 $\mu g\ m^{-3}$ the random error is within 10%. This value is comparable to that reported by Zwart *et al.* (1994) for 1 min averages. The error in hourly average c^* values as a result of random errors generated by the system is thus comparable to that estimated by Zwart *et al.*. At concentrations above 5 $\mu g\ m^{-3}$ this error increases rapidly.

The NO_2 measurements started on the first of May, because of late delivery of special parts of the NO_x system. For this reason, about 35% of the data in 1995 was not available. Most NO_2 data were rejected as a result of technical problems. Because of the very warm summer, temperatures in the monitor box rose to very high levels, which could not be lowered far enough by the air conditioning.

Table 19. Selection criteria for gradients measured over the Speulder forest and the percentage of measurements left after selection in 1995 (remaining total: 2557 hours of continuous SO_2 measurements 1352 hours of NO_x measurements and; 1516 hours of continuous NH_3).

Criteria	percentage of remaining SO_2 data	percentage of remaining NO_2 data	percentage of remaining NH_3 data
Technical problems; calibration; maintenance; installation	80	28	47
Validity of flux profile relations u>1or u*>0.2 m/s,	64	22	37
Fetch requirements: θ<330 and θ> 30°	53	17	29
SO_2: Deviation between two monitors: $\|\Delta C\| < 3$ μg/m^3; C>3 μg/m^3; no gradient: c* > 0 NH_3: C>0.1 μg/m^3; no gradient: c* > 0 NO_x: C>5 μg/m^3; no gradient: c* > 0	31	16	18
$\|V_d\| < 2\ V_d$ max	30	16	17

For NH_3, data from the period February to December 1995 have been processed. About 17% of the data remained after selection, see Table 19. Most data were rejected as a result of incorrect operation of instrumentation due to e.g. freezing of the solutes in the denuders, or technical problems.

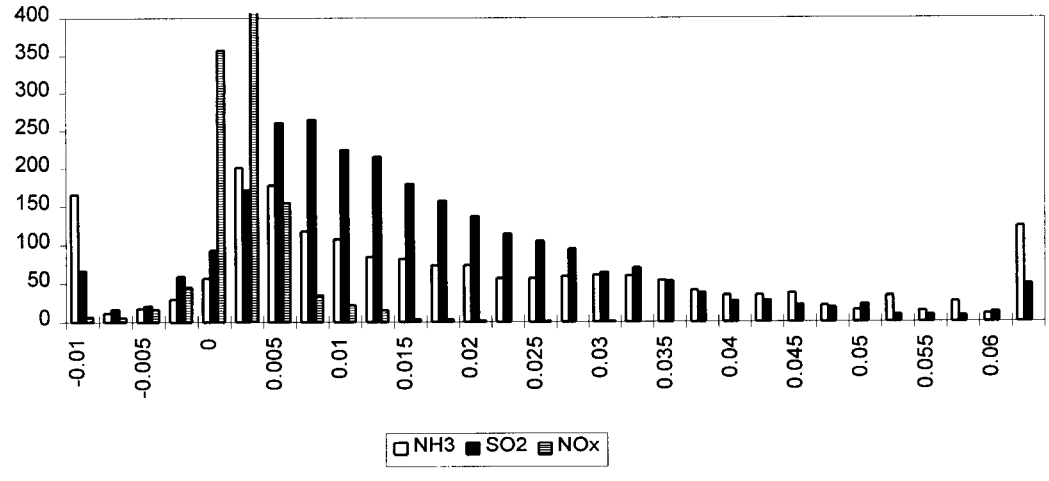

Figure 34. Frequency distribution of Vd values for selected hours (m s^{-1}).

The frequency distribution of dry deposition velocities for SO_2, NH_3 and NO_x for the remaining (selected) hours are given in Figure 34. The distribution shows a log-normal curve, with a normal distribution of random errors. Most negative values for SO_2 are the result of the random error in vertical concentration gradient measurements, although 'real' emission fluxes have been observed after periods with high sulphur loads due to high concentrations, followed by some hours with very low ambient concentrations. The accumulated sulphite concentrations not yet fixed as SO_4^{2-} can be evaporated during these conditions. The same effect, even stronger, is observed for NH_3 (Erisman and Wyers, 1993; Wyers and Erisman, 1996) in addition to stomatal emissions. If ambient concentrations fall below the compensation points for NH_4^+ concentrations in stomatal apoplast, and/or for NH_4^+ concentrations at the outer leaf surface, emission of NH_3 is expected. This effect varies

strongly between different years (Wyers and Erisman, 1996), probably as the result of variations in the accumulated flux and frequency of decreasing ambient concentrations after strong accumulations. This in turn is related to variations in the lengths dry and wet periods and fluxes during dry periods.

Some statistical parameters for dry deposition velocities in selected periods are given in Table 20. The median values are lower than the averages, as the result of the log-normal distributions. NH_3 deposition velocities are highest, SO_2 show a surface resistance to uptake at the surface. NO_x show a log-normal distribution, with highest values just above zero.. Errors listed in the table are estimated by:

$$R.E. = \sqrt{(1/\rho^2 - 1)/(N-2)} \qquad [25]$$

where ρ is the correlation coefficient of the hourly average vertical concentration gradient and N is the number of levels where concentrations were measured. In the table median values are given, because the distribution of hourly values is log-normal and averages are therefore influenced by a few very high values. The error for selected Vd values is 30% for SO_2, 45% for NO_x and 23% for NH_3, these values are relatively small, reflecting the high quality of the measurements. The uncertainty estimates are in reasonable agreement with those derived by Zwart *et al.* (1994), for the SO_2 measurements made over the Speulder forest (50% random error and 20% systematic). The measuring scheme is optimised to minimise errors after the suggestions by Zwart *et al.*. The error is largest for NO_x, because gradients are usually very small, and thus the needed accuracy for measuring the concentration measurements very high.

Table 20. Statistical parameters for Vd (m s^{-1}) derived from measurements of selected hours.

Statistic	SO_2	NH_3	NO_x
Average	0.0148	0.0203	0.00094
Standard deviation	0.0166	0.0285	0.00307
Median	0.012	0.019	0.00049
Min	-0.073	-0.151	-0.0132
Max	0.124	0.113	0.0281
Error (median value, %)	30	23	45

Frequency distributions of Rc for SO_2, NH_3 and NO_x are shown in Figure 35. The R_c classes most represented for SO_2 and NH_3 are those between 0 and 50 s m^{-1}. The median R_c value for SO_2 is 32 s m^{-1}, whereas that for NH_3 is somewhat lower : 12 s m^{-1}. R_c values for NO_x do not show a distinct distribution. Median R_c value for NO_x is 371 s m^{-1}.

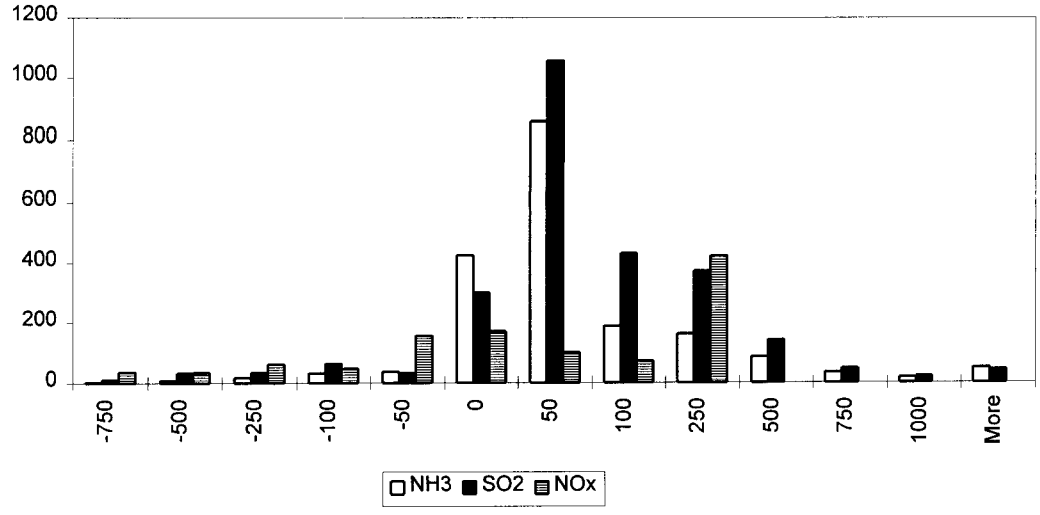

Figure 35. Frequency distribution of Rc values for selected hours (s m^{-1}).

The representativity of the conditions for the hours in the selected dataset were compared to those for the rejected dataset (Erisman *et al.*, 1996). The comparison of the distributions of the selected and rejected dataset for SO_2 shows that the distributions are reasonable in agreement. Daytime and night-time is equally represented. The number of dry hours, relative humidity and temperature is somewhat higher for the rejected data than for the selected data. The number of hours wet is also higher for the rejected data (45%) than for the selected data (37%). However, most of the combinations of circumstances occur in both datasets. This is not true for NH_3. The percentage of hours where surface wetness occurred is about equal (40%), but situations with high SO_2 concentrations are clearly over-represented in the selected dataset. Application of the selection criteria in Table 19 may have lead to a bias in the dataset.

Testing of dry deposition parametrisations

Using hourly average data, R_a, R_b and R_c were estimated with the parametrisations in section 3.4. Values of V_d and F were derived from these resistances and the gas concentration. For the selected periods, these parametrised data were compared to measured values of V_d and F. Table 21 shows averages, standard deviations and correlation coefficients of measured and modelled dry deposition fluxes. The results show that the average dry deposition fluxes of SO_2 do not differ significantly. For NH_3 and NO_x the modelled values are significantly higher than the measured values. This is because in the measurements of NH_3 more net upward fluxes occur than in the modelled values. The parametrisations are therefore insufficient to describe the surface exchange of NH_3. The uncertainty in NO_x measurements is probably too high to draw conclusions.

Table 21. Statistical data for comparison of parametrised values and those derived from measurements.

	NO_x		SO_2		NH_3	
	measured	modelled	measured	modelled	measured	modelled
Number of hours		1352		2557		1516
R^2		0.099		0.34		0.36
Average	0.019	0.043	0.126	0.144	0.082	0.123
Standard deviation	0.059	0.060	0.148	0.113	0.149	0.119
Maximum	0.516	0.378	1.191	1.101	1.184	0.768
Minimum	-0.229	0.001	-0.369	0.007	-0.539	0.001

The fluxes for SO_2 are compared in a scatter diagram in Fig. 36. Figure 37 shows the comparison for NH_3 and Figure 38 that for NO_x. Given is the average modelled and measured values per class of modelled values. The error bars represent variation as well as uncertainty. These figures confirm the significant different values for NH_3 and NO_x. For SO_2 a small overestimation of modelled fluxes is shown at higher fluxes.

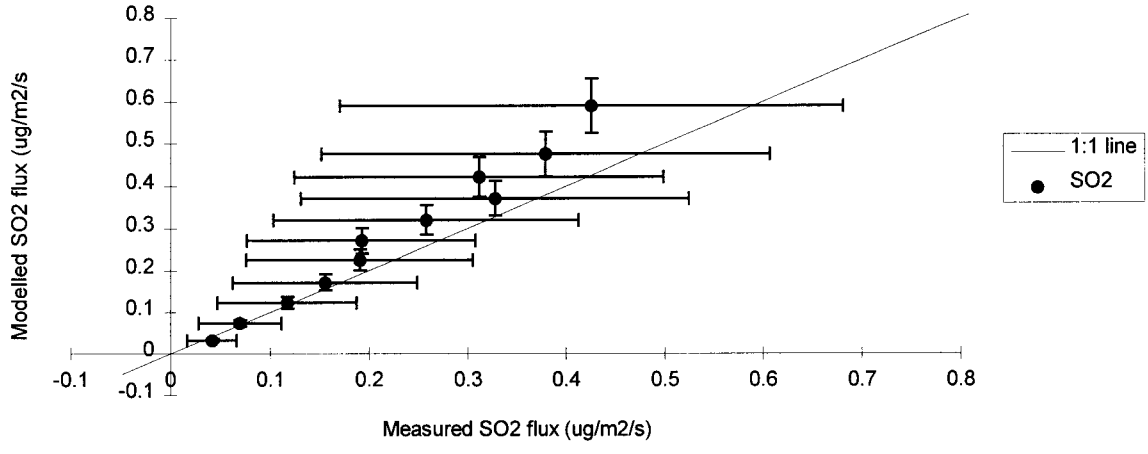

Figure 36. Comparison of modelled and measured fluxes for SO_2.

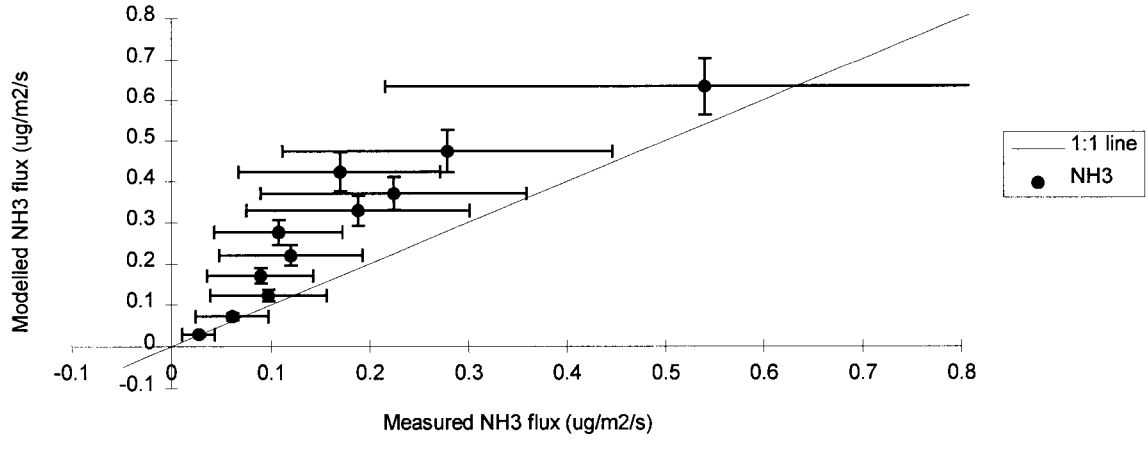

Figure 37. Comparison of modelled and measured fluxes for NH_3.

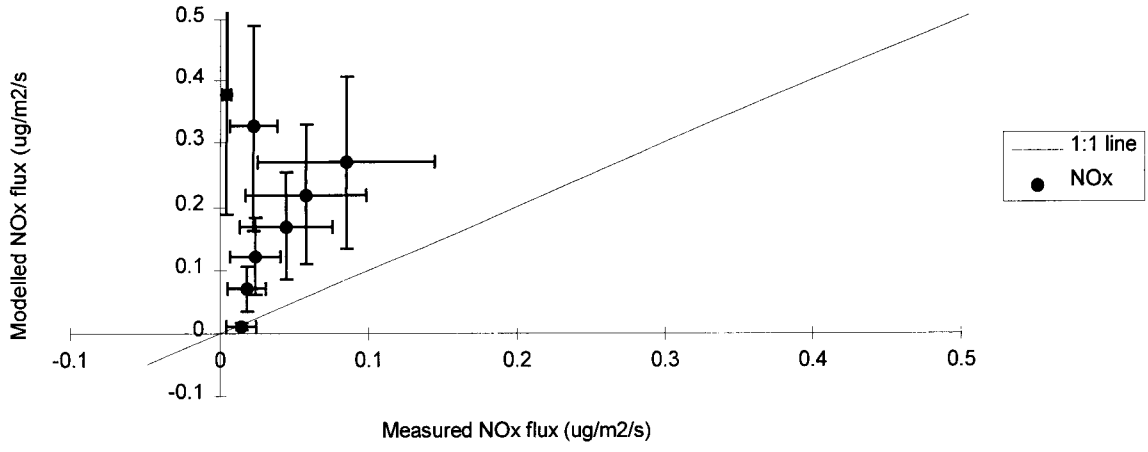

Figure 38. Comparison of modelled and measured fluxes for NO_x

Dry deposition velocities

Dry deposition velocities are estimated every hour using measured quantities and the dry deposition parametrisations outlined in Appendix A. For SO_2, NH_3 and NO_x only the V_d's for hours which are rejected after selection are calculated using the parametrisation, the other $_{Vd}$ values are from measured concentration gradients. V_d for selected periods are discussed in section 4.1. Here the annual average diurnal variations and annual averages are given.

Diurnal variations

Diurnal variations of V_d for gases and aerosols are displayed in Fig. 39 and 40, respectively. As turbulence intensities are higher during daytime than at night, Vd values are generally higher during daytime than at night. V_d values for HNO_3 are highest, because it is assumed that uptake rates are entirely governed by turbulent transport, without any surface resistance. SO_2 and NO_2 show diurnal variations determined by turbulence, although the influence of the surface cannot be neglected. NO_2 deposition is determined by stomatal uptake, and SO_2 uptake is both determined by stomata and external leaf water layers. This explains the higher V_d values for SO_2 , although the shape of both curves is identical. The diurnal variation in NH_3 deposition velocities shows a dip during the middle of the day as the result of net upward fluxes. These occur when the ambient concentrations fall below stomatal or external leaf surface compensation points (Wyers and Erisman, 1996).

Model results for aerosols show the same diurnal variations. There is only a difference in magnitude of V_d values: base cation Vd being highest, followed by NO_3^-, SO_4^{2-} and NH_4^+, respectively. This reflects the size distributions of these particles. Indications of the distribution of particle concentration with size can be obtained from the concentration differences for PM 2.5 and 10 as shown in Table 19. Base cation concentrations are higher in the PM 10 classes, whereas e.g. NH_4^+ is nearly only found in the PM 2.5 class.

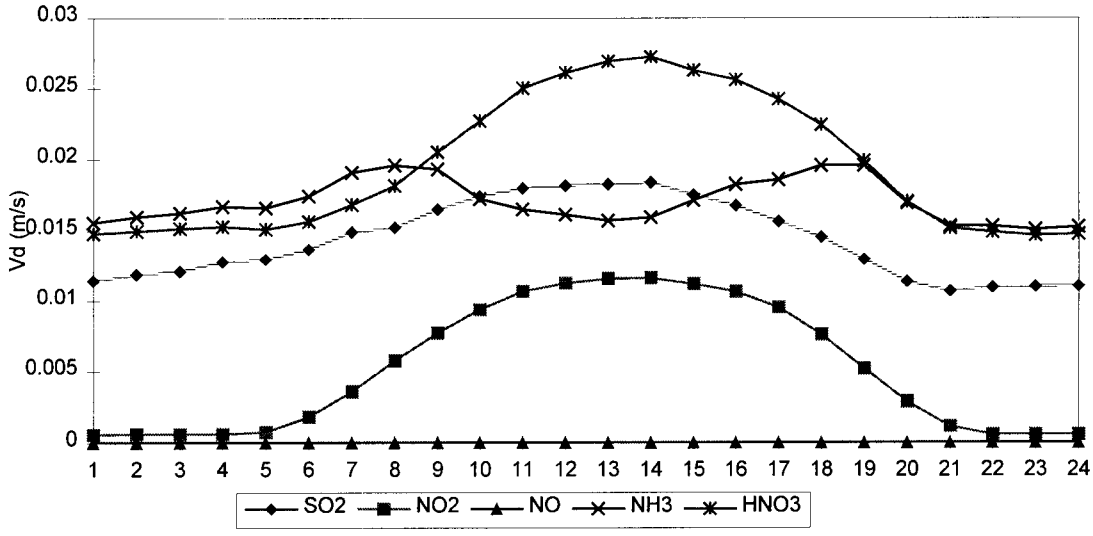

Figure 39. Diurnal variations of gas Vd (m s^{-1}) at 36 m height. V_d *HNO_2 is assumed equal to that of SO_2 and V_d HCl is assumed to equal V_d HNO_3.*

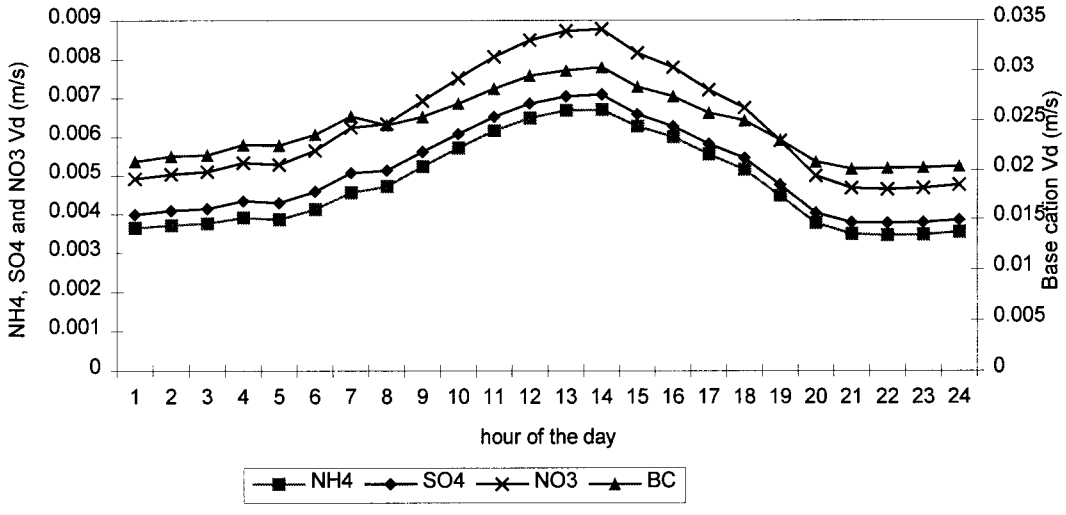

Figure 40. Diurnal variations of aerosol Vd (m s^{-1}) at 36 m height.

Annual averages

Annual averages, standard deviation and median values of V_d are listed in Table 22. Average V_d values are rather high as the result of the high turbulence induced by the forest. Highest V_d is estimated for base cations and chloride, about 2.5 cm s^{-1}. The maximum V_d for gases is about 2 cm s^{-1}, estimated for HNO_3 and HCl with a negligible surface resistance. SO_2 and NH_3 deposition velocities are quite high, showing only small resistances to uptake. This is mainly the result of the occurrence of surface wetness, which is about 50% of the time.

Table 22. Annual dry deposition velocities estimated from measurements over Speulder forest in 1995 (cm s^{-1}).

Component	Average	Standard deviation	No. of hours	Min	Max	Median
SO_4	0.51	0.42	7027	0	3.01	0.43
SO_2	1.38	1.26	7027	-7.25	12.35	1.18
NH_4	0.47	0.37	7027	0	2.55	0.42
NH_3	1.68	1.74	7027	-15.11	11.30	1.54
NO_x	0.24	0.30	7027	-1.33	2.81	0.05
NO_3	0.63	0.51	7027	0	3.6	0.53
HNO_3	1.95	1.06	7027	0.01	4.68	1.95
HNO_2[a]	1.43	0.93	7027	0.01	4.74	1.3
Cl	2.43	1.7	7027	0.67	12.02	1.93
HCl	1.95	1.06	7027	0.01	4.68	1.95
Na	2.43	1.7	7027	0.67	12.02	1.93
Ca	2.43	1.7	7027	0.67	12.02	1.93
K	1.22	0.85	7027	0.34	6.01	0.97
Mg[b]	2.43	1.7	7027	0.67	12.02	1.93
Zn[b]	0.51	0.42	7027	0	3.01	0.43
Pb[b]	0.51	0.42	7027	0	3.01	0.43
Cd[b]	0.51	0.42	7027	0	3.01	0.43
Cu[b]	0.51	0.42	7027	0	3.01	0.43
Ni[b]	0.51	0.42	7027	0	3.01	0.43
Cr[b]	0.51	0.42	7027	0	3.01	0.43

[a] assumed to be similar to SO_2

[b] assumed to be similar to SO_4^{2-} (< 2.5 μm)

Dry deposition fluxes

Diurnal variations

The annual average diurnal variation in dry deposition fluxes is given in Fig. 42 and 42. The diurnal variation shows a midday peak value of about 700 mol ha^{-1} a^{-1} for SO_2. HNO_3 and HCl, NO_x and particles show highest dry deposition fluxes in the afternoon, as the result of highest turbulence. NH_3 does not show a distinct minimum or maximum. This is because there is an anti-correlation between concentrations and V_d. HNO_2 shows maximum values in early morning, when turbulence intensities increase and concentrations are highest.

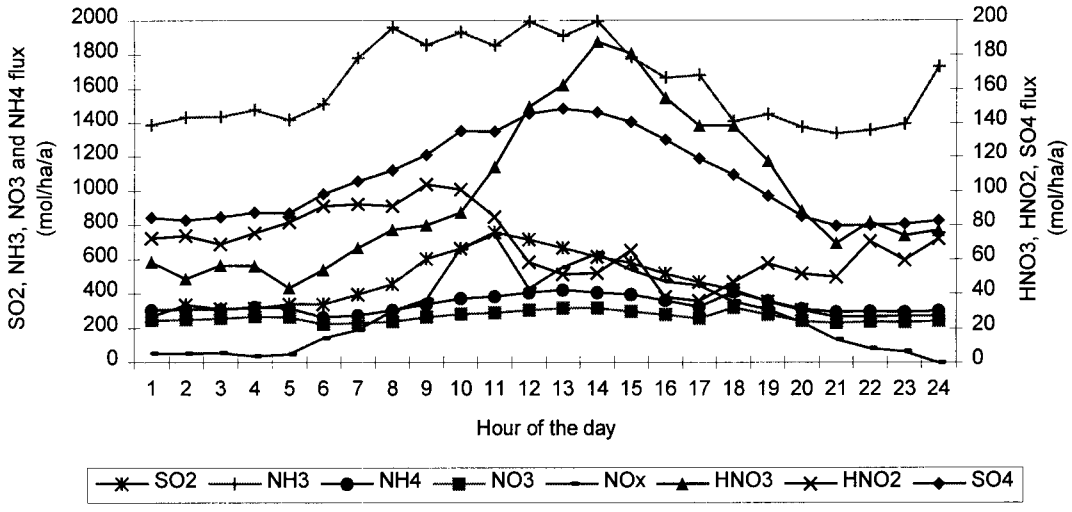

Figure 41. Annual diurnal variation in dry deposition fluxes of SO_2, SO_4^{2-}, NH_3, NH_4^+, HNO_2, HNO_3 and NO_3^- (mol ha^{-1} a^{-1}).

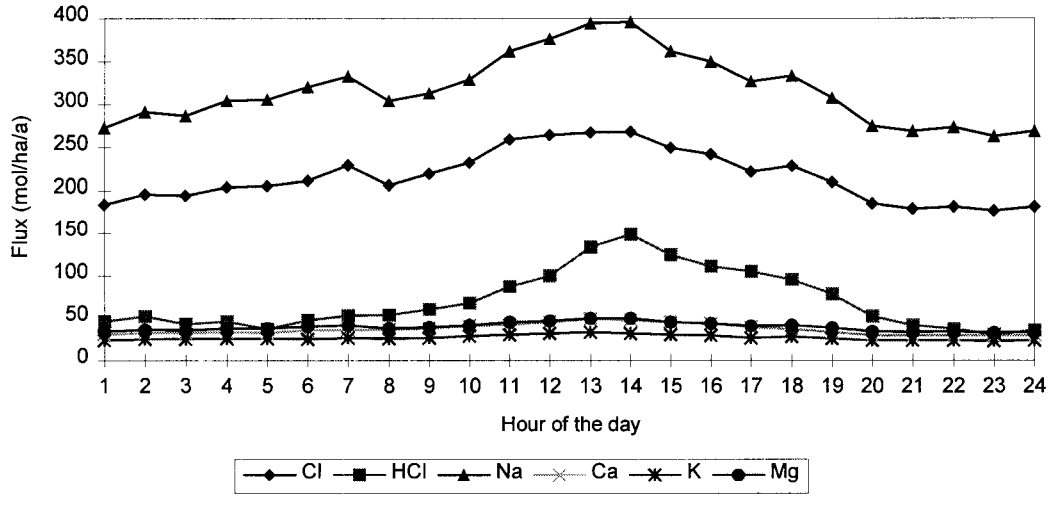

Figure 42. Annual diurnal variation in dry deposition fluxes of HCl, Cl, Na^+, Ca^{2+}, Mg^{2+}, and K^+ (mol ha^{-1} a^{-1}).

Annual average fluxes

Annual average dry deposition fluxes, standard deviations, minimum, maximum and median values are listed in Table 23. Highest input is from NH_3, about 1300 mol ha^{-1} a^{-1}. NH_4^+

aerosol deposition contributes about 21% to the total NH_x dry deposition. The contribution of SO_4^{2-} aerosol to the total SO_x deposition is about 25% and of NO_3^- to NO_y 42%. Chloride input is dominated by aerosol input, mainly as the result of sea salt particles. Speulder forest is located relatively near the coast (about 100 km). Median values are generally lower than averages as the result of the log-normal distribution of the fluxes. SO_2, NH_3 and NO_x show a large negative minimum and a positive maximum. These extreme values are the result of relatively high random errors. Base cation input is relative large, mainly as the result of the relatively small distance to the North sea (Na^+, Mg^{2+}) and as the result of nearby emissions from unpaved roads and agricultural practice. Dry deposition of heavy metals is generally small. Highest input is from zinc (5 mol ha^{-1} a^{-1}). Lowest input is from cadmium, concentrations of this metal were usually near to the detection limit. The uncertainty in this value is therefore very high.

Table 23. Annual statistics of dry deposition fluxes inferred at Speulder forest.

Component	Average	Standard deviation	Count	Min	Max	Median
SO_4	106	99	5745	3	911	77
SO_2	345	570	6381	-1816	5871	139
NH_4	337	325	4977	7	2517	227
NH_3	1277	2214	4157	-14697	25441	688
NO_X	203	503	2418	-2402	5418	86
NO_3	267	242	5955	3	2320	199
HNO_3	97	125	820	0	1058	54
HNO_2	69	65	766	0	483	46
Cl	214	299	5836	2	2936	101
HCl	69	71	815	0	627	43
Na	317	374	5031	15	4124	188
Ca	37	36	4783	4	482	28
K	25	19	6400	3	169	19
Mg	40	45	5031	3	468	24
Zn	5	4	4785	0	54	3
Pb	0.88	0.79	4603	0.05	6.65	0.62
Cd	0.03	0.03	4838	0.00	0.25	0.02
Cu	0.66	0.59	4856	0.04	6.21	0.45
Ni	0.25	0.23	4367	0.02	2.01	0.18
Cr	0.11	0.19	4017	0.01	5.29	0.07

Total sulphur, nitrogen and base cation inputs are listed in Table 25. The total potential acid dry deposition, calculated as $2SO_x+NO_y+NH_x$ (Heij and Schneider, 1991) is about 3160 mol ha^{-1} a^{-1}. The largest contribution to the potential acid deposition is from NH_x, 51%. Base cation deposition, calculated as K+2Ca+2Mg is estimated to be 180 eq ha^{-1} a^{-1}, about 6% of total dry potential acid deposition. Na^+ is assumed not to contribute to the neutralisation of acids as it originates from sea salt.

Table 24. Total sulphur, nitrogen and base cation input by dry deposition (eq. ha^{-1} a^{-1}).

Component	Dry deposition flux (eq. ha^{-1} a^{-1})
SOx	450
NOy	633
NHx	1620
potential acid	3153
BC	180

3.3.4 Wet deposition and cloud/fog deposition

Wet deposition
Wet deposition was measured using wet-only samplers placed in an open heathland (Speulderveld) about 3 km from the Speulder forest. Weekly samples were collected and transported to ECN in Petten to be analysed for anions and cations. Table 25 shows the annual average fluxes and standard deviations of the wet deposition measurements for all components considered in this project. Standard deviations reflect the variability in weekly fluxes. The standard deviation is highest for sea salt components (Na^+, Cl^- and Mg^{2+}) because very high fluxes occurred during periods with strong south-westerly winds with showers in winter, whereas during other periods fluxes were much lower. Potential acid wet deposition fluxes amount about 1760 eq ha^{-1} a^{-1}, the main contribution is formed by NH_4^+ (46%). Base cation deposition contributes about 280 eq ha^{-1} a^{-1}, 16% of the potential acid deposition.

Table 25. Annual average wet deposition fluxes and standard deviations measured over the Speulderveld (mol ha^{-1} a^{-1}).

Component	Average	Standard deviation
SO_4^{2-}	291	193
NO_3^-	374	279
NH_4^+	806	554
Cl^-	855	1208
Na^+	646	914
Ca^{2+}	46	28
K^+	29	30
Mg^{2+}	78	106
Zn^{2+}	4	7
Pb^{2+}	0.11	0.08
$Cd^{@+}$	0.04	0.08
Cu^{2+}	0.19	0.20
Ni^+	0.06	0.05
Cr^{2+}	0.07	0.28

Cloud/fog deposition
A cloud/fog detector and sequential sampling system was installed in January 1995 at 26 m height in the mast. Until November 1995 no mist occurred in this region of the country. In November after a period of several days with mist occurrence, it appeared that the sampler did not function. Even after some improvements, the instruments did not function during a second period with mist occurrence. No mist was detected after this period. Therefore, there are no cloud/fog measurements available for Speulder forest.

3.3.5 Annual average deposition fluxes

Table 26 shows the overall average dry, wet and total deposition for the period 1-2-95 to 1-12-95 (extrapolated to annual averages). Wet deposition is generally lower than dry deposition, except for base cations. Highest input on equivalent basis is for SO_x and NH_x. The contribution of NH_x to the total nitrogen deposition is twice that for NO_y. Total potential acid

deposition to the Speulder forest amounted 4914 mol H^+ ha^{-1} a^{-1} in 1995. The total base cation depositions was 456 eq ha^{-1} a^{-1}, 9% of the total potential acid flux. Total nitrogen deposition was 3430 mol ha^{-1} a^{-1} (48 kg ha^{-1}).

Table 26. Average dry, wet and total deposition fluxes to the Speulder forest for the period 1-2-95 to 1-12-95 (mol ha^{-1} a^{-1}).

Component	Dry deposition	Wet deposition	Total deposition
SO_4	106	291	397
SO_2	345		345
SO_x	*452*		*742*
NH_4	337	806	1143
NH_3	1277		1277
NH_x	*1615*		*2420*
NO_x	203		203
NO_3	267	374	641
HNO_3	97		97
HNO_2	69		69
NO_y	*636*		*1010*
Cl	214	855	1069
HCl	69		69
Cl_x	*284*		*1139*
Na	317	646	963
Ca	37	46	83
K	25	29	54
Mg	40	78	118
Zn	5	4	9
Pb	0.88	0.11	0.99
Cd	0.03	0.04	0.07
Cu	0.66	0.19	0.85
Ni	0.25	0.06	0.31
Cr	0.11	0.07	0.18

3.4 Synthesis

3.4.1 Comparison of three sites

The locations of the three sites on a map of Europe is shown in Figure 43. Some site specific characteristics are listed in Table 27 for the three sites.

Figure 43. Location of the three monitoring sites.

Table 27. Site specific characteristics.

	Auchencorth Moss	Melpitz	Speulder forest
Type of vegetation	peat bog /heath	grassland	Douglas fir
Vegetation height (m)	0.10	0.15	22
Roughness length (m)	0.01	0.04	1.20
Displacement height (m)	-	0.05	140
SO_2 measuring heights	3.0, 1.2, 0.5	5.3, 3.6, 2.5, 1.0	36, 32, 28, 24
NO_x measuring heights	3.0, 1.2, 0.5	5.3, 3.6, 2.5, 1.0	36, 32, 28, 24
NH_3 measuring heights	3.4, 1.4, 0.4	4.53, 1.80, 0.76	34,28,24
Particles	1.8	1.84	26
Acid gases	1.8	1.84	26
Wet-only collectors	1.5	1.5	1.5 (3km from the forest)

The sites were selected for their difference in land use type, surface characteristics and environmental climates. The northern Scottish site can be classified as humid background site. Speulder forest is characterised as a rough surface in a humid, sea climate with moderate pollution levels, except for NH_3. Melpitz can be considered as a site with a land climate, with relatively high sulphur loads. The difference in surface characteristics is reflected in the dry deposition velocities and surface resistances determined from the gradients measured at the different sites. The influence of surface wetness, stomatal uptake, but also coupling of uptake at the external leaf surface between different components is clearly shown. One important result of this project is that it is shown that the variations in processes affecting surface uptake is not yet quantified by current surface resistance parametrisations. This reflects the need for these long-term measurements, as the large variability has up till now not yet been identified by campaign type of measurements. As the climate and pollution level is so important for surface uptake, several other conditions should be found, which are not covered by these three sites, e.g. southern Europe warm, dry conditions. Surface resistance parametrisations were tested and applied here. No improvements in surface resistance parametrisations were made yet, as this was not within the aims of this project. Data, however, will be used in the coming year to improve models for surface uptake.

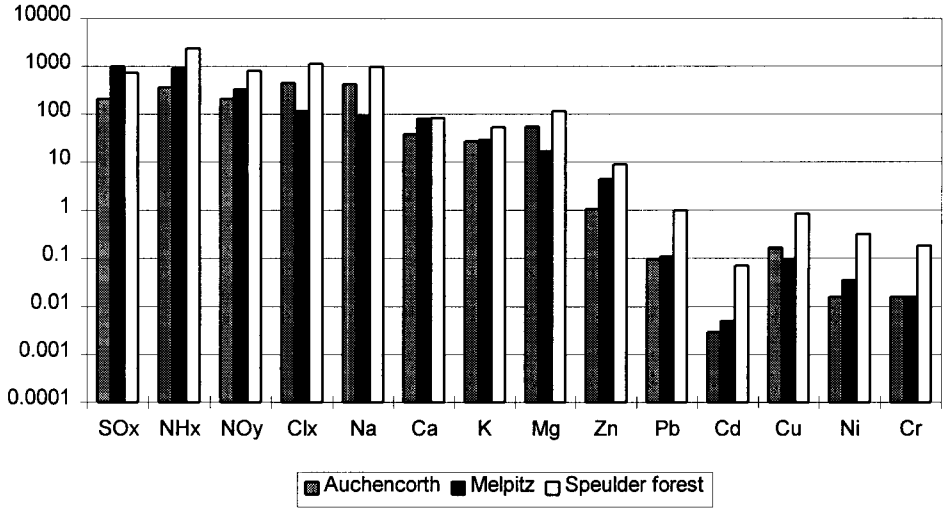

Figure 44. Total deposition for each component in 1995 at the three sites (mol ha^{-1} a^{-1}).(axis represents a logarithmic scale).

The differences in pollution level is clearly identified in the different fluxes measured at the sites. Figure 44 shows a comparison of the total deposition measured at the three sites. This figure shows that generally the fluxes at Auchencorth Moss are lowest, except for components of sea salt origin (Na^+, Mg^{2+}, Cl^-). For these components, Melpitz has lower fluxes than Auchencorth Moss, as the result of the difference in distance to the sea. For these components wet deposition is higher than dry deposition (Figure 45). Speulder forests yields highest input for all components, mainly as the result of the roughness of the forest and the resulting high dry deposition velocities. Heavy metal inputs are much lower than gases and base cations, because concentrations are much lower, but also the dry deposition velocities are much lower. It is remarkable that fluxes are much higher in Auchencorth than in Melpitz. Heavy metal inputs are mainly resulting from wet deposition (Figure 45). It must be emphasised here that uncertainties associated with heavy metal inputs are highest of all (see next section). Figure 45 shows the contribution of wet deposition to the total deposition for the three sites. The

percentage wet deposition of the total varies very much per component and per site. At Auchencorth Moss, the background site, wet deposition is clearly the dominant input. At the higher pollution sites, dry deposition becomes more important, and is generally dominating total deposition at the forest site (high roughness).

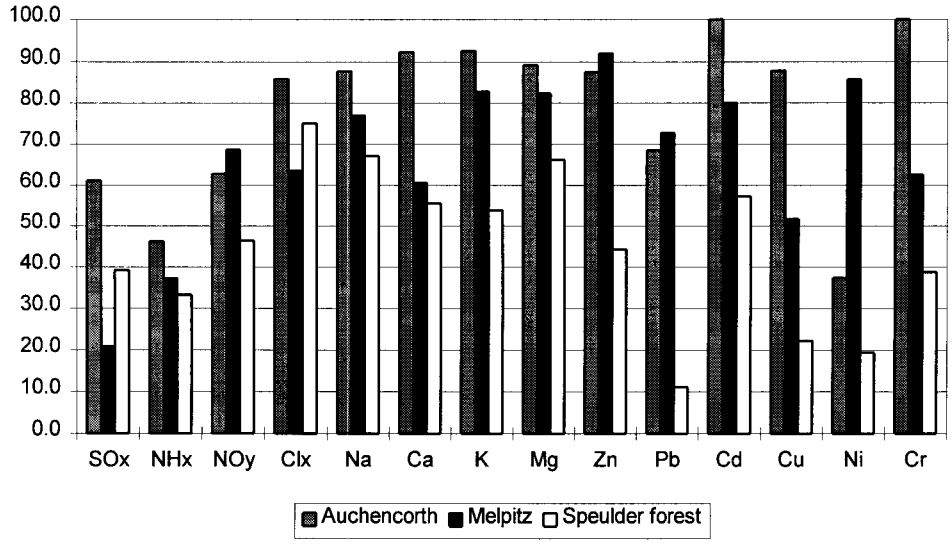

Figure 45. Contribution wet deposition to total deposition for the three sites (%).

3.4.2 Uncertainty

The uncertainty has not been investigated extensively. However, for each site the uncertainty has been estimated based on the comparison of modelled and measured V_d, quantification of major uncertainty sources and expert judgement. Uncertainty ranges are given in Table 28. The table shows that the uncertainty in particle input is highest, especially for heavy metals. Particle deposition velocities are uncertain, and for heavy metals, the detection of concentration is uncertain as the result of the very low concentrations. For forests, especially for Speulder forest, there is more information on particle deposition than for low vegetation. In a recent study, many methods to determine particle deposition were used, in order to evaluate particle deposition models for rough surfaces (Erisman *et al.*, 1994). Therefore, uncertainty in particle fluxes to the forest is lower than for other sites. Gas deposition yields lower uncertainties for low vegetation than for rough surfaces, because the vertical concentration differences are higher and because much more measurements are available over low vegetation. The highest uncertainty for gaseous input is found for NO_x. In the future, these components clearly need more attention.

Table 28. Analysis of uncertainties in annual fluxes at the three sites.

	Auchencorth Moss	Melpitz	Speulder forest	
1-Dry deposition				
Trace gases				***Major source of error***
SO_2	30	50	40	
NH_3	30	40	30	NH_3 concentration
O_3	20	30	-	Air chemistry ?
NO	80	60	50	NO concentration
NO_2	50	50	50	Air chemistry
HNO3	50	30	40	HNO_3 concentration
HNO_2	90	50	40	HNO_2 concentration
HCl	90	40	40	HCl concentration
Aerosols				
SO_4-S, NO_3-N	90	40	40	Vd formulation
NH_4-N	90	40	40	Vd formulation
Cl, K, Mg, Ca, Na	90	40	40	Vd formulation
Pb, Cu, Zn	90	40	50	Vd formulation
Ni, Cd, Cr	90	45	50	low concentrations
2-Wet deposition				
Ions				
SO_4-S, NO_3-N	10-20	10-20	15-20	Rain collection
NH_4-N	10-20	10-20	25	efficiency
Cl, K, Mg, Ca, Na	10-20	10-20	25	" "
Pb, Cu, Zn	10-20	10-20	30	" "
Ni, Cd, Cr	10-20	10-20	30	low concentrations

4. Generalisation

Investigations on abatement strategies based on the critical load concept require relevant deposition data of acidifying substances and base cations on both local and regional scales (Nilsson and Grennfelt, 1988; Hettelingh *et al.*, 1991; 1995; Lövblad *et al.*, 1993). On the local scale, large variations in deposition over landscape features and their variations in sensitivity make it essential to compare the critical load value for a specific ecosystem with the actual deposition so as to determine the exceedance value. On the larger regional scale, the essential parameters are dispersion and deposition which must be estimated in order to assess the relevant abatement strategies. For pollution deposition over Europe and budget estimates, the regional-scale approach is required (e.g. Tuovinen *et al.*, 1994). The local-scale approach covers the calculation of the more site specific critical load exceedances. The two approaches should be linked in order to evaluate the complete chain from emission to deposition and to develop relevant abatement strategies. This requires parametrisation of the deposition processes on ecosystem level (Erisman and Draaijers, 1995). On the national level some studies have shown the local variation in deposition: in the UK (URGAR, 1990), in Sweden (Lövblad *et al.*, 1991) and in the Netherlands (Erisman, 1993). The dry deposition flux is inferred as the product of ambient concentration of the components of interest and its dry deposition velocity, whereas the wet deposition flux is obtained by interpolating wet deposition measurements.

Up to now, no reliable information is available on the spatial pattern of base cation deposition over Europe. There is lack of knowledge on the spatial and temporal variation of emissions and concentrations, hampering accurate deposition mapping. Here, a method is used to estimate local-scale deposition fluxes of acidifying substances in Europe by applying a combination of long-range transport modelling and local scale inferential deposition modelling (Erisman, 1993; Erisman and Baldocchi, 1994, van Pul *et al.*, 1992, 1995) as applied in the EDACS model. Furthermore, base cation deposition maps are presented which are based also on the inferential modelling technique. In this chapter, the method is explained and results of local scale deposition fluxes for the surroundings of the monitoring locations used in this project are presented.

4.1 Method description: EDACS

Acidifying substances

The deposition model which was developed at RIVM is the EDACS model (Estimation of Deposition of Acidifying Components on a Small scale in Europe, Van Pul *et al.*, 1995). The outline of the EDACS model to estimate local and regional scale deposition fluxes is presented in Figure 46. The basis for the two estimates is formed by results of the EMEP long-range transport model. With this model dry, wet and total deposition is estimated on a 150x150 km grid over Europe using emission maps for SO_2, NO_x and NH_3 (e.g. Tuovinen *et al.*, 1994). These maps, together with interpolated meteorological observations over Europe and large scale land use data, form the input of the EMEP-MSC West Long Range Transport model. The model results are used for estimating country-to-country budgets, as a basis of sulphur and nitrogen protocols, and for assessments. The local-scale approach used by RIVM depends strongly on LRT model results. Calculated ambient concentrations of the acidifying

components (daily averages) are used along with a detailed land use map and meteorological observations to estimate small-scale dry deposition fluxes (Figure 46). By using calculated concentration maps, the relationship between emissions and deposition is maintained and scenario studies, budget studies and assessments can be carried out on different scales. Wet deposition is added to the dry deposition to estimate total local scale deposition in Europe. Wet deposition can either be obtained directly from the EMEP model, or from measurements made in Europe. The latter method is used here and will be described in the next section.

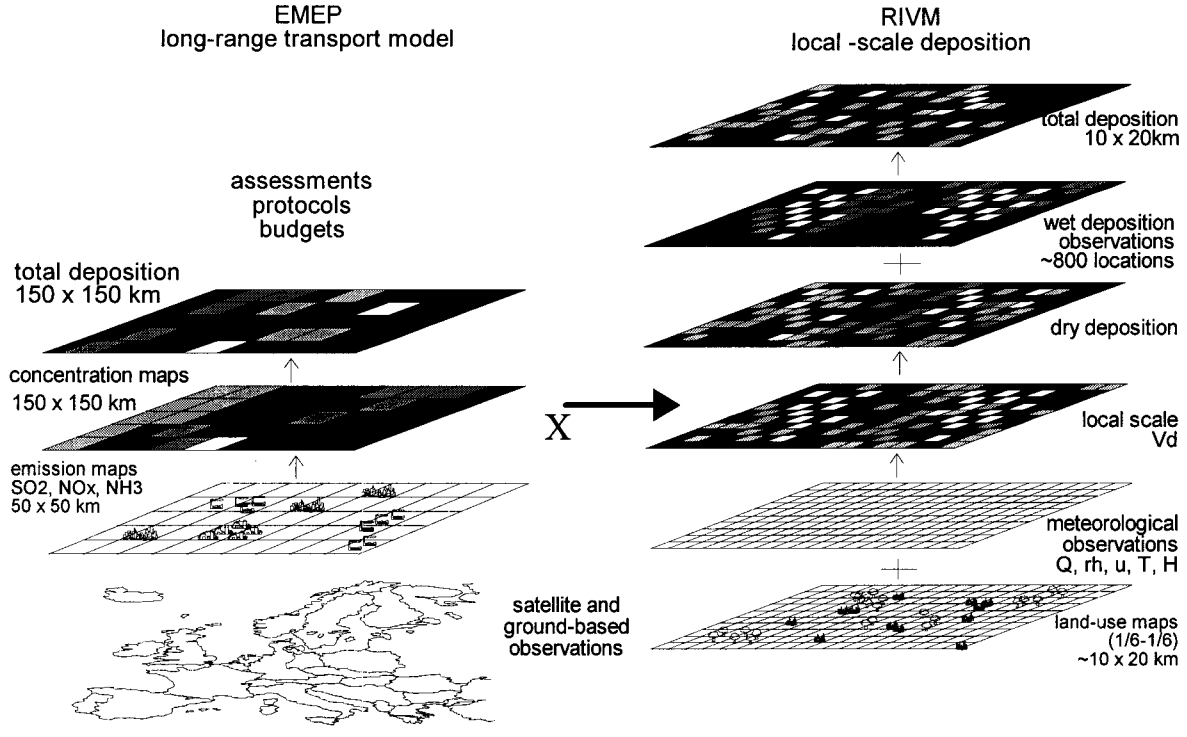

Figure 46. Outline of method to estimate local scale deposition fluxes.

Base cations

The dry deposition flux of base cations is calculated as the product of the dry deposition velocity and air concentration at a reference height above the surface. In the inferential technique, the choice for a reference height (50 m) is a compromise between the height where the concentration is not severely affected by local deposition or emission and is still within the constant flux layer (Erisman, 1992). For this height, dry deposition velocity fields over Europe are constructed with EDACS. The parametrisation of the dry deposition velocity for particles was based on the model of Slinn (1982) and tested with micrometeorological measurements recently performed at the Speulder forest in the Netherlands (Ruijgrok et al., 1994; Erisman et al., 1994b). It includes both turbulent exchange and sedimentation of coarse particles. Six-hourly based dry deposition velocity fields were aggregated to annual means before they were combined with annual mean air concentration fields, yielding dry deposition estimates on a small scale over Europe. This in contrast to the acidifying components where 6 hour average concentrations and deposition velocities are used.

Surface-level air concentrations were estimated from precipitation concentrations using scavenging ratios. These were derived from simultaneous measurements of base cation

concentrations in precipitation and surface-level air performed by Eder and Dennis (1990) in Canada and Römer and Te Winkel (1994) in The Netherlands. This approach to estimate air concentrations is based on the premise that cloud droplets and precipitation efficiently scavenge aerosols resulting in a strong correlation between concentrations within precipitation and the surface-level air (Eder and Dennis, 1990). This assumption will only be valid for well-mixed conditions at sufficient distance from sources. Factors that will influence the magnitude and variability of scavenging ratios include particle size distribution and solubility, precipitation amount and rate, droplet accretion process and storm type (Galloway et al., 1993). Event scavenging ratios can range several orders of magnitude even for single species at a single location but scavenging ratios have been found reasonably consistent when averaged over one year or longer (Galloway et al., 1993). Therefore, annual mean precipitation concentrations were used to infer annual mean air concentrations of Na^+, Mg^{2+}, Ca^{2+} and K^+. Precipitation concentration data were taken from Van Leeuwen et al. (1995) as described in the next section.

Deposition of Na^+ and part of the deposition of Mg^{2+}, Ca^{2+} and K^+ will be the result of sea spray. In sea spray these ions are mainly associated with Cl^-, and thus do not contribute to neutralisation of atmospheric acid. To estimate what fraction of Mg^{2+}, Ca^{2+} and K^+ is of non-sea salt origin, correction factors have been derived based on the composition of sea water (Asman et al., 1981). It is assumed that Na^+ originates exclusively from sea spray and that the ratio between the concentration in sea spray for the component to be corrected and Na^+ is the same as in bulk sea water. Using such a correction will only yield reliable estimates on non-sea salt Mg^{2+}, Ca^{2+} and K^+ in areas where sea salt is the only source of Na^+ in ambient air.

4.2 V_d parametrisations and concentration data

The method for dry deposition has been developed by Van Pul *et al.* (1992; 1995) for acidifying substances and by Draaijers *et al.* (1996) for base cations. Both methods are based on the methods used for the Netherlands (Erisman, 1993). Dry deposition in EDACS is inferred from the combination of long-range transport model concentrations provided by EMEP, or base cation concentrations derived from wet deposition measurements, and parametrised dry deposition velocities (Van Pul *et al.*, 1995). Concentrations at 50 m above the surface (blending height) are used. At this height it is assumed that concentrations and meteorological parameters are not influenced by surface properties to a large extent (Erisman, 1993). Dry deposition velocities of gases and particles at this height are calculated on a small scale using a land use map, routinely available meteorological data and the inferential technique (Erisman *et al.*, 1994). In the inferential technique the deposition at the surface is inferred from the concentration and the deposition velocity at the same height (Hicks *et al.*, 1987). The deposition velocity is calculated using a resistance model in which the transport to and absorption or uptake of a component by the surface is described. Resistances are modelled using observations of meteorological parameters and parametrisation of surface exchange processes for different receptor surfaces and pollution climates as described in Erisman *et al.* (1994). The V_d parametrisations used to describe the regional depositions are those listed in chapter 2, and equal therefore those used for the extension of the selected monitoring data. Meteorological parameters (wind speed, friction velocity, radiation, temperature, humidity and precipitation) are obtained from the ODS (Observational Data Set) for every 6 h and interpolated over Europe on a $1/6^0$ x $1/6^0$ grid.

4.3 Maps of regional deposition

Wet deposition of acidifying components and basic cations was mapped on a 50x50 km scale over Europe for 1989 and 1993, based on results of field measurements made at approximately 750 locations (the number of locations differs per component) (Van Leeuwen *et al.*, 1995). Information on concentrations of ions in precipitation in 1989 and 1993 was obtained from the EMEP database and from organisations responsible for wet deposition monitoring in their countries. Concentrations measured with bulk samplers were corrected for the contribution of dry deposition onto the funnels of these samplers. Sulphate concentrations were corrected for the contribution of sea salt. Point observations were interpolated to a field covering the whole of Europe using the kriging interpolation technique. The 50 x 50 km data for 1993 were used here to determine the wet deposition in the three areas surrounding the three monitoring sites. The deposition velocity is calculated at 50 m height for the land use class coverage for each 10 x 20 km grid cell. The average V_d for a grid cell is calculated by applying the land use specific parametrisations. The dry deposition is calculated by multiplying the 150 x 150 km average concentration with the sub-grid average dry deposition velocities. The daily average dry deposition fluxes are averaged to annual values. These annual values are added to the wet deposition values to obtain total deposition.

4.5 Comparison with measurements at the three sites

The grids where the measuring sites are situated in were selected and modelled annual average deposition fluxes were compared to measured values. The main emphasis is on dry deposition, as in EDACS interpolated measured wet deposition fluxes are used. EDACS results are only available for 1993, whereas measured data are for 1995. Results of measured and modelled deposition are displayed in Figure 47. It is clear that EDACS overestimates sulphur deposition. This is mainly the result of the neglecting of horizontal concentration gradients and of the deposition velocity parametrisation. For ammonia, EDACS underestimates the deposition. This is due to the neglecting of horizontal concentration gradients, which is especially of importance for NH_3, because sources vary considerably and because NH_3 is emitted from the ground level. Both effects leading to strong horizontal and vertical concentration gradients. At Auchencorth Moss, e.g., NH_3 input is dominated by two local sources. These sources are not represented in the concentrations estimated by the EMEP model. In order to distinguish between the contribution of concentration or V_d to the difference between modelled and measured fluxes, the V_d values are compared in Figure 48. The differences between modelled and measured V_d values are much smaller than those of the fluxes. Generally, V_d values are within 30% of each other, except for SO_2, HNO_3, HCl, and NO_x at Auchencorth, NO_x at Melpitz and Speulder forest, where differences are within 50%, and for Na^+ where differences are up to 200% at Auchencorth!.

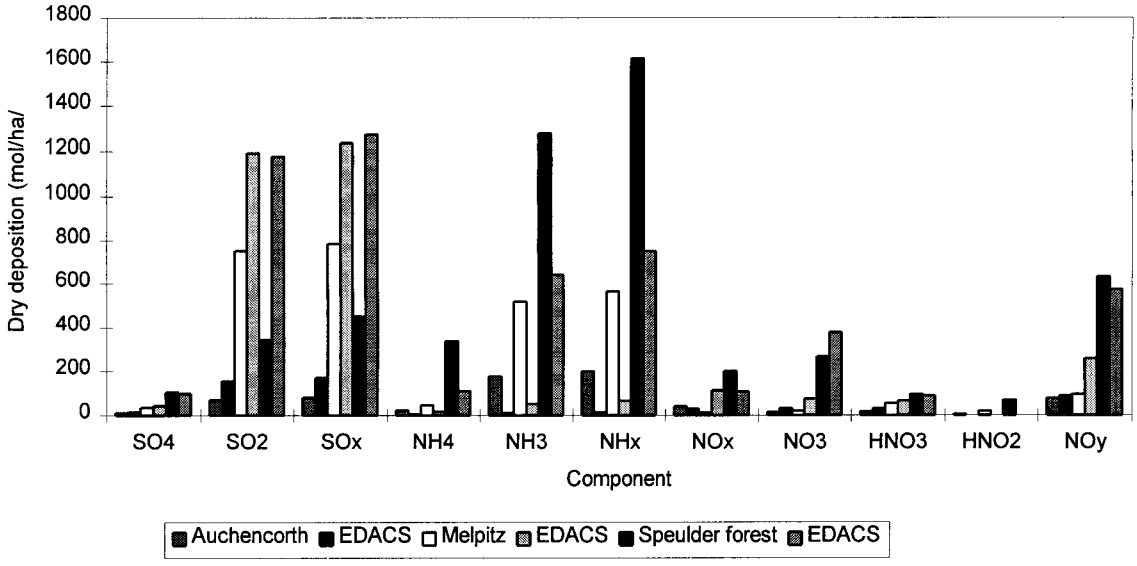

Figure 47. Comparison of modelled and measured fluxes at the three sites.

It is clear from this comparison that the model needs further development to estimate local (ecosystem specific) inputs. Main emphasis must be on development of concentration resolution and surface resistance parametrisations.

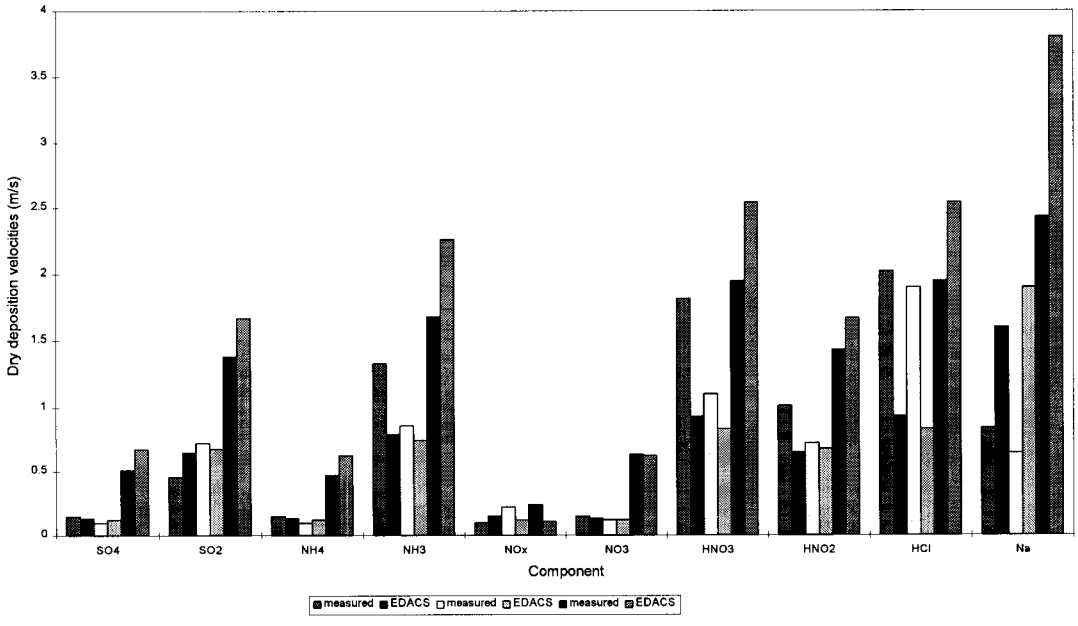

Figure 48. Comparison of modelled and measured V_d values at the three sites.

5. Monitoring and modelling strategy

5.1 Development of a deposition monitoring strategy of Europe

It is clear that for individual ecosystems deposition in general, and dry deposition in particular, can still not be quantified with sufficient accuracy using deposition models. The various methods have different advantages and drawbacks and the choice of a certain method for estimation of the flux of a specific pollutant to a specific ecosystem may in many cases depend on the purpose of the study and on requirements on accuracy and costs. For the time being, it is impossible to obtain an accurate annual average deposition map of Europe based on actual deposition measurements. Dry, cloud and fog deposition show very strong horizontal gradients due to variations in ambient concentrations in land use, in surface conditions and in meteorology. Deposition maps are generated based on a combination of models and measurements (e.g. van Pul *et al.*, 1992; Erisman *et al.*, 1996). Regarding spatial and temporal scales, measurements are supplementary to models in such a method. Furthermore, measurements are used for developing process descriptions and for evaluation of model results. Finally, measurements can act as an independent tool for assessing policy targets (trend detection). These issues, outlined below, require different measuring/monitoring and modelling strategies.

Process-oriented studies
The process-oriented studies are primarily used to provide insight into deposition processes for different components, and to obtain process descriptions and parameters to be used in models. Micrometeorological methods provide the best methods for these purposes. In cases where micrometeorological methods cannot be used, such as complex terrain and within forest stands, the throughfall method is the only one available up to now. Process-oriented studies can be used to test or verify simple/cheap measuring methods, which might be used for other purposes such as monitoring.

Evaluation of models
For evaluation or validation of model results, preferably simple and cheap monitoring methods are desired. In general, monthly to annual average fluxes are used for validation. The uncertainty in results obtained by these monitoring methods should be within acceptable limits. Furthermore, results should be representative for areas used as receptor areas in the model. Validation of LTRAP model results can be done using area representative measurements of wet deposition and of ambient concentrations. Micrometeorological measurements suitable for monitoring might be used for evaluating model dry deposition fluxes (Hicks *et al.*, 1991; Erisman *et al.*, 1996; Erisman and Draaijers, 1995). Throughfall measurements might be used as a validation method for spatial variability in S, Na^+ and Cl^- dry (and total) deposition, provided that several criteria on the method and site are met (e.g. Draaijers *et al.*, 1996). It is advisable to equip several monitoring locations in Europe with dry deposition monitoring systems, wet-only sensors, and cloud and fog deposition measuring methods (see this report), which act as reference stations for testing of low cost equipment and which can serve to derive surface exchange parametrisations used in deposition models. The locations with so called 'intensive monitoring methods' should be selected on the basis of

pollution climates and type of vegetation. Furthermore, the surroundings should be homogeneous and no sources should be near the site.

Detection of trends
If the purpose of measurements is trend detection, the annual averages should be measured as accurately as the magnitude of the trends. Ambient concentration and wet deposition measurements can be used (EMEP monitoring network) for trend detection. The trend in concentrations is representative for the dry deposition trend, which cannot be measured accurately enough at present. The disadvantage of using only concentration measurements is that a change in dry deposition due to ecosystem response (as a result of reduced loads or climatic change) or due to changes in surface conditions (interaction with other gases, etc.) cannot be detected. Extensive deposition monitoring (see previous section) might be useful for trend detection, especially at larger emission reductions, otherwise intensive methods should be applied.

Modelling
An essential component of the project is the use of process based models to complete dry deposition inputs from existing air concentration monitoring networks (Fowler et al., 1991; Erisman, 1992; Lövblad et al., 1993, Erisman *et al.*, 1996). These models will be applied for sulphur and nitrogen compounds, base cations and heavy metals to quantify ecosystem specific inputs of these components. The core dry deposition monitoring stations and the low cost deposition monitoring network will provide the validation data to test and refine models for pollution climates and land uses in Europe.

Monitoring and modelling strategy
Currently, the EDACS model is the most advanced method to estimate small scale deposition fluxes, and critical load exceedances in Europe. The resolution is not yet good enough to estimate ecosystem specific inputs. For this, new, more detailed land use data are necessary. As shown here is that the concentration resolution, which is currently 150x150 km, should be improved to reduce uncertainty in model estimates. Furthermore, surface resistance parametrisations should be more detailed to describe the complex surface exchange of gasses. The monitoring stations provided good data to evaluate models and to improve parametrisations under a range of climates and conditions. The data are, however, not representative for the total range of ecosystems, climates and conditions in Europe. It is therefore necessary to extend the three sites with a few more, in order to cover most of the ranges. As the measurements show, it is not so much the ecosystem itself that regulates the deposition, as the roughness characteristics and the surface conditions (wetness, snow cover, etc.). It is therefore not necessary to cover most of the ecosystems, but only a few in strong varying conditions (dry weather, cold, wet, etc.), and check whether the assumptions on the roughness characteristics are right. To our opinion about 10 sites, including the three used here, need to be equipped with monitoring stations as developed in this project. Two or three of such stations are needed in southern Europe, three or four in central Europe and three in background areas. For validation of the spatial representativity of model results several (about 100) sites in Europe are needed, in addition to current concentration monitoring networks. The intensive monitoring sites are, however, much too expensive for large scale application. Therefore, the development of low cost deposition monitoring methods, which should be used at the 100 sites, is needed (see next section).

5.2 Description of monitoring methods to be used for deposition monitoring

Current monitoring methods used for deposition monitoring comprise the throughfall method, micrometeorological methods (supplemented/supported by inference) and watershed balance methods. Generally, these methods yield similar estimates of the annual mean total deposition of sulphur within acceptable uncertainly limits. A larger uncertainty exists to estimate reduced or oxidised nitrogen and base cation fluxes (Erisman and Draaijers, 1995).

To obtain a deposition monitoring network with an area coverage that allows interpolation with confidence, many more stations will be required in addition to the presently operational three intensive monitoring sites. This is only feasible when the costs of the additional stations will be substantially lower than the costs of the currently employed intensive monitoring stations. In addition it is important that these methods can be applied to a wide range of relevant atmospheric constituents. In the last few years new, simple methods to measure deposition fluxes have become available. These are the so called Relaxed Eddy Accumulation (REA) method and a long term gradient method.

In the REA method air is sampled in one of two containers depending on the direction of the vertical wind speed. Field experiments have demonstrated that this method is potentially a valuable tool to measure fluxes of bulk gases such as methane (Businger and Oncley, 1990). The possibility to use the new REA method for routine monitoring remains to be demonstrated.

The new REA method could be used to monitor the deposition of trace gases as well as particle bound components. The instrumentation consists of a simple sonic anemometer and two air sampling devices. During up-draughts (as sensed by the anemometer) air is sampled in one of the two samplers. During down-draughts air is sampled in the other. The flux is derived from the difference in the average concentration of the compound in the updraughts and in the down-draughts (Oncley *et al,* 1993). Fluxes of bulk gases such as carbon dioxide and methane measured with this method have been compared with good results with measurements by other classical micrometeorological methods. In this case standard gas sample bags were used as collection devices. In principle however other collection devices such as bubblers, denuders or filter-foams can be used as well. Using multi-component analysers the flux of several trace gases can thus be measured at the same time.

The possibility of the method to measure the flux of several acidifying and ecotoxic compounds such as sulphur dioxide and nitric acid over extended periods of a week or more should be investigated. First of all, the REA-method should be compared with the eddy correlation method using ozone and carbon dioxide as tracers. This test will be valuable to validate the method and investigate possibilities for long term monitoring fluxes of gaseous components such as sulphur dioxide, nitrogen dioxide and nitric acid and fluxes of aerosol bound components such as heavy metals and Persistent Organic Pollutants (POP).

The use of weekly averaged gradients to estimate deposition fluxes should also be investigated. Schjoerring *et al,* (1992) have suggested that the net vertical exchange of for example ammonia can be estimated from the mean horizontal fluxes measured by passive samplers at different heights above the surface. If it can be demonstrated that this method may provide reasonable estimates of ammonia exchange it is relatively easy to extend its

application to other compounds such as sulphur dioxide and nitrogen dioxide using dedicated passive samplers.

For the new monitoring methods the following features have been formulated :
- a cost reduction of a factor of 3 to 4 compared to costs of equipment for dry deposition measurements of the current LIFE monitoring stations
- an accuracy which is comparable to that of the currently employed LIFE monitoring stations.

6. Conclusions

Monitoring methods for deposition of acidifying components, eutrophying components, base cations and heavy metals were developed and tested in the first year of this project. At the end of 1994 three monitoring stations were equipped: one in a moorland in Scotland, near to Edinburgh: Auchencorth Moss; one in a grassland in Germany near to Leipzig: Melpitz and one over a coniferous forest in The Netherlands: Speulder forest. After installation, the monitoring equipment was almost immediately operational. Data coverage for all three sites is quite high, except for some minor technical problems. The accuracy of the (selected) gradient measurements of SO_2 and NH_3 is on the average within 30%. The accuracy of the NO_x gradients is lower, mainly because of the very small concentration differences and the photostationary equilibrium affecting the gradients. Dry deposition velocity estimates using a surface resistance parametrisation agreed well for Speulder forest measurements, but revealed systematic differences for Auchencorth Moss and Melpitz. These parametrisations need further development.

Dry deposition was inferred from concentration measurements and deposition velocity estimates. Wet deposition was obtained directly from rain chemistry measurements and rainfall amounts, using wet-only samplers. Cloud/fog deposition was determined using a sequential fog collector. For all sites it was found that fog occurrence and estimated inputs were insignificant compared to dry and wet deposition.

Fluxes at Auchencorth Moss are lowest for all components, except for those much influenced by the sea as a source. As Melpitz is located far away from seas, at this site these components are lowest. Wet deposition is the dominant source of input at Auchencorth, whereas at Speulder forest, through its roughness and pollution climate, dry deposition is dominant. At this site Vd's are highest. Melpitz is a polluted site. Especially sulphur deposition is high. The ratio of NH_3 relative to SO_2 deposition appears to be of importance for SO_2 deposition. At low NH_3 deposition, surface saturation of SO_4^{2-} might occur, leading to a decrease in sulphur uptake at the surface.

The results of this project show that the methods implemented to monitor the deposition can be successfully applied. Routine application is possible and annual fluxes derived from the measurements are within reasonable accuracy. Next to annual fluxes, improved surface exchange parametrisations can be derived from the gradient measurements. This is necessary, because current parametrisations are inadequate to estimate dry deposition for the range of conditions and ecosystems of Europe. Both a comparison of hourly modelled and measured dry deposition values and a comparison between annual modelled and measured values revealed large differences. As such models are used for policy development and abatement strategy using the critical load concept, it is necessary to improve models and reduce uncertainty in exceedance estimates. In this way optimal measures can be taken, protecting ecosystem 'vitality' against lowest costs.

The model used for policy development is the EMEP model. The resolution of model results is 150x150 km. This is inadequate for determining ecosystem inputs. Currently, the EDACS model is the most advanced method to estimate small scale deposition fluxes, and critical load exceedances in Europe. Ecosystem specific deposition inputs can be determined with EDACS,

provided that data on ecosystem type, roughness length and location are available. Site specific data are not only necessary to determine the critical load exceedance, but also to provide a means of comparison of modelled inputs with measurements. As the dry deposition varies strongly within regions, it is impossible to obtain an integrated measured flux over a region, and as such, evaluate low resolution models. The monitoring stations provided good data to evaluate model estimates and to improve parametrisations under a range of climates and conditions. The comparison shows that current models need improvement for more accurately determine the critical load exceedance. Systematic differences were found between model estimates and measurements, which means that policy development might be systematically biased. For the EDACS model improvement it is most important that the concentration resolution is improved and that surface resistance parametrisations are extended. EMEP is currently developing their models to estimate 50x50 km concentrations and depositions, which is a mayor improvement. Surface resistance parametrisations could be improved using the measurements reported here.

The monitoring data obtained at the three sites are not representative for the total range of ecosystems, climates and conditions in Europe. For a thorough evaluation of models and of policy development, more measuring sites of deposition are needed in Europe. For development and testing of deposition models, more 'intensive' sites, as developed within the project reported here, placed at different ecosystems in different conditions are needed. As the measurements show, it is not so much the ecosystem itself that regulates the deposition, as the roughness characteristics and the surface conditions (wetness, snow cover, etc.). It is therefore not necessary to cover most of the ecosystems, but only a few in strong varying conditions (dry weather, cold, wet, etc.), and check whether the assumptions on the roughness characteristics are right. To our opinion about 10 sites, including the three used here, need to be equipped with monitoring stations as developed in this project. Two or three of such stations are needed in southern Europe, three or four in central Europe and three in background areas. For validation of the spatial representativity of model results several (about 100) sites in Europe are needed, in addition to current concentration monitoring networks. The intensive monitoring sites are, however, much too expensive for large scale application. Therefore, the development of low cost deposition monitoring methods, which should be used at the 100 sites, is needed (see next section). These 100 low cost sites, together with the maximum of 10 intensive sites should provide the minimum of measurements for model development and evaluation, and for policy evaluation in Europe, based on measurements. It is therefore strongly recommended to extend the current EMEP concentration and wet deposition network with dry deposition monitoring facilities. The EMEP monitoring data, together with the EMEP and EDACS model then provides good quality information for policy development for reducing excessive inputs of pollutants to ecosystems in Europe.

Acknowledgement

John Garland and Johan Sliggers are acknowledged for reviewing this report.

References

Allen, A.G., Harrison, R.M. and Erisman, J.W. (1989) Field measurements of the dissociation of ammonium nitrate and ammonium chloride aerosols. Atmospheric Environment, 23:1591-1599

Asman, W.A.H., Slanina, J. and Baard, J.H. (1981), Meteorological interpretation of the chemical composition of rain water at one measurement site, *Water, Air and Soil Pollution*, 16, 159-175.

Bache, D.H. (1986) On the theory of gaseous transport to plant canopies. Atmospheric Environment, 20:1379-1388.

Baldocchi, D.D., Hicks, B.B., and Camara, P. (1987) A canopy stomatal resistance model for gaseous deposition to vegetated surfaces. Atmospheric Environment, 21:91-101.

Baldocchi, D.D., Hicks, B.B. and Meyers, T.P. (1988) Measuring biosphere-atmosphere exchanges of biologically related gases with micro meteorological methods. Ecology , 69:1331-1340.

Beljaars, A.C.M., Holtslag, A.A.M. and Westrhenen, R.M. van (1987a) Description of a software library for the calculation of surface fluxes. Technical report TR-112, Royal Netherlands Meteorological Institute, De Bilt, The Netherlands.

Brost, R.A., Delany, A.C. and Huebert, B.J. (1988) Numerical modelling of concentrations and fluxes of HNO_3, NH_3 and NH_4NO_3 near the surface. J. Geophys. Res., 93:7137-7152.

Buijsman, E. and Erisman, J.W. (1988) Wet deposition of ammonium in Europe. J. Atmos. Chem., 6:265-280.

Buijsman, E. (1989) Onderbouwende informatie over het Landelijk Meetnet Luchtkwaliteit. I: Het Landelijk Meetnet Regenwatersamenstelling. Report No. 228703006, National Institute of Public Health and Environmental Protection, Bilthoven, The Netherlands.

Businger, J.A. (1986) Evaluation of the accuracy with which dry deposition can be measured with current micrometeorological techniques. J. Climate Appl. Meteor., 25:1100-1124.

Businger, J.A., S.P. Oncley (1990) Flux Measurement with conditional sampling Journal of Atmospheric and Oceanic Technology, 349-352

Chamberlain, A.C. (1966) Transport of gases from grass and grass-like surfaces. Proc. R. Soc. Lond., A290:236-265.

Chamberlain, A.C. (1975) The movement of particles in plant communities. In: J.L. Monteith (Editor), Vegetation and the atmosphere - 1. Academic Press, New York.

Davenport, A.G. (1960) Rationale for determining design wind velocities. J. Struct. Div. Am. Soc. Civ. Eng., 86:39-68.

Davidson, C.I. and Wu, Y.L. (1990) Dry deposition of particles and vapors. In: S.E. Lindberg, A.L. Page and S.A. Norton (Editors), Acidic Precipitation, Vol. 3. Springer-Verlag, New York.

Denmead, O.T. (1983) Micrometeorological methods for measuring gaseous losses of nitrogen in the field. In: J.R. Freney and J.R. Simpson (Editors), Gaseous loss of nitrogen from plant-soil systems. Martinus Nijhoff/Dr W. Junk, The Hague, The Netherlands, pp. 133-158.

Dollard, G.J., Unsworth, M.H. and Harvey, M.J. (1983) Pollutant transfer in upland regions by occult precipitation. Nature, 302:241-243.

Dollard, G.J., Davies, T.J. and Lindstrom, J.P.C. (1986) Measurements of the dry deposition rates of some trace gas species. In: G. Angeletti and G. Restell (Editors), Proc. of the 4th

European Symposium on Physico-chemical behaviour of atmospheric pollutants. Stresa, Italy, 23-25 September 1986.

Draaijers, G.P.J., Leeuwen, E.P.van, Jong, P.G.H. de, Erisman, J.W. (1996) Deposition of base cations and their role in acid neutralization and forest nutrition. Report no. 722108017. National Institute of Public Health and the Environment, Bilthoven, The Netherlands.

Droppo, J.G. Jr. (1985) Concurrent measurements of ozone dry deposition using eddy correlation and profile flux methods. J. Geophys. Res., 90:2111-2118.

Duyzer, J. H., Bouman, A.M.M., Aalst, R.M. van and Diederen, H.S.M.A. (1987) Assessment of dry deposition of NH_3 and NH_4^+ over natural terrains. In: Proc. of the EURASAP Symposium on Ammonia and Acidification. Bilthoven, The Netherlands, 13-15 April 1987.

Duyzer, J.H. and Bosveld, F.C. (1988) Measurements of dry deposition fluxes of O_3, NO_X, SO_2 and particles over grass/heathland vegetation and the influence of surface inhomogeneity. Report No. R 88/111, TNO, Delft, The Netherlands.

Duyzer (1991) Inputs of nitrogen compounds and photo-oxidants as components of the pollution climate of Europe (progress report). Report No. R 91/005, TNO, Delft, The Netherlands.

Dyer, A.J. and Hicks, B.B. (1970) Flux gradient relationships in the constant flux layer. Q. J. Roy. Met. Soc., 96:715.

Eder, B.K. and Dennis, R.L. (1990) On the use of scavenging ratios for the inference of surface-level concentrations and subsequent dry deposition of Ca^{2+}, Mg^{2+}, Na^+ and K^+. Water Air Soil Pollut., 52:197-215.

Erisman J.W., Vermetten A.W.M., Asman W.A.H., Slanina J. and Waijers-IJpelaan A. (1988) Vertical distribution of gases and aerosols: the behaviour of ammonia and related components in the lower atmosphere. Atmospheric Environment, 22:1153-1160.

Erisman J.W., Versluis A.H., Verplanke T.A.J.W., de Haan D., Anink D., van Elzakker B.G., Mennen M.G., van Aalst R.M. (1989) Monitoring the dry deposition of SO_2 in the Netherlands. Report No. 228601002. National Institute of Public Health and Environmental Protection, Bilthoven, The Netherlands.

Erisman, J.W. (1992) Atmospheric deposition of acidifying compounds in the Netherlands. Ph.D. Thesis, Utrecht University, The Netherlands.

Erisman, J.W. (1993a) Acid deposition onto nature areas in the Netherlands; Part I. Methods and results. Water Soil Air Pollut.,71:51-80.

Erisman, J.W. and Wyers, G.P. (1993a) Continuous measurements of surface exchange of SO_2 and NH_3; implications for their possible interaction in the deposition process. Atmospheric Environment, 27A:1937-1949.

Erisman, J.W., Versluis, A.H., Verplanke, T.A.J.W., Haan D. de, Anink, D., Elzakker, B.G. van, Mennen, M.G. and Aalst, R.M van. (1993b) Monitoring the dry deposition of SO_2 in the Netherlands. Atmospheric Environment, 27:1153-1161.

Erisman, J.W., Mennen, M., Hogenkamp, J., Goedhart, D., Pul, A. van and Boermans, J. (1993c) Evaluation of dry deposition measurements for monitoring application over the Speulder forest. Report no. 722108002, National Institute of Public Health and the Environment, Bilthoven, The Netherlands.

Erisman, J.W. and Baldocchi, D.D. (1994) Modelling dry deposition of SO_2. Tellus, 46B:159-171.

Erisman, J.W., Pul, A. van and Wyers, P. (1994a) Parameterization of dry deposition mechanisms for the quantification of atmospheric input to ecosystems. Atmospheric Environment, 28:2595-2607.

Erisman, J.W., Draaijers, G.J.P., Duyzer, J.H., Hofschreuder, P., Leeuwen, N. van, Römer, F.G., Ruijgrok, W. and Wyers, G.P. (1994b) Contribution of aerosol deposition to atmospheric deposition and soil loads onto forests. Report No. 722108005, National Institute of Public Health and Environmental Protection, Bilthoven, The Netherlands.

Erisman, J.W. and Draaijers, G.P.J. (1995) Atmospheric deposition in relation to acidification and eutrophication. Studies in Environmental Research 63, Elsevier, the Netherlands.

Erisman, J.W., G.P.J. Draaijers, M.G. Mennen, J.E.M. Hogenkamp, E. van Putten, W. Uiterwijk, E. Kemkers, H. Wiese, J. H Duyzer, R. Otjes, G. P. Wyers. Towards development of a deposition monitoring network for air pollution of Europe; Deposition monitoring over the Speulder forest, Report no. 722108014, National Institute of Public Health and the Environment, Bilthoven, The Netherlands.

Erisman, J.W., Potma, C., Draaijers, G.P.J., van Leeuwen, E.P. (1996) A generalised description of the deposition of acidifying pollutants on a small scale in Europe. Water, Air and Soil Pollut., 85,pp2101-2106.

Erisman, J.W., Potma, C., Draaijers, G.P.J., van Leeuwen, E.P. (1996) A generalised description of the deposition of acidifying pollutants on a small scale in Europe. Water, Air and Soil Pollut., 85,pp2101-2106.

Fowler, D. (1978) Dry deposition of SO_2 on agricultural crops. Atmospheric Environment, 12:369-373.

Fowler, D. (1984) Transfer to terrestrial surfaces. Phil. Trans. R. Soc. Lond., B30: 281-297.

Fowler, D., Cape, J.N. and Unsworth, M.H. (1989) Deposition of atmospheric pollutants on forests. Phil. Trans. R. Soc. Lond., B 324:247-265.

Fowler, D. and Duyzer, J.H. (1990) Micrometeorological techniques for the measurement of trace gas exchange. In: M.O. Andrae and D.S. Schimel (Editors), Exchange of trace gases between terrestrial ecosystems and the atmosphere. John Wiley and Sons, pp. 189-207.

Fowler, D., Duyzer, J.H., and Baldocchi, D.D. (1991) Inputs of trace gases, particles and cloud droplets to terrestrial surfaces. Proc. R. Soc. Edinburgh, 97B:35-59.

Fowler, D., Cape, J.N., Sutton, M.A., Mourne, R., Hargreaves, K.J., Duyzer, J.H. and Gallaghar, M.W. (1992) Deposition of acidifying compounds. In: T. Schneider (Editor), Acidification research: evaluation and policy applications. Elsevier, Amsterdam, pp. 553-572.

Fowler, D., Flechard, C.R., Milford, C., Hargreaves, K.J., Storeton-West, R.L., Nemitz, E., Sutton, M.A. (1996) Towards development of a deposition monitoring network for air pollution in Europe; Measurements of pollutant concentration and deposition fluxes to moorland at Auchencorth Moss in Southern Scotland, 1995. Institute of Terrestrial Ecology, Edinburgh, Scotland.

Gallagher, M.W., Choularton, T.W., Morse, A.P. and Fowler, D. (1988) Measurements of the site dependence of cloud droplet deposition at a hill site. Q.J. R. Met. Soc., 114:291-303.

Galloway, J.N., Savoie, D.L., Keene, W.C. and Prospero, J.M. (1993), The temporal and spatial variability of scavenging ratios for nss sulfate, nitrate, methanesulfonate and sodium in the atmosphere over the North Atlantic Ocean, *Atmospheric Environment*, 27A, 235-250.

Garland, J.A. (1977) The dry deposition of sulphur dioxide to land and water surfaces. Proc. R. Soc. Lond., A354:245-268.

Garland, J.A. (1978) Dry and wet removal of sulfur from the atmosphere. Atmospheric Environment, 12:349.

Garratt, J.R. and Hicks, B.B. (1973) Momentum, heat and water vapour transfer to and from natural and artificial surfaces. Q. J. R. Met. Soc., 99:680-687.

Grennfelt, P. (1987) Deposition processes for acidifying compounds. Environ. Tech. Lett., 8:515-527

Grennfelt, P and Thörnelöf, E. (Editors), Proc. on Critical loads for nitrogen, Report No. Nord 1992:41, Lökeberg, Sweden, 6-10 April 1992. Nordic Council of Ministers, Copenhagen, Denmark.

Hettelingh, J.P., Downing, R.J. and Smet, P.A.M. de (1991) Mapping critical loads for Europe, CCE report no.1, Report No. 259101001. Coordination Centre for Effects, National Institute of Public Health and Environmental Protection, Bilthoven, The Netherlands.

Hicks, B.B., Baldocchi, D.D., Meyers, T.P., Hosker Jr., R.P. and Matt, D.R. (1987) A preliminary multiple resistance routine for deriving dry deposition velocities from measured quantities. Water Air Soil Pollut., 36:311-330.

Hicks, B.B., Draxler, R.R., Albritton, D.L., Fehsenfeld, F.C., Hales, J.M., Meyers, T.P., Vong, R.L., Dodge, M., Schwartz, S.E., Tanner, R.L., Davidson, C.I., Lindberg, S.E. and Wesely, M.L. (1989) Atmospheric processes research and procecess model development. State of Science/Technology, Report No. 2. National Acid Precipitation Assessment Program.

Hicks, B.B., Hosker, R.P., Meyers, T.P. and Womack, J.D. (1991) Dry deposition inferential measurement techniques - I. Design and tests of a prototype meteorological and chemical system for determining dry deposition. Atmospheric Environment, 25A:2345-2359.

Holtslag, A.A.M. and Bruin, H.A.R. de (1988) Applied modelling of the nighttime surface energy balance over land. J. Appl. Met., 27:689-704.

Huebert, B.J. and Robert, C.H. (1985) The dry deposition of nitric acid to grass. J. Geophys. Res., 90:2085-2090.

Iversen, T., Halvorsen, N., Mylona, S. and Sandnes, H. (1991) Calculated budgets for airborne acidifying components in Europe, 1985, 1987, 1988 and 1990. MSC-West, Norwegian Meteorological Institute, Oslo.

Jans, W.W.P., Roekel, G.M. van, Orden, W.H. van and Steingröver, E.G. (1994) Above ground biomass of adult Douglas fir. A dataset collected in Garderen and Kootwijk from 1986 onwards. IBN-DLO Research Report No. 94/1, 58 pp.

Joslin, J.D. and Wolfe, M.H. (1992) Tests of the use of net throughfall sulfate to estimate dry and occult sulfur deposition. Atmospheric Environment, 26A:63-72.

Kramm, G. (1989) A numerical method for determining the dry deposition of atmospheric trace gases. Boundary-Layer Met., 48:157-176.

Leeuwen, E.P. van, Potma, C., Draaijers, G.P.J., Erisman, J.W. and Pul, W.A.J. van (1995) European wet deposition maps based on measurements. RIVM Report 722108006, National Institute for Public Health and Environmental Protection, Bilthoven, The Netherlands.

Lenschow (1982) Reactive trace species in the boundary layer from a micrometeorological perspective. J. Met. Soc. Japan, 60:

Lovett, G.M. (1988) A comparison of methods for estimating cloud water deposition to a New Hampshire USA. subalpine forests. In: M.H. Unsworth and D. Fowler (Editors), Acid deposition at high elevation sites. Kluwer, Dordrecht, The Netherlands, pp. 309-320.

Lövblad, G. and Erisman, J.W. (1992) Deposition of nitrogen in Europe. In: P. Grennfelt and E. Thörnelöf (Editors), Proc. on Critical loads for nitrogen, Report No. Nord 1992:41, Lökeberg, Sweden, 6-10 April 1992. Nordic Council of Ministers, Copenhagen, Denmark.

Lövblad, G., Erisman, J.W. and Fowler, D. (1993) Models and methods for the quantification of atmospheric input to ecosystems. Report No. Nord 1993:573 Göteborg, Sweden, 3-7 November 1992. Nordic Council of Ministers, Copenhagen, Denmark.

Mallant, R.K.A.M. and Kos, G.P.A. (1990) An optical device for the detection of clouds and fog. Aerosol Sci. Technol., 13:196-202.

Mennen, M.G., Erisman, J.W., Elzakker, B.G.van and Zwart, E. (1992) A monitoring system for continuous measurement of the SO_2 dry deposition flux above low vegetation. In: Air Pollution Report 39. CEC, Brussels, Belgium.

Mennen M.G., Hogenkamp J.E.M., Zwart H.J.M.A. and Erisman J.W. (1996) Flow distortion errors by rigid obstacles in dry deposition measurements, *Boundar-Layer Meteorology* (submitted).

Mennen M.G., Uiterwijk J.W., Putten E.M. van, Hellemond J. van, Wiese C.W., Regts T.A., Hogenkamp J.E.M., E. Kemkers, R. Otjes and Erisman J.W. (1996) Dry deposition monitoring over the Speulder forest; 2. Description of the equipment and evaluation of the measuring methods. Report no. 722108016, National Institute of Public Health and the Environment, Bilthoven, The Netherlands.

Milford, J.B. and Davidson, C.I. (1985) The sizes of particulate trace elements in the atmosphere - A review JAPCA, 35:1249-1260.

Montheith, J.L. (1975; 1976) Vegetation and the atmosphere. Academic Press, London, UK.

Nilsson, J. and Grennfelt, P. (1988) Critical loads for sulphur and nitrogen. Proceedings of the workshop in Skokloster, Sweden.

Oncley, S. P., A.C. Delany, T.W. Horst (1993) Verification of flux measurements using relaxed eddy accumulation Atmospheric Environment, 27A, 15 2417-2426

Pasquill, F. and Smith, F.B. (1983) Atmospheric diffusion. John Wiley and Sons, New York.

Pul, W.A.J. van, Erisman, J.W., Jaarsveld, J.A. van and Leeuw, F.A.A.M. de (1992) High resolution assessment of acid deposition fluxes. In: T. Scneider (Editor), Acidification research: evaluation and policy application. Studies in Environmental Science 50. Elsevier, Amsterdam.

Pul, W.A.J., Potma, C., Leeuwen, E.P. van, Draaijers, G.P.J. and Erisman, J.W. (1995) EDACS: European Deposition maps of Acidifying Compounds on a Small scale. Model description and results. RIVM Report 722401005.

Ridder, T.B., Baard, J.H. and Buishand, T.A. (1984) The impact of sample strategy and analysis protocol on concentrations in rainwater (in Dutch). Royal Netherlands Meteorological Institute, Report No. TR-55.

RIVM (1994) Jaaroverzicht 1993. Report No. 722101014, National Institute of Public Health and Environmental Protection, Bilthoven, The Netherlands.

Römer, F.G. and Winkel, B.W. te (1994) Droge depositie van aerosolen op vegetatie: verzurende componenten en basische kationen. Report 63591-KES/MLU 93-3243, KEMA, Arnhem, The Netherlands.

Ruijgrok, W., Tieben, H. and Eisinga, P. (1994) The dry deposition of acidifying and alkaline particles on Douglas fir. Report No. 20159-KES/MLU 94-3216, KEMA, Arnhem, The Netherlands.

Schaug, J., Pedersen, U. and Skjelmoen, J.E. (1991). EMEP Co-operative programme for monitoring and evaluation of the long-range transmission of air pollutants in Europe, Data Report 1989, part 1: Annual Summaries, Norwegian Institute for Air Research, EMEP/CCC-Report 2/91.

Schjoerring, J.K., M. Ferm, S.G. Sommer (1992) Measurement of NH3 emission and deposition by the gradient method: Can passive flux samplers be used to obtain the net exchange of NH3 through periods of several days with varying wind speed and atmospheric NH3 concentration. Proceedings of the Workshop " Development of analytical techniques

for atmospheric pollutants", Rome, April, April 13-15, 1992. I. Allegrini (ed). ISBN 2-87263-082-1

Schwela, D. (1977) Die trockene Deposition gasförmiger Luftverunreinigungen. Schriftenreihe de Landesanstalt für Immissionsschutz, Heft, 42:46-85.

Sehmel, G.A. (1980) Particle and gas dry deposition: a review. Atmospheric Environment, 14:983-1011.

Slanina, J. Römer, F.G. and Asman, W.A.H. (1982) Investigation of the source regions for acid deposition in the Netherlands. Proc. CEC Workshop on Physic-Chemical behaviour of atmospheric pollutants, 9 September, Berlin, 1982.

Slinn, W.G.N. (1982) Predictions for particle deposition to vegetative surfaces. Atmospheric Environment, 16:1785-1794.

Spindler, G. and Grüner, A (1996) Towards development of a deposition monitoring network for air pollution of Europe; The Melpitz site in Germany - Results of measurements made in 1995, IFT, Leipzig, Germany.

Steingröver, E.G. and Jans, W.W.P. (1994) Physiology of forest-grown Douglas-fir trees. Effects of air pollution and drought. Final Report, APV III project 793315. IBN-DLO Research Report No. 94/3.

Thom, A.S. (1971) Momentum absorption by vegetation. Quarternary Journal of the Royal Meteorological Society, 97:414-428.

Thom, A.S. (1975) Momentum, mass and heat exchange of plant communities. In: J.L. Monteith (Editor), Vegetation and Atmosphere. Academic Press, London, pp. 58-109.

Thorne, P.G., Lovett, G.M. and Reiners, W.A. (1982) Experimental determination of droplet impaction on canopy components of Balsem fir. J. Appl. Met., 23:1413-1416.

Tuovinen, J.P., Barrett, K. and Styve, H. (1994) Transboundary acidifying pollution in Europe: Calculated fields and budgets 1985 - 1993. EMEP/MSC-W, Report 1/94, Norwegian Meteorological Institute, Oslo.

UK Review group on acid rain (1990) Acid deposition in the United Kingdom 1986-1988. Warren Spring Laboratory, UK.

Vermeulen, A.T., Wyers, G.P., Römer, F.G., Leeuwen, N.P.M. van, Draaijers, G.P.J. and Erisman, J.W. (1994) Fog deposition on Douglas fir forest, ECN Report RX-94-100, Petten, The Netherlands.

Voldner, E.C., Barrie, L.A. and Sirois, A. (1986) A literature review of dry deposition of oxides of sulfur and nitrogen with emphasis on long-range transport modelling in North America. Atmospheric Environment, 20:2101-2123.

Waldman, J.M., Munger, J.W., Jacob, D.J., Flagan, R.C., Morgan, J.J. and Hoffman, M.R. (1982) Chemical composition of acid fog. Science, 218:677-680.

Weathers, K.C., Likens, G.E., Bormann, F.H., Eaton, J.S., Bowden, W.B., Anderson, J.L., Cass, D.A., Galloway, J.N., Keene, W.C., Kimball, K.D., Huth, P. and Smiley, D. (1986) A regional acidic cloud/fog water event in the eastern United States. Nature, 319:657-658.

Wesely, M.L. and Hicks, B.B. (1977) Some factors that affect the deposition rates of Sulfur Dioxide and similar gases on vegetation. J. Air Pollut. Contr. Assoc., 27:1110-1116.

Wesely, M.L., Cook, D.R., and Hart, R.L. (1985) Measurements and parameterization of particulate sulphur dry deposition over grass. J. Geophys. Res., 90:2131-2143.

Wesely, M.L. (1989) Parametrization of surface resistances to gaseous dry deposition in regional-scale numerical models. Atmospheric Environment, 23:1293-1304.

Wesely, M.L., Sisteron, D.L., Hart, R.L., Drapapcho, D.L. and Lee, I.Y. (1989) Observations of nitric oxide fluxes over grass. J. Atmos. Chem., 9:447-463.

Wieringa, J. (1992) Updating the Davenport roughness classification. J. Wind Engin. Indust. Aerodynamics, 41.

Wu, Y.L., Davidson, C.I., Dolske, D.A. and Sherwood, S.I. (1992) Dry deposition of atmospheric contaminants to surrogate surfaces and vegetation. Aerosol Sci. Technol., 16:65-81.

Wyers, G.P., Otjes, R.P. and Slanina J. (1993) A continuous-flow denuder for the measurement of ambient concentrations and surface exchange fluxes of ammonia. Atmospheric Environment, 27A:2085-2090.

Wyers, G.P., Veltkamp, A.C., Vermeulen, A.T., Geusebroek, M., Wayers, A. and Möls, J.J. (1994) Deposition of aerosol to coniferous forest. Report No. ECN-C--94-051, ECN, Petten, The Netherlands.

Wyers, G.P. and Erisman, J.W. (1996) Ammonia exchange over coniferous forest. Atmospheric Environment, in press..

Zeller, K.W., Massman, D., Stocker, D.G., Stedman, D. and Hazlett, D. (1989) Initial results from the Pawnee eddy correlation system for dry acidic deposition research. U.S.D.A. Forest Service Research Paper RM-282.

Zwart H.J.M.A., Hogenkamp J.E.M., Mennen M.G. and Erisman J.W. (1994) Performance of a monitoring system for measurement of SO_2 and NO_2 dry deposition fluxes to a forest. Report no. 722108001, National Institute of Public Health and the Environment, Bilthoven, The Netherlands.

Appendix A. Surface resistance parametrisations

Surface exchange parametrisations for gases and particles used in this project were derived from lterature and measurements by Erisman *et al.* (1994). The parametrisations are summarised in this Appendix.

A.1.1 Surface resistances for gases

The surface resistance of a gas consists of a series of resistances reflecting different pathways of uptake. They are either determined by the actual state of the receptor, or by a memory effect. R_c is a function of the canopy stomatal resistance R_{stom} and mesophyll resistance R_m; the canopy cuticle or external leaf resistance R_{ext}; the soil resistance R_{soil} and in-canopy resistance R_{inc}, and the resistance to surface waters or moorland pools R_{wat} (Eqn. 16). In turn, these resistances are affected by leaf area, stomatal physiology, soil and external leaf surface pH, and presence and chemistry of liquid drops and films. The stomatal resistance, external leaf surface resistance and soil resistance act in parallel:

$$\begin{aligned} &\textit{vegetative surface:} && R_c = \left[\frac{1}{R_{stom} + R_m} + \frac{1}{R_{inc} + R_{soil}} + \frac{1}{R_{ext}}\right]^{-1} \\ &\textit{water surfaces:} && R_c = R_{wat} \\ &\textit{bare soil:} && R_c = R_{soil} \\ &\textit{snow cover:} && R_c = R_{snow} \end{aligned} \qquad [16]$$

This section gives a short overview of the most important resistances for each gas. These have extensively been described in Erisman *et al.* (1994d). Table 2 lists values of surface resistances obtained with the parametrisations in Erisman *et al.* (1996), given for three different pollution climates as examples.

SO_2

The deposition of SO_2 on vegetation has been shown to be regulated mainly by stomatal resistance and the presence of surface water on the foliage. The stomatal uptake can be modelled satisfactorily. However, an understanding of the variations of surface resistance due to surface wetness chemistry is limited. It is assumed here that when the surface is wet, deposition of SO_2 is regulated by external leaf uptake. At low SO_2 concentrations, the buffering capacities of vegetation leaves are probably sufficient to maintain low R_c values. At high SO_2 concentrations other neutralising components, such as NH_3, might become important. The surface may be moistened by high relative humidity, dew, guttation, rain or fog, and cloud deposition. Deposition of SO_2 to soil is dependent on the relative humidity and on the soil pH.

NH_3

NH_3 is emitted from fertilised soils and from pasture during grazing. In addition, emission takes place from crops, ungrased pasture and semi-natural vegetation under dry, warm conditions during daytime at low ambient concentrations. In other cases NH_3 is mainly deposited. Deposition in these cases is regulated by stomatal uptake and by deposition to

external leaf surfaces. R_c values for semi-natural vegetation and forests are low (in the range of 0-50 s m^{-1}), and depend on surface wetness.

NO_X

NO is not taken into account here as a depositing pollutant. Deposition of NO_2 is mainly regulated by stomata. The deposition to external leaf surfaces, water surfaces and soils is one order of magnitude less than stomatal uptake.

PAN, HNO_2, HNO_3, HCl

PAN deposition is slow with an overall surface resistance of 500-1000 s m^{-1}. Knowledge about HNO_2 deposition is scarce; since HNO_2 is a week acid, just like SO_2, it is treated as SO_2 until more information becomes available. Thus uptake of HNO_2 is regulated by stomata and external leaf surfaces when the surface becomes moist. The strong acids HNO_3 and HCl deposit efficiently to all surfaces, with negligible R_c values. Only at low temperatures with a surface covered with snow R_c increases up to 50-100 s m^{-1}

O_3

The uptake of ozone by vegetation is mainly via the stomata. The resistance of the remaining plant parts (the cuticle) to ozone is found to be larger than 1000 s m^{-1}. The surface resistance to ozone deduced from measurements above water and snow are about 1000-2000 s m^{-1}, which can be explained by the lower water solubility. R_c may sometimes be lower depending on the chemical content of the water layer. The soil resistance to ozone is largely dependent on the type of soil and the soil water content. The soil resistance is typically 100 s m^{-1} under dry soil conditions. This value increases typically up to 500 s m^{-1} at a waterlogged stage of the soil (20-30% water content).

Table 29. Examples of averaged surface resistances (s m^{-1}) for different gases during daytime under different climates, with the stomatal resistance (R_{stom}) also given

	Moist (rain or *rh*>90%), moderate temperature		Winter, snow covered surface		Dry, warm summer (*rh*<60%), well watered soil	
	Coniferous forest	Grassland	Coniferous forest	Grassland	Coniferous forest	Grassland
R_{stom}	200	60	400	closed stomata	150	50
SO_2	0[b]	0[b]	500	500	300	100
NH_3	0[b]	0[b]	500	500	500[a]	500[a]
NO_2	320	100	640	1000	240	80
HNO_2	0[b]	0[b]	500	500	300	100
HNO_3	0[b]	0[b]	10	50	0[b]	0[b]
HCl	0[b]	0[b]	10	50	0[b]	0[b]
PAN	500	500	1000	1000	500	500
O_3	320	100	640	1000	240	80

[a] Under these conditions NH_3 is expected to be emitted from the vegetation. The upward flux is estimated with this R_c value in Equation [3].

[b] R_c values are set to 1 s m^{-1} to avoid unrealistically high deposition velocities at low values of R_a and R_b.

A.1.2 Particles

The Slinn (1982) model developed to describe particle deposition was simplified to include all relevant routinely available parameters, resulting in parametrisations for the deposition of particles to forests (Ruigrok *et al.*, 1994). Current models for generalisation of deposition, such as DEADM (Erisman, 1993a), use a parametrisation of V_d for *low vegetation* based on relations of Wesely *et al.* (1985):

$$V_d = \frac{u_*}{300} \quad \textit{for stable conditions and}$$
$$V_d = \frac{u*}{300}\,[1 + (\frac{-300}{L})^{2/3}]\ \textit{for unstable and neutral conditions} \qquad [17]$$

Routinely available data include meteorological parameters such as wind speed, radiation, temperature, relative humidity, u_* and L, and land use and z_0 values.

Slinn (1982) proposes to use a simplification of his model by splitting V_d for *forests* in a turbulent contribution and a surface deposition velocity, the latter being dependent on the collection efficiency of the surface and thus surface properties:

$$V_d = [V_{dt}^{-1} + V_{ds}^{-1}]^{-1}, \qquad [18]$$

where the surface deposition velocity is given as $V_{ds} = E\ u_*^2/u_h$, with u_h the wind speed at canopy height, E the collection efficiency and V_{dt} the turbulent contribution, represented by the inverse of the aerodynamic resistance: $R_a(z=36)^{-1}$. The collection efficiency, E, is different for different size classes as different processes become important. E is determined by parametrisation of modelled E values for Speulder forest based on data such as u_*, z_0, d, u_{36}, rh, surface wetness, etc. (Ruigrok *et al.*, 1994). The following relations were found.
The general form for V_d at 36 m high is:

$$V_d = \frac{1}{\frac{1}{V_{ds}} + Ra(50)} \qquad [19]$$

where V_{dS} can be estimated from:

$$V_{ds} = \frac{u_*^2}{u_h} E \qquad [20]$$

u_h is the wind speed at canopy height which is extrapolated from the wind speed measured at 36 m to 22 m (canopy height) using measured u_* values and flux profile relations; E is given for different components and conditions in Table 3. For the large particles, represented by Na^+ in Table 3, the sedimentation velocity has to be added:

$$V_s = 0.0067\ ms^{-1} \qquad rh \le 80\%$$
$$V_s = 0.0067 EXP\left(\frac{0.0066 rh}{1.058 - rh}\right)\ m\,s^{-1}\ rh > 80\% \qquad [21]$$

The data for Na^+ in Table 3 are also representative for Mg^{2+} and Ca^{2+}. V_{ds} for K^+ can be taken half the value of Na^+, because the MMD for K^+ is much smaller than that of Na^+.

Table 30. Parametrisations of E values for different components and conditions

	Wet surface		Dry surface	
Compound	rh ≤ 80	rh > 80	rh ≤ 80	rh > 80
NH4	$0.066u_*^{0.41}$	$0.066u_*^{0.41}[1+0.37EXP\left(\frac{rh-80}{20}\right)]$	$0.05u_*^{0.23}$	$0.05u_*^{0.23}[1+0.18EXP\left(\frac{rh-80}{20}\right)]$
SO_4	$0.08u_*^{0.45}$	$0.08u_*^{0.45}[1+0.37EXP\left(\frac{rh-80}{20}\right)]$	$0.05u_*^{0.28}$	$0.05u_*^{0.28}[1+0.18EXP\left(\frac{rh-80}{20}\right)]$
NO_3	$0.10u_*^{0.43}$	$0.10u_*^{0.43}[1+0.37EXP\left(\frac{rh-80}{20}\right)]$	$0.063u_*^{0.25}$	$0.063u_*^{0.25}[1+0.18EXP\left(\frac{rh-80}{20}\right)]$
Na	$0.679u_*^{0.56}$	$0.679u_*^{0.56}[1+0.37EXP\left(\frac{rh-80}{20}\right)]$	$0.14u_*^{0.12}$	$0.14u_*^{0.12}[1-0.09EXP\left(\frac{rh-80}{20}\right)]$